The Effect of Spindle Geometry on the Establishment of Merotelic Kinetochore Attachment and Chromosome Mis-segregation

William T. Silkworth

Dissertation submitted to the faculty of the Virginia Polytechnic Institute and State University in partial fulfillment of the requirements for the degree of

Doctor of Philosophy
In
Biological Sciences

Daniela Cimini, chair
Young Ju
Jeffrey Kuhn
Richard Walker

June 26th 2012
Blacksburg, VA

Keywords: mitosis, aneuploidy, chromosome mis-segregation, merotelic kinetochore attachment, mitotic spindle geometry

The Effect of Spindle Geometry on the Establishment of Merotelic Kinetochore Attachment and Chromosome Mis-segregation

William T. Silkworth

Abstract

At any given time there are on the order of one hundred million cells undergoing mitosis in the human body. To accurately segregate chromosomes, the cell forms the bipolar mitotic spindle, a molecular machine that distributes chromosomes equally to the daughter cells. To this end, microtubules of the mitotic spindle must appropriately attach the kinetochores: protein structures that form on each chromatid of each mitotic chromosome. The majority of the time correct kinetochore microtubule attachments are formed. However, mis-attachments can and do form. Mis-attachments that are not corrected before chromosome segregation can give rise to aneuploidy, an incorrect number of chromosomes. Aneuploidy occurring in the germ line can cause both miscarriage and genetic diseases. Furthermore, aneuploidy is a major characteristic of cancer cells, and aneuploid cancer cells frequently mis-segregate chromosomes at high rates, a phenotype termed chromosomal instability (CIN). CIN has been correlated with both advanced tumorigenesis and poor patient prognosis and over the years there have been many hypotheses for what causes CIN. In this study, we identified two distinct mechanisms that are responsible for CIN. Both of these mechanisms cause a transient, abnormal geometric arrangement of the mitotic spindle. Specifically, cancer cells possess supernumerary centrosomes, which lead to the assembly of multipolar spindles during early mitosis when attachments between kinetochores and microtubules are forming.

Supernumerary centrosomes facilitate the formation of merotelic attachments, in which a single kinetochore binds microtubules from more than one centrosome. As mitosis progresses the supernumerary centrosomes cluster, giving rise to a bipolar spindle by the time of chromosome segregation. However, the high rates of merotelic attachments formed during the transient multipolar stage result in high rates of chromosome mis-segregation. The second geometric defect characterized is caused by failure of centrosomes to separate before kinetochore-microtubule attachments begin to form. This mechanism, too, leads to high rates of kinetochore mis-attachment formation and high rates of chromosome mis-segregation. Finally, this study shows that the mechanisms characterized here are prevalent in human cancer cells from multiple organ sites, thus revealing that both mechanisms are a common cause of CIN.

Dedication

Dedicated to Sylvia Barbato, my grandmother.

Acknowledgements

First and foremost, I thank my mentor Daniela Cimini, who is without question the greatest scientist I know. Daniela has a passion for both her students and science, which is a rare trait that makes it a pleasure to be a member of her laboratory. While I can attempt to appreciate the amount of work and long hours she has dedicated to both her profession and students, I will neither fully understand nor appreciate it until I am in a similar position. To Daniela, I owe a debt which I will never be able to repay. As I move forward in my own career, I will try to by implementing everything I have learned from her. Additionally, I thank my committee members. It is with their guidance that I have learned to challenge myself and approach questions from different vantage points.

I thank all the members of the Cimini lab but perhaps none more than Isaac Nardi. Working with Isaac was truly a phenomenal experience. Without his help I do not think that we would have accomplished so much or had such a great time while working the odd hours that facilitated the collection of this data.

Lastly, I would like to thank my family, especially my parents. It is with their constant support that I have been able to achieve all I set out to accomplish. I would also like to thank all my friends for their endless patience in listening to me while I have been working towards this degree. Whether or not these people know it or not, they have helped immensely and allowed me to weigh many decisions and choose the best course of action. To everyone mentioned above I must express a sincere thank you for all the support that has been given to me. Thank you.

Table of Contents

List of Figures

Chapter 1

Chapter 2

Chapter 3

Chapter 4

List of Tables

Chapter 1

Introduction and literature review

Overview

The survival and development of organisms depend on the ability of cells to maintain and pass the correct complement of chromosomes to subsequent generations. The segregation of chromosomes into daughter cells occurs during a highly orchestrated process named mitosis. Accurate transport of the genetic material to each daughter cell occurs thanks to the rearrangement of interphase cell components into specialized mitotic organelles and structures, such as the mitotic spindle and the kinetochore (KT) [1-3].

The importance of mitotic chromosome segregation is illustrated by the fact that in humans, at any time, there are ~2.5 X 10^8 cells dividing [4]. If inaccuracies in mitosis are not kept to a minimum, the possibility exists for cells to accumulate errors [4], which may produce a number of outcomes. Specifically, inaccurate chromosome segregation can lead to the production of aneuploid daughter cells, i.e. cells possessing an abnormal number of chromosomes. Aneuploidy is well known for its role in inducing severe genetic diseases and is the leading cause of miscarriage in humans [5-7]. Indeed, the only autosome aneuploidies that can result in a live birth are trisomy 21 (an extra copy of chromosome 21), which causes Down's syndrome, trisomy 18, which causes Edward's syndrome, and trisomy 13, which causes Patau's syndrome. Of these three, Down's syndrome is the only one compatible with development into adulthood, whereas the other two cause death within the first year of life [8]. Sex chromosome aneuploidies occur at higher frequencies than do numerical changes in autosomes [8] and can induce less severe syndromes, such as Turner's syndrome (X0 individuals, i.e. females with only one copy of the X chromosome), and Klinefelter's syndrome (XXY males). The suggested reason for sex chromosome aneuploidies to be better tolerated than most autosomes is the

relatively low number of genes carried by such chromosomes [9-11]. The frequency of aneuploidy in somatic human cells is largely unknown [12, 13]. However, most cancer cells are aneuploid (Table 1.1) [13, 14], suggesting that aneuploidy arising in somatic cells might be the leading cause of cancer development, a hypothesis proposed by Theodor Boveri over 100 years ago [15].

The goal of this study is to investigate how defects in the mitotic apparatus may lead to establishment of kinetochore-microtubule mis-attachments and chromosome mis-segregation, and to determine whether the mechanisms studied here contribute to chromosomal instability in cancer cells. A thorough investigation of mitotic defects requires a comprehensive understanding of normal mitotic division, the mitotic apparatus, and the mechanisms of chromosome segregation. Thus, the remainder of Chapter 1 will focus on a detailed literature review of the following topics: the stages of mitosis, components of the mitotic spindle and its role in chromosome segregation, the kinetochore, the spindle assembly checkpoint, the types and fates of different types of attachments between the microtubules of the mitotic spindle and kinetochore, and finally this chapter will conclude with a discussion of aneuploidy and its role in cancer initiation and progression. Chapters 2 and 3 describe two cellular mechanisms that cause transient defects of the mitotic apparatus that lead to chromosome mis-segregation and aneuploidy. Finally, chapter 4 investigates the potential role that the mechanisms described in chapter 2 and 3 may have in causing chromosomal instability in different cancer cell types, and reaches the conclusion that the mechanisms of abnormal spindle assembly characterized here appear to be common among a variety of cancer cells and may provide promising targets for chemotherapeutic agents.

Mitosis

Accurate distribution of the genetic material is crucial to the proper functioning and perpetuation of cells and organisms. Chromosomes are replicated during S-phase, but the two sister chromatids will not be separated until the next M-phase, through a process named mitosis. Mitosis consists of five distinct phases: prophase, prometaphase, metaphase, anaphase, and telophase (Figure 1.1). Upon mitotic entry each chromosome is constituted of two sister chromatids, a kinetochore assembles on each chromatid, and the duplicated centrosomes give rise to a microtubule-based machine named the mitotic spindle. Together, chromosomes, kinetochores, and the mitotic spindle form the mitotic apparatus [16].

Prophase (Figure 1.1, first panel), the first stage of mitosis, occurs when the genetic material becomes condensed into individual chromosomes. These chromosomes resemble worm-like structures that are encapsulated by the nuclear membrane. As this stage progresses, chromosomes become more condensed and better defined. Cohesin molecules hold the two sister chromatids of each chromosome together, and a kinetochore assembles on each chromatid. The interphase microtubule cytoskeleton depolymerizes and reorganizes into short and more dynamic microtubules (MTs). The replicated centrosomes nucleate a radial array of microtubules that, along with the action of microtubule motors, separate the centrosomes to opposite sides of the nucleus [17-19]. The breakdown of the nuclear envelope marks progression from prophase into prometaphase.

Prometaphase (Figure 1.1, second panel) is the stage at which the sister chromatids are exposed to the dynamic microtubules that constitute the mitotic spindle. The kinetochores are fully assembled by this time and form attachments with microtubules. Initial attachment of microtubules to a kinetochore results in the rapid poleward movement of the chromosome [20]. This process usually results in an orientation of sister chromatids that allows for the unattached sister kinetochore to face the opposite spindle pole. Non-kinetochore microtubules interact with the sister chromatid arms and produce polar ejection forces [21]. These forces assist in the movement of the sister chromatid between the spindle poles and facilitate microtubule capture of the unattached kinetochore. When the unattached sister kinetochore binds microtubules, the chromosome starts a congressional movement towards the spindle equator [22].

Metaphase (Figure 1.1, third panel) is achieved when all kinetochores are attached to microtubules and all chromosomes are aligned at the spindle equator. The structure formed by the aligned chromosomes is referred to as the metaphase plate. In many cell types, the aligned chromosomes are not stationary but undergo short poleward and anti-poleward oscillations (directional instability) [21]. These oscillations are due to dynamic instability exhibited by microtubules. The mitotic spindle at this stage achieves its typical fusiform structure.

The initiation of anaphase (Figure 1.1, fourth panel) occurs upon the degradation of cohesin subunits that hold together sister chromatids [23]. The sudden elimination of cohesin allows for the synchronized poleward movement of sister chromatids (now daughter chromosomes). The kinetochores function to transport chromosomes poleward

toward their respective spindle pole. As the kinetochore is involved in this process, so are kinetochore microtubules. These microtubules shorten without losing their attachment to the kinetochore, thus drawing chromosomes to the spindle poles (anaphase A). In conjunction with this movement there is also an increase in spindle pole-to-pole distance (anaphase B). This further separation of the spindle poles allows for the additional separation of sister chromatids toward opposite sides of the parent cell.

Telophase (Figure 1.1, fifth panel) is the final stage of mitosis, when the chromosomes are significantly moved away from the metaphase plate, and the nuclear envelope starts reassembling. Mitosis is followed by cytoplasmic division, or cytokinesis (Figure 1.1, fifth panel). An actin-based contractile ring starts forming during the later stages of mitosis at the spindle equator. This contractile ring keeps contracting after completion of mitotic chromosome segregation to cleave the cytoplasm into two roughly equal cells. A cytoplasmic bridge can persists between the two daughter cells for many hours before complete cleavage. The completion of cytokinesis, along with the previous steps of mitosis, yields two genetically identical daughter cells.

Mitotic Spindle

The mitotic spindle is a key molecular machine that separates chromosomes during mitosis. Upon mitotic entry, the interphase microtubules break down to re-polymerize into a fusiform bi-polar array of shorter and more dynamic microtubules [24]. This structure is completely assembled by metaphase, at which stage the mitotic spindle appears as a symmetric radial array of microtubules emanating from two distinct regions located at opposite sides of the cell. These two regions are commonly referred to as

spindle poles, centrosomes, or microtubule-organizing centers, and serve as nucleation sites from which microtubules emanate [25, 26]. Microtubules fan out toward the center of the spindle, where they interact with the chromosomes (Figure 1.2). Spindle poles, microtubules, and chromosomes form a prominent structure that can be easily followed by simple light microscopy. Thus, the spindle is one of the best-studied cellular structures.

Each microtubule consists of thirteen tubulin protofilaments organized to form a hollow tube. Each tubulin molecule consists of two very similar globular subunits called α- and β-tubulin. Tubulin dimers assemble so that α– and β–subunits regularly alternate within the protofilament. This linear arrangement gives microtubules a structural polarity. The two ends of a microtubule are referred to as the minus end (with exposed α-subunits), located at the centrosome, and the plus end (with exposed β-subunits), away from the centrosome. Microtubules undergo a process of slow polymerization and rapid disassembly of subunits termed dynamic instability [27]. This instability is primarily seen at the plus ends of microtubules while the minus end remains relatively stable. It is this process of dynamic instability which facilitates capture and subsequent segregation of chromosomes during mitosis.

Within a mitotic spindle, three classes of microtubules can be identified (Figure 1.2), depending on which structures they contact with their plus end and the role they serve during mitosis. These three classes are: astral, interpolar, and kinetochore microtubules (Figure 1.2). Astral microtubules are those in which the plus ends seemingly probe the cytoplasm and contact the cell cortex [28]. Their primary function is to orient the mitotic spindle within the cell. Molecular motors travel along interpolar

microtubules and function to separate centrosomes to opposite sides of the nucleus [28]. The anti-parallel arrangement allows for specific microtubule motors, such as the kinesin Eg5, to "walk" towards the plus ends of two overlapping microtubules, which results in centrosome separation [17-19]. Interpolar microtubules are also responsible for anaphase B movement in which the spindle poles separate to allow for complete chromosome segregation [29]. Microtubules whose plus end interacts with kinetochores are referred to as kinetochore microtubules. Vertebrate kinetochores bind multiple kinetochore microtubules, which form a microtubule bundle also called a kinetochore-fiber, or K-fiber. Kinetochore microtubules constitute the link between the chromosomes and the mitotic spindle and govern mitotic chromosome dynamics [30]. (A number of microtubule-associated proteins (MAPs) also bind microtubules to stabilize them.)

In vertebrate somatic cells, centrosomes are located at the two spindle poles, and function as the microtubule organizing centers at those sites (Figure 1.2). Centrosomes are regions of amorphous pericentriolar material in which a pair of centrioles are located. Each centriole consists of a truncated array of microtubules that are organized into a triplet arrangement in which nine groups of three microtubules form a cylindrical structure [25, 26]. Two such cylinders are positioned orthogonally to one another to form a centriole pair. The centrioles are surrounded by a matrix, named pericentriolar material, which is primarily composed of pericentrin, a protein that acts as a scaffold to which other proteins are attached [31]. A special component of the centrosome is γ-tubulin. γ-tubulin is a third type of tubulin [32, 33] that is found exclusively at the centrosome, and is very well conserved in all eukaryotes [32]. γ-tubulin was found to bind one or more proteins to form the γ-tubulin ring complex, or γ-TuRC, a ring-like structure with

diameter of ~25nm (same as microtubules) [34]. γ-TuRCs are believed to be the sites of microtubule nucleation at the centrosome. Newly nucleated microtubules interact with proteins such as HSET, NuMA, and TPX2, that contribute to the maintenance of bipolar spindles with focused spindles poles [35, 36].

Although centrosomes have been shown to function as microtubule nucleation sites, many meiotic cells and other specialized cells assemble acentrosomal spindles [37]. A tubulin polymer stabilizing gradient localized in the vicinity of the chromosomes may initiate microtubule assembly, which leads to the formation of the characteristic bipolar spindle through the action of motor proteins such as cytoplasmic dynein [38, 39], and minus-end associated proteins, such as NuMA (*Nu*clear/*M*itotic *A*pparatus protein) [40-42].

Kinetochore

The kinetochore is a proteinaceous structure that serves as the interface between the chromosomes and spindle microtubules [43]. Various molecular components of the kinetochore facilitate the attachment of chromosomes to the plus ends of microtubules. In addition, key motor proteins that reside at the outermost kinetochore area, promote chromosome movement during mitosis [44]. The kinetochore assembles on centromeric DNA and each sister chromatids assembles one kinetochore, thus ensuring faithful segregation of the genetic material. The centromere, or primary constriction, is the location on each chromosome that is visible during mitosis as it is significantly narrower compared to the rest of the chromosome. The centromeric regions of chromosomes vary among species, but, with the exception of those organisms that possess holocentric

chromosomes, such as *Cenorhabditis elegans*, are frequently characterized by the presence of repetitive sequences at a specific locus. In *Saccharomyces cerevisiae* a 125bp sequence is indispensable for the construction of the kinetochore [45]. In human cells, centromeres consist of repetitive sequences 171bp long, also referred to as α-satellite or alphoid DNA, arranged in a head to tail fashion and spanning several megabases [46].

Electron micrographs of the vertebrate kinetochore reveal a trilaminar structure atop the centromeric DNA with heterochromatin flanking both sides of the centromeric DNA [47]. The microtubules can be visualized entering the most distal domain of this organelle. The three domains visible by electron microscopy are commonly referred to as the inner kinetochore, the outer kinetochore, and the fibrous corona [47-49] Specific proteins localize to each of these domains (Figure 1.3) and determine kinetochore structure and function.

The inner kinetochore is composed of constitutive proteins, three of which were the first kinetochore proteins to be identified because they were recognized by antisera from patients with *c*alcinosis, *r*eynaud's, *e*sophageal, *s*clerodactyly, and *t*elangiectasia (CREST) syndrome [47]. These are *cen*tromere *p*roteins A, B, and C (CENP-A, CENP-B, and CENP-C, respectively) (Figure 1.3) [50].

The kinetochore protein CENP-A is a histone H3 homolog and is conserved from yeast through humans [51-53]. CENP-A substitutes for Histone H3 in the centromeric region of chromosomes (Figure 1.3) and provides the molecular marker and basis for kinetochore assembly [52]. Perturbations of CENP-A have calamitous consequences. For example, CENP-A null mice do not develop beyond embryogenesis due to failure of kinetochore formation and cell death [54]. CENP-A is targeted to the kinetochore during

late mitosis-early G1 [55]. Although the precise mechanism that targets CENP-A to the centromere in vertebrates remains unknown, it has been shown that budding yeast CENP-A localizes in a sequence-dependent manner [56].

Like CENP-A, CENP-B is a DNA binding protein. It recognizes the CENP-B box, a specific 17bp sequence within the alphoid DNA [57]. Interestingly, cells derived from CENP-B null mice do not exhibit mitotic defects [58, 59]. Recently, it has been seen that CENP-B is involved in chromatin remodeling, which appears necessary for the formation of functional kinetochores [57]. However, neocentromeres in human patients were found in regions of DNA that do not contain alpha satellite sequences (and therefore no CENP-B binding sites) [60], suggesting that CENP-B is not required for kinetochore formation. Given such contradictory data, further studies will be necessary to determine if CENP-B plays a significant functional role. However, it is possible that CENP-B's role at the kinetohcore might be solely structural and not functional. Early studies indicated that CENP-B is found at both kinetochores of stable dicentric chromosomes, as opposed to CENP-C, which instead localizes only at the active kinetochore of stable dicentric chromosomes [61]. These data suggests a functional role for CENP-C. Since the identification of the first three CENPs, many other inner kinetochore proteins have been identified and the list currently includes CENP-H, CENP-I, CENP-K – U (Figure 1.3) [62-64]. These CENPs are present at the inner kinetochore throughout the cell cycle and most of them are constitutively associated with CENP-A nucleosomes. Not all of these inner kinetochore proteins seem to play a critical role in chromosome segregation [48], although some of them may be responsible for the loading of CENP-A on centromeric DNA [64]. The inner kinetochore proteins CENP-H, CENP-

I, CENP-K – U have been recently named the *c*onstitutively *c*entromere-*a*ssociated *n*etwork (CCAN) [62-64]. Members of the CCAN control the localization of some outer kinetochore proteins [63], such as Mis12 and Ndc80 [65, 66].

The outer kinetochore consists of fewer proteins than does the inner kinetochore and becomes fully assembled after entry into mitosis [48]. The members of this region belong to three protein complexes (KNL1, Mis12, and Ndc80, also referred to as the KMN network) (Figure 1.3) and play a critical role in establishment of kinetochore attachment to microtubules [43, 48]. KNL1 was shown to target multiple outer kinetochore proteins both in C. elegans [67] and vertebrates [63], and its depletion results in defective chromosome segregation [63]. Mis12 plays an important role in chromosome segregation [68, 69], presumably by promoting kinetochore attachment. The Ndc80 complex, conserved in a wide range of eukaryotes, consists of four proteins: Hec1, Nuf2, Spc24, and Spc25 [70-72]. These molecules are required for the establishment of stable kinetochore attachment to the spindle [73] and proper chromosome segregation [74, 75]. The plus ends of microtubules interact specifically with Hec1 and Nuf2, while Spc24 and Spc25 are located proximal to the inner kinetochore [73, 76]. Spc24 and Spc25 seemingly fasten the microtubule binding domain of this functional complex to the kinetochore scaffold [77]. A current model proposes that both KNL1 and the Ndc80 complex, possibly with the cooperation of Mis12, bind to a microtubule lattice promoting the stable end-on microtubule connections (Figure 1.3) [77, 78].

The fibrous corona derives its name from its meshwork-like aspect in electron micrographs. This region is the first to come into contact with microtubule plus ends and microtubules become embedded in it. Proteins found at the fibrous corona include:

spindle assembly checkpoint (SAC) proteins; CENP-E; CENP-F; the RZZ complex (Rod, ZW 10, and Zwilch); Dynein/Dynactin; and a number of *p*lus end *t*rack*i*ng *p*roteins (+TIPs; CLASP, CLIP-170, EB1, APC) (Figure 1.3) [79, 80]. All these proteins play disparate roles, from SAC signaling (SAC proteins, RZZ complex, CENP-E) [48, 81] [82], to SAC silencing (dynein) [83]; from directing chromosome congression (CENP-E, dynein) [84-86], to establishment of stable end-on kinetochore attachments (dynein, RZZ, CENP-F) [87-90]; from mitotic chromosome movement (dynein) [86, 91-93], to coordination between microtubule dynamics and kinetochore movement (+TIPs) (reviewed in [94]).

Spindle Assembly Checkpoint

Upon mitotic entry, each chromosome consists of two sister chromatids held together by a molecular complex, cohesin, that is necessary for proper bi-orientation of sister chromatids [95]. Initially located throughout the length of mitotic chromosomes, cohesin molecules become reduced during mitosis until all but the centromeric region appears to maintain this adhesion [96]. Anaphase onset coincides with cohesin degradation, which allows the sister chromatids to be partitioned to the two daughter cells in a coordinated manner. If this process were to occur before chromosome alignment, the result would be mis-segregation of chromosomes and aneuploid daughter cells. Fortunately, a mechanism is in place to prevent such chromosome mis-segregation during mitosis. This mechanism is a biochemical signaling pathway known as the *s*pindle *a*ssembly *c*heckpoint, or SAC. Work performed by Rieder et al. (1994 and 1995) illustrates the importance of kinetochore attachment to the spindle for SAC signaling [97,

98]. In these studies, anaphase onset was prevented in the presence of an unattached kinetochore [99]. Ablation of a single unattached kinetochore resulted in anaphase onset [97]. This revealed two critical pieces of information. First, the SAC ensures that all chromosomes become properly attached to the mitotic spindle, second the signal that prevents progression into anaphase (the "wait anaphase" signal) is produced at or near the kinetochore. Since this early report, our knowledge of the SAC pathway has substantially increased, allowing a more comprehensive understanding of molecular interactions at work.

As described above, cohesin molecules hold replicated condensed sister chromatids together. Degradation of the cohesin is carried out by an enzyme named separase. However, before anaphase onset this enzyme is sequestered in a complex with the protein securin. The metaphase to anaphase transition depends on the degradation of securin, which in turn allows separase to become active [100] and cleave the cohesin complex, thus inducing separation of sister chromatids (Figure 1.4). The degradation of securin molecules is dependent on the action of the proteasome [4, 101]. The *a*naphase *p*romoting *c*omplex/*c*yclosome, APC/C, an E3 ubiquitin ligase, marks securin for degradation through ubiquitination [102, 103]. A positive regulator, Cdc20, is necessary for the activation of APC/C [104]. The SAC effectively inhibits the activity of the Cdc20-APC/C complex thereby preventing cohesin degradation until all kinetochores become attached to spindle microtubules and all chromosomes become aligned at the metaphase plate (Figure 1.4) [105].

The first SAC proteins were identified through genetic screens of *Saccharomyces cerevisiae* exposed to microtubule perturbing compounds [106, 107]. The

characterization of mutants that did not arrest in mitosis in the presence of MT drugs, led to the identification of six SAC genes: *m*itotic *a*rrest-*d*eficient Mad1, Mad2, and Mad3 (BubR1 in vertebrates), *b*udding *u*ninhibited in *b*enzimidazoles, Bub1, Bub3, and *m*ono*p*olar *s*pindle 1, Mps1 [48, 108, 109]. It was subsequently found that these members share significant homology throughout eukaryotes [110, 111]. In addition to these core SAC proteins, a number of proteins have been shown to contribute to checkpoint signaling in various ways. These proteins include CENP-E [112, 113], Dynein [83], and the RZZ (Rod, ZW 10, and Zwilch) complex (reviewed in [81]). The shared homology throughout eukaryotic cells illustrates the importance and efficacy of the SAC to prevent chromosome loss during mitosis. It is currently thought that there are two portions of the SAC [99, 114].

The first portion of the SAC consists of an attachment sensing mechanism that ensures all kinetochores become occupied by a full complement of microtubules before anaphase onset [97, 115, 116]. The second portion is one in which tension across sister kinetochores is monitored [114, 117-119].

Throughout the early stages of mitosis unoccupied kinetochores produce a signal to inhibit the APC/C, thus delaying onset of anaphase [97, 99]. Preceding production of this inhibitory signal, during kinetochore assembly, Hec1 and Nuf2 members of the Ndc80 complex, function to recruit Mps1, Mad1, and Mad2 [115, 120]. Interestingly, Mps1 appears to be responsible for the localization of both Mad1 and Mad2; however, it is the kinase activity of Mps1 that is responsible for localization of Mad2 [121].

Localization of Mad2 to the kinetochore is dependent on the absence of microtubules [115], and activation of the SAC is dependent on the presence of Mad2 at

the kinetochore [122]. Both Mad1 and Mad2 localize to the kinetochore from prophase until metaphase, just prior to sister chromatid separation [123]. Mad2 [105, 124], BubR1, and Bub3 [125] were shown to form a complex with Cdc20. This protein complex, named mitotic checkpoint complex, or MCC, inhibits the ubiquitination ability of APC/C, thereby preventing degradation of securin [111]. Therefore, the MCC complex ensures well regulated control of the APC/C and contributes to the "wait anaphase" signal produced by kinetochores [97, 125].

Complementing the previously discussed attachment mechanism appears to be a more subtle tension sensing mechanism of the vertebrate SAC [114, 126, 127]. As chromosomes align at the metaphase plate, they accumulate a full complement of kinetochore microtubules. This results in the development of inter-kinetochore tension, visible as an increase in the distance between sister kinetochores. Lack of tension across sister kinetochores results in the accumulation of Bub1 and BubR1, but not Mad2, at the kinetochores [114]. This suggests that Bub1 and BubR1, but not Mad2, are involved in the branch of the SAC that senses tension across sister kinetochores. BubR1 has been shown to interact with CENP-E [127], and BubR1 kinase activity is dependent on the interaction with CENP-E. Kinetochores that are unattached promote CENP-E mediated activation of BubR1 kinase [127], and this BubR1 kinase activity causes a delay in progression through mitosis [127].

A link between the "attachment" and "tension" hypotheses is suggested by the fact that tension increases stability of microtubule attachment, and thus the number of attached microtubules, thus leading to kinetochore full occupancy by microtubules [128]. As the last kinetochore achieves microtubule attachment and becomes aligned at the

metaphase plate, the SAC is inactivated [97, 99] and the cell enters anaphase. Silencing of the checkpoint is thought to occur via two pathways: removal of kinetochore associated checkpoint proteins in a dynein-dependent manner [83, 129] and breakdown of the MCC complex [129]. The dynein/dynactin complex is an attractive mechanism for silencing the SAC upon microtubule attachment. During prometaphase, the dynein/dynactin complex localizes to unattached kinetochores along with Mad1, Mad2, and BubR1 [123, 130]. At metaphase, these proteins are depleted from kinetochores [130] and travel towards the minus end of kinetochore microtubules in a dynein-dependent manner [83]. The inhibition of dynein/dynactin impairs poleward movement of checkpoint proteins and effectively delays entry into anaphase through the maintenance of an active checkpoint [83]. For the MCC breakdown process, a key player was recently identified in $p31^{comet}$ [131]. $p31^{comet}$ promotes mitotic exit by inhibiting the "wait anaphase" signal produced at the kinetochore once complete kinetochore attachment and chromosome alignment have occurred [132, 133]. $p31^{comet}$ participates in the removal of checkpoint proteins from the MCC complex, thus reversing the inhibitory action exerted by the MCC on the APC/C complex [129]. These two methods for checkpoint inactivation most likely function together to allow for swift inactivation that coordinates organized segregation and exit from mitosis.

Kinetochore mis-attachments

Each vertebrate kinetochore can bind 20-40 kinetochore microtubules [49, 134]. For accurate chromosome segregation, the two sister kinetochores must bind microtubules from opposite spindle poles (amphitelic orientation; Figure 1.5A).

However, during kinetochore capture by the mitotic spindle microtubules, other types of attachment can form between kinetochores and microtubules. Namely, these attachments include: monotelic, syntelic, and merotelic attachments [12, 13].

Monotelic attachments are formed when growing microtubules from one spindle pole attach to one sister kinetochore, while the other sister kinetochore is devoid of microtubules (Figure 1.5B). Monotelic attachment results in the positioning of the mis-attached chromosome near the spindle pole to which it is attached (Figure 1.5B, left panel). Thus, progression through mitosis in the presence of monotelic chromosomes would inevitably result in the production of a trisomic daughter cell (three copies of the same chromosome) and a monosomic one (Figure 1.5B, right panel). However, this type of mis-attachment is an obligatory step in early mitosis, and the unattached kinetochore generates the "wait anaphase" signal that maintains the SAC active until amphitelic attachment is achieved [99]. Therefore, under unperturbed cellular conditions, monotelic attachment is an unlikely cause of chromosome mis-segregation.

Syntelic attachment occurs when both sister kinetochores bind microtubules from the same spindle pole (Figure 1.5C). Like monotelic chromosomes, syntelic chromosomes position close to the pole to which they are attached (Figure 1.5C, left panel), and progression into anaphase in the presence of this mis-attachment would result in the production of aneuploid daughter cells (Figure 1.5C, right panel). However, this type of mis-attachment is observed very rarely in unperturbed mammalian cells [135], suggesting that either syntelic attachment occurs at very low frequencies, or it is rapidly converted into a different type of kinetochore attachment. It is currently debated if syntelic kinetochore attachment can generate a SAC signal. However, it is possible that

lack of tension associated with syntelic attachment prevents kinetochore microtubules from attaining proper stabilization and does not allow achievement of full kinetochore occupancy by microtubules, thus activating the spindle assembly checkpoint [114, 119, 128].

Merotelic attachments are those in which one sister kinetochore binds microtubules from both spindle poles (Figure 1.5D) [12, 13]. This type of mis-attachment occurs frequently in early mitosis [136]. Furthermore, all microtubule binding sites of the kinetochore are occupied by microtubules and sufficient tension is generated between sister kinetochroes, thereby evading detection by the SAC [137-141]. However, an Aurora B-dependent mechanism can correct merotelic attachment before anaphase onset by promoting kinetochore microtubule turnover [142, 143], possibly through phosphorylation of the Ndc80 complex [76]. As opposed to monotelic and syntelic attachments, merotelic kinetochore attachment does not affect the ability of the chromosome to align at the metaphase plate (Figure 1.5D, left panel) [137, 138]. Because merotelic attachments are not detected by the SAC, cells can enter anaphase in the presence of merotelic kinetochores. When this happens, the normally attached sister moves poleward, whereas the behavior of the merotelic kinetochore and its chromatid (now a chromosome) depends on the specific ratio of microtubules to the two spindle poles. If the microtubule bundles attached to opposite poles are different in size (i.e., ratio $R>1$), the merotelic kinetochore will move towards the pole attached to the thicker bundle [138]. Conversely, if the two microtubule bundles are similar in size (i.e., ratio $R\sim1$), the merotelic kinetochore will induce an anaphase lagging chromosome [138], that is a chromosome that lags behind at the cell equator after anaphase onset (Figure 1.5D,

middle panel). Lagging chromosomes are found in ~1% untreated cultured mammalian cells [136, 137, 144, 145]. When the cytokinetic furrow ingresses, the lagging chromosome can be pushed on either side [137], thus producing aneuploid daughter cells ~50% of the time (Figure 1.5D, right panels). Whether the lagging chromosome ends up in the correct or incorrect daughter cell, it will form a micronucleus upon mitotic exit (Figure 1.5D, right panels) [137]. Interestingly, micronuclei are frequently found in cancer cells [146, 147], and recent evidence suggests that the presence of micronuclei in peripheral blood lymphocytes is predictive of increased risk of cancer in humans [148]. Because merotelic kinetochore attachment can evade the SAC, it represents a serious threat to the maintenance of a proper chromosome number [12, 13]and represents a major mechanism of aneuploidy in mammalian cells [145].

Aneuploidy and Cancer

Aneuploidy is a defining characteristic of cancer cells (Table 1.1) [13, 149, 150]. This feature, together with the propensity to mis-segregate chromosomes at high rates, is commonly referred to as *C*hromosomal *In*stability, or CIN. The CIN phenotype is often associated with the advanced stages of tumor development [151].

Certain CIN colorectal cancer cells harbor a frameshift mutation resulting from a deletion in the Bub1 gene essential for the fidelity of the SAC [152]. However, analysis of other CIN cancer cells revealed that mutations in SAC genes are not common [153-158] and most CIN cancer cells have a robust SAC [159, 160]. Because complete absence of fundamental components of the SAC results in cell death [161], a partial expression or function is a more likely scenario that will lead to aneuploidy. Indeed, a number of

studies in mice haploinsufficient for genes involved in SAC signaling [161-165] showed an increase in development of spontaneous [162, 164, 165] or chemically-induced [161, 163, 165] tumors.

Although much work has been aimed at establishing what exactly causes CIN, a unifying mechanism has not yet been identified. In an attempt to determine the order of events that lead to chromosomal instability and high levels of aneuploidy in cancer cells, two predominant hypotheses have emerged. The first postulates that aneuploidy represents an initial stage of cancer progression [149, 166, 167]. The second proposes the emergence of a polyploid intermediate before the onset of aneuploidy [168-172]. The polyploid cell would then be genetically unstable and would be prone to mis-segregate chromosomes, which would lead to the high degree of aneuploidy observed in cancer cells [170, 171]. It has been suggested that the polyploid intermediate could originate from cytokinesis failure [170, 171], a hypothesis that has been tested experimentally by Fujiwara and colleagues (2005), who inhibited cytokinesis in p53-null mouse cells and found that these cells underwent transformation [172]. Whereas this work suggests that polyploidy-induced malignant transformation requires the inactivation of p53, other studies found a p53-independent correlation between polyploidization and tumorigenesis [173, 174]. In support of the polyploidy hypothesis is also the observation that polyploidy is common in some pre-cancerous conditions such as Barrett's esophagus [168].

Nevertheless, it has been observed that polyploid cancer cells are rare, whereas cancer cells with 50-70 chromosomes are very common [13, 14, 149]. These data support the aneuploidy hypothesis, which proposes that the gain or loss of one or few chromosomes is a first step towards tumorigenesis. This hypothesis is also supported by

the haploinsufficiency studies described above [162-164], which showed a correlation between chromosome mis-segregation and tumorigenesis. It has been suggested that aneuploidy is the only mechanism that can result in a large enough change in gene expression that would contribute to the progression of cancer [169]. Specifically, a two-stage mechanism has been proposed to explain how aneuploidy might lead to cancerous transformation. First, cells undergo a chromosome mis-segregation event; this original mis-segregation event would then destabilize the karyotype and lead to further mis-segregation, increased aneuploidy, and eventually to the emergence pre-cancerous cells [169, 175]. Because the initial chromosome mis-segregation event could be induced by a defect in the mitotic apparatus, this hypothesis also explains how non-genotoxic compounds can induce transformation [176, 177]. The aneuploidy hypothesis also postulates that either a critical number of chromosome losses/gains or aneuploidy for specific chromosomes would be required for cancerous transformation to arise [178]. This would justify the length of time required for cancer development [175] and would also explain why under certain conditions, such as sex chromosome aneuploidy and some autosomal trisomies (e.g., trisomy 21), aneuploidy occurs without the appearance of cancer.

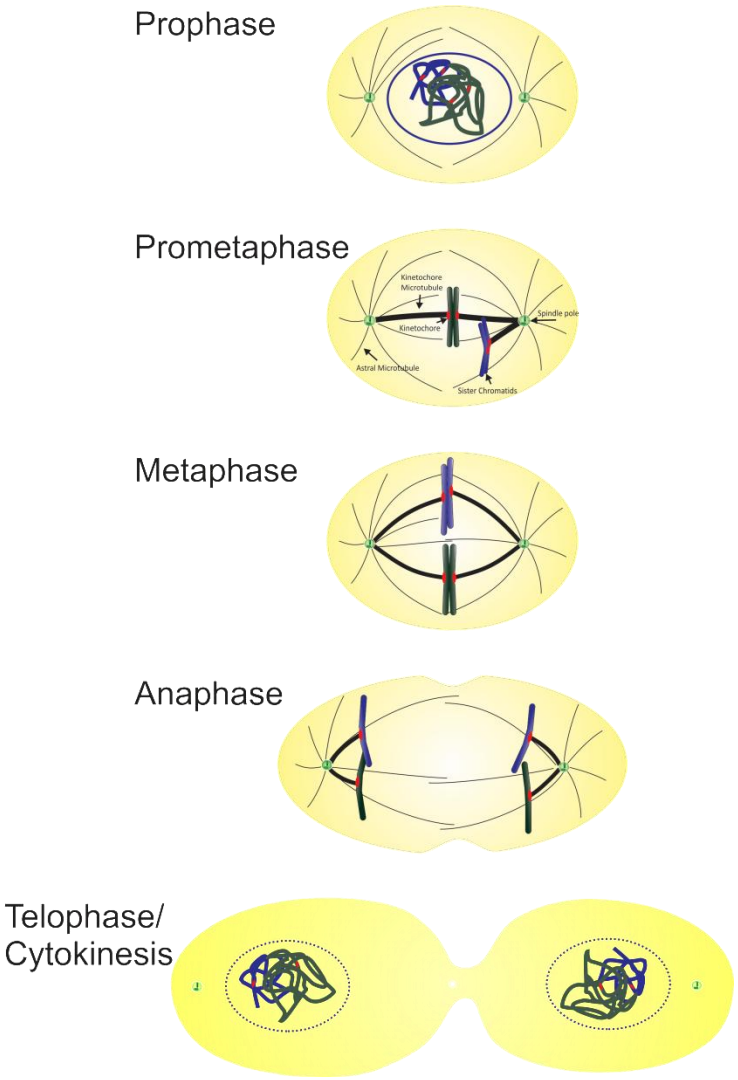

Figure 1.1: *Overview of M-Phase in a typical animal cell*. Cells begin mitosis in prophase where replicated chromosomes condense. Nuclear envelope breakdown marks the entrance into prometaphase, were kinetochores can bind to microtubules. Metaphase is when attached chromosomes align between the centrosomes at the spindle equator. During anaphase sister chromatids segregate and move to what will become two genetically identical daughter cells. Telophase occurs when the nuclear envelope begins to reform around the recently segregated chromosomes. The invagination of the plasma membrane marks cytokinesis, the cleavage of the mother cell into two independent daughter cells.

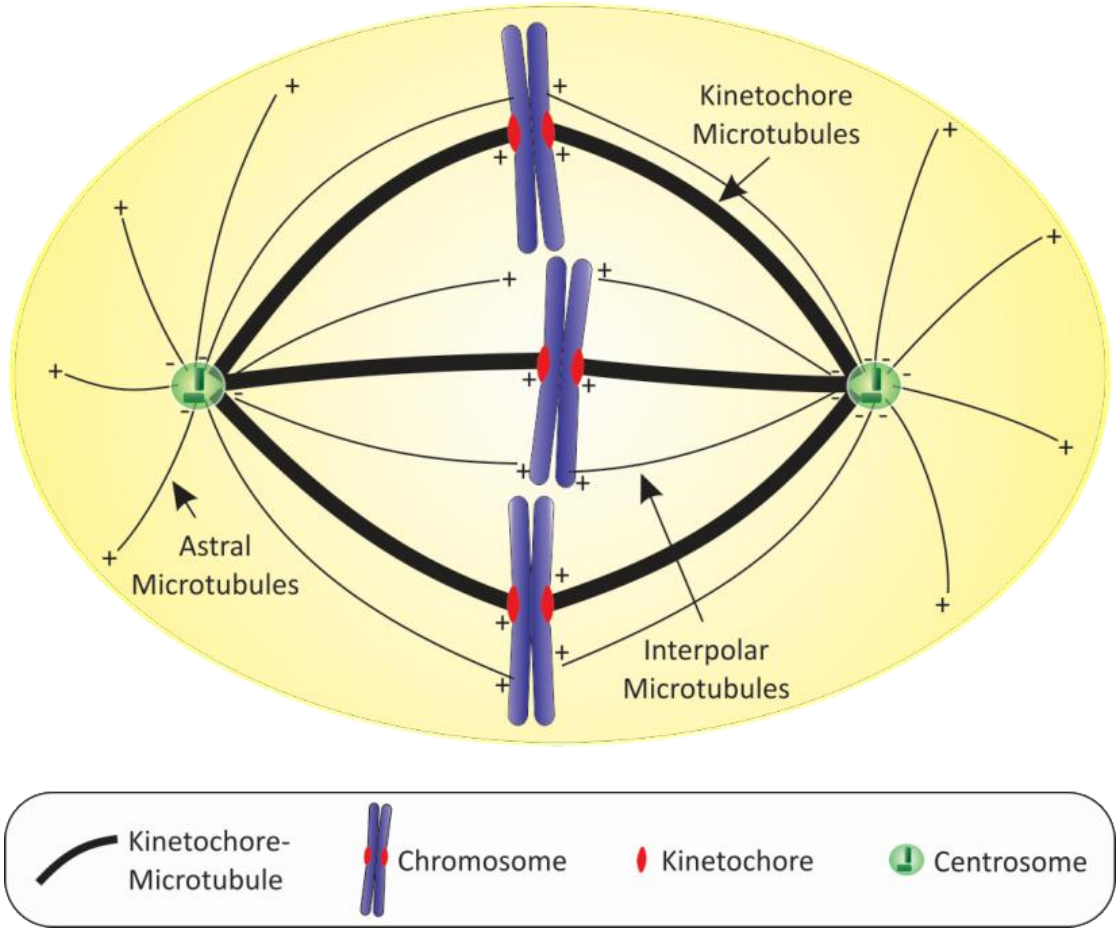

Figure 1.2: *Organization and components of the mitotic apparatus*. Diagram of major structural components of the mitotic spindle. Microtubules are shown in black. Given the inherent polarity of tubulin subunits, the pluses (+) indicate the β end while the minuses (-) represent the α end of tubulin subunits.

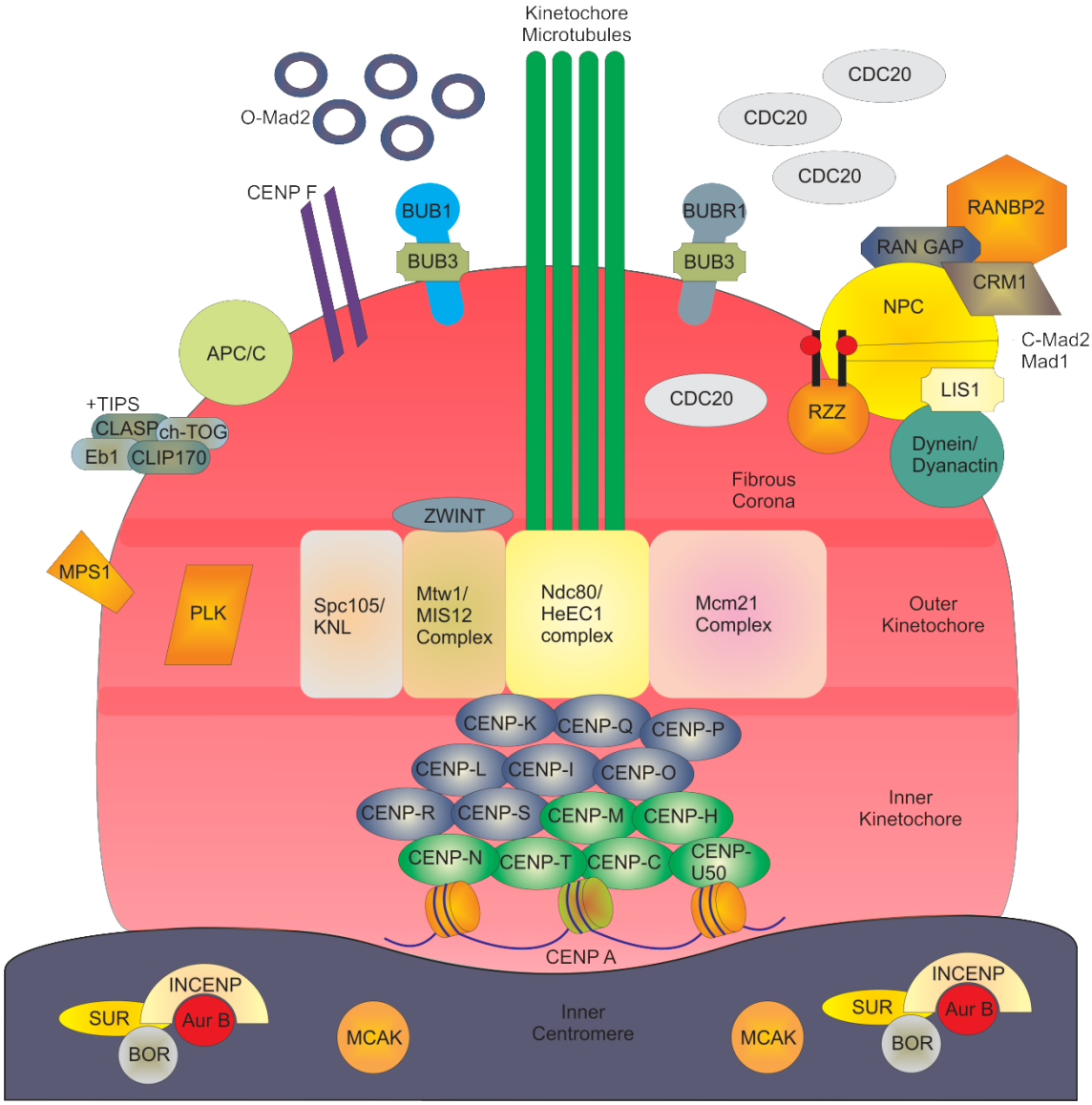

Figure 1.3: *Components of the vertebrate kinetochore*. A diagrammatic representation of the three major regions of the kinetochore: inner kinetochore, outer kinetochore, and fibrous corona. Within each region are the proteins that contribute to both the structure and function of the kinetochore.

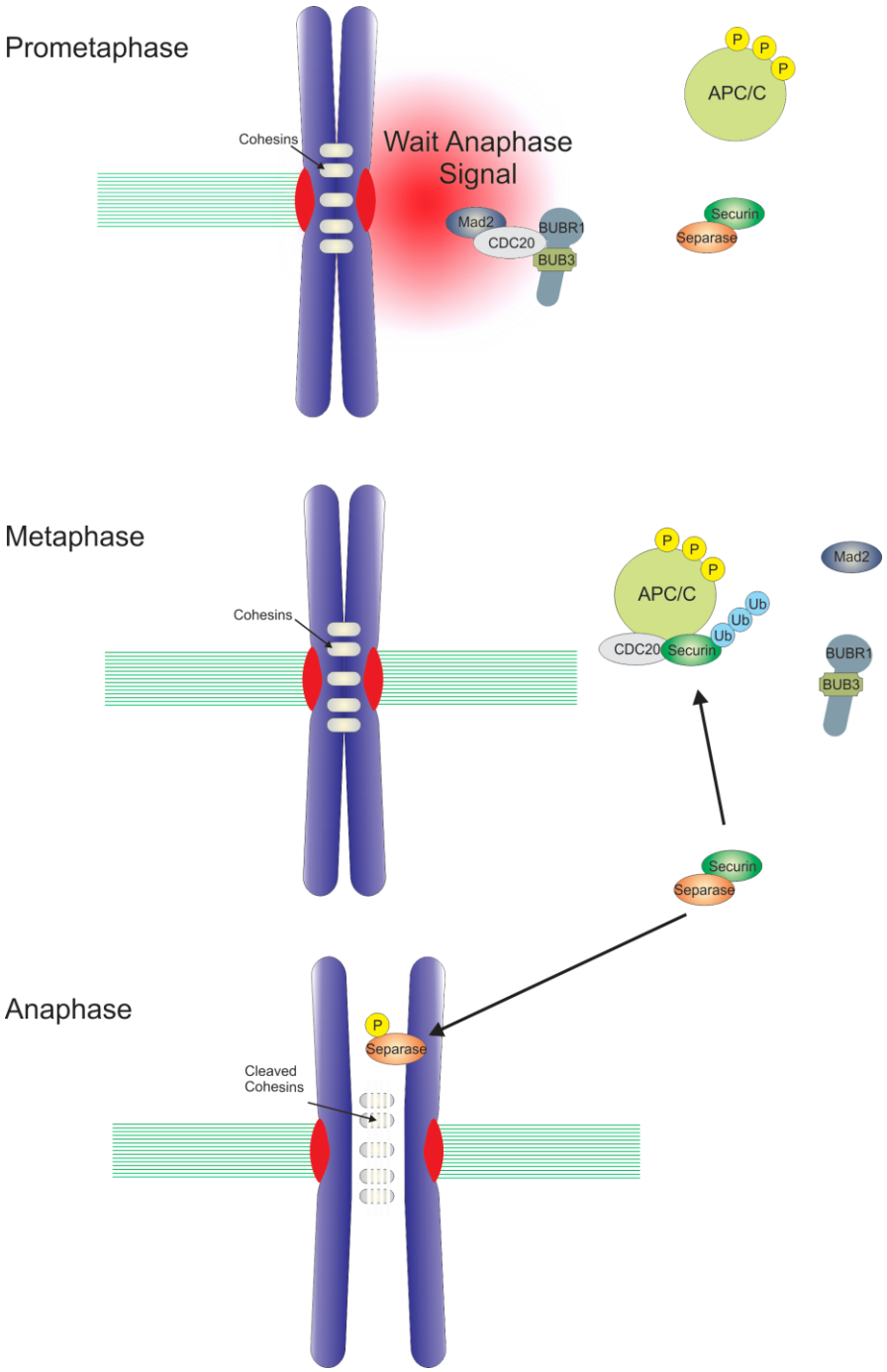

Figure 1.4: *The spindle assembly checkpoint*. Kinetochore-microtubule attachment silences the SAC and activates APC/C, which in turn activates separase through securin degradation. Separase activity cleaves the cohesion molecules that hold sister chromatids together. The outcome is progression into anaphase.

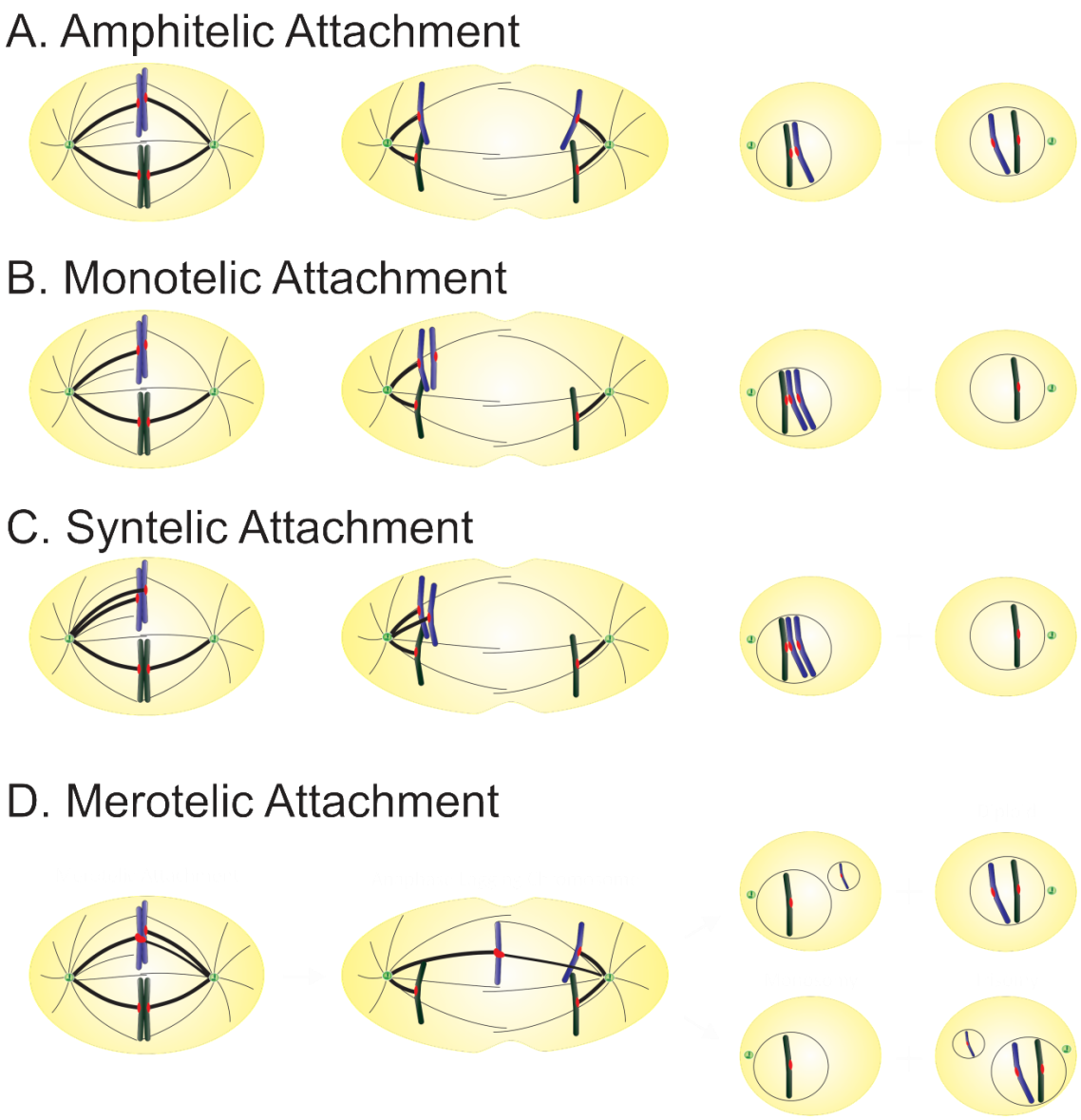

Figure 1.5: *The four types of kinetochore attachments that may form during mitosis*. Panels in the left column show kinetochore attachment and chromosome positioning in metaphase. Panels in the middle column show anaphase progression in the presence of different types of kinetochore attachment, without correction. Panels in the right column show the daughter cells produced by progression through mitosis in the presence of different types of kinetochore attachment.

Table 1.1. ***Aneuploidy in cancer cells from ten of the most commonly affected sites in humans.***

	Aneuploid cancers (Total)
Lung	413/435 (94.9%)
Colon	301/340 (88.5%)
Breast	598/800 (74.8%)
Prostate	151/186 (81.2%)
Stomach	167/180 (92.8%)
Liver	110/155 (71.0%)
Cervix uteri	75/84 (89.3%)
Corpus uteri	116/165 (70.3%)
Ovary	386/422 (91.5%)
Bladder	157/192 (81.8%)

Information assembled from: Mitelman Database of Chromosome Aberrations in Cancer. [150]

Chapter 2

Multipolar spindle pole coalescence is a major source of kinetochore mis-attachment and chromosome mis-segregation in cancer cells.

Silkworth WT, Nardi IK, Scholl LM, Cimini D.
PLoS One. 2009 Aug 10;4(8):e6564.

Author Contributions

Conceived and designed the experiments: WTS IKN DC. Performed the experiments: WTS IKN LMS. Analyzed the data: WTS IKN LMS DC. Contributed reagents/materials/analysis tools: DC. Wrote the paper: WTS DC

Abstract

Many cancer cells display a CIN (*C*hromosome *In*stability) phenotype, by which they exhibit high rates of chromosome loss or gain at each cell cycle. Over the years, a number of different mechanisms, including mitotic spindle multipolarity, cytokinesis failure, and merotelic kinetochore orientation, have been proposed as causes of CIN. However, a comprehensive theory of how CIN is perpetuated is still lacking. We used CIN colorectal cancer cells as a model system to investigate the possible cellular mechanism(s) underlying CIN. We found that CIN cells frequently assembled multipolar spindles in early mitosis. However, multipolar anaphase cells were very rare, and live-cell experiments showed that almost all CIN cells divided in a bipolar fashion. Moreover, fixed-cell analysis showed high frequencies of merotelically attached lagging chromosomes in bipolar anaphase CIN cells, and higher frequencies of merotelic attachments in multipolar vs. bipolar prometaphases. Finally, we found that multipolar CIN prometaphases typically possessed γ-tubulin at all spindle poles, and that a significant fraction of bipolar metaphase/early anaphase CIN cells possessed more than one centrosome at a single spindle pole. Taken together, our data suggest a model by which merotelic kinetochore attachments can easily be established in multipolar prometaphases. Most of these multipolar prometaphase cells would then bi-polarize before anaphase onset, and the residual merotelic attachments would produce chromosome mis-segregation due to anaphase lagging chromosomes. We propose this spindle pole coalescence mechanism as a major contributor to chromosome instability in cancer cells.

Introduction

Accurate mitotic chromosome segregation is necessary to maintain a diploid chromosome number. Most cancer cells are aneuploid [13, 14] and aneuploidy was suggested, already a century ago, to be a cause of cancer [15]. In addition to this aneuploid state, many cancer cells exhibit high rates of chromosome mis-segregation (i.e., gain or loss of whole chromosomes) at each cell cycle, a condition referred to as chromosome instability or CIN [179-181], which contributes to maintaining high levels of aneuploidy. A number of studies have tried to identify the defect(s) in mitotic chromosome segregation potentially responsible for CIN. Early studies suggested defects in the mitotic checkpoint as the main cause of CIN [152]. However, subsequent work has shown that most CIN cancer cells have a robust checkpoint [159] and their response to mitosis perturbing treatments is undistinguishable from the response of non-CIN cells [159, 160]. Cytokinesis failure has also been suggested in the past as a possible cause of CIN [182, 183]. However, cytokinesis failure would produce a single polyploid daughter cell, and could not explain CIN, which is defined as the mis-segregation of chromosomes at higher rates. As a result, CIN produces both high levels of aneuploidy and large variability in chromosome copy number within the population [179], whereas cytokinesis failure would simply result in a doubling of the chromosome number. Thus, cytokinesis failure *per se* cannot explain CIN, unless it is followed by other chromosome mis-segregation events in which single chromosomes (rather than the whole genome) are mis-segregated. Other studies suggested multipolarity as a potential cause of CIN [184-187] based on the observation that cancer cells from numerous sites (reviewed in [13]) frequently assemble multipolar spindles (usually accompanied by centrosome

amplification). Although multipolar chromosome segregation would certainly lead to extensive chromosome mis-segregation, a number of studies suggested that many of these multipolar cells might undergo a process of spindle pole coalescence/clustering [188, 189], which would prevent the massive chromosome mis-segregation that would be associated with multipolar chromosome segregation. It has been suggested that this spindle pole coalescence mechanism would confer a selective advantage to cells whose aneuploidy levels would otherwise be so severe to result in cell death [190, 191]. Finally, a number of studies have found high frequencies of anaphase lagging chromosomes (i.e., chromosomes that do not segregate to the spindle pole, but lag behind at the spindle equator during anaphase) in various cancer cells, including oral cancer cells [147, 192], human breast cancer cells [193, 194], ovarian carcinoma cells [195], and colorectal cancer cells [193]. One of these studies [193] also showed that the lagging chromosomes were merotelically oriented (i.e., their kinetochore was bound to microtubules from both spindle poles rather than just one). In summary, many alternative mechanisms of CIN have been proposed over the years; however, a comprehensive theory of how CIN is perpetuated is still lacking, and it is not clear if any correlation between some of these mechanisms exists.

In this study, we used CIN colorectal cancer cells as a model system to investigate the possible cellular mechanism(s) underlying CIN. We found that CIN cells frequently assembled multipolar spindles in early mitosis, but multipolar anaphases were very rare, and almost all CIN cells divided in a bipolar fashion. We also found that bipolar anaphase CIN cells exhibited high frequencies of merotelically attached lagging chromosomes. Moreover, a significant fraction of bipolar metaphase/early anaphase CIN cells possessed

more than one centrosome at a single spindle pole. Finally, we found high frequencies of merotelic attachments in multipolar prometaphases. Taken together, our data suggest a model by which merotelic kinetochore attachments can easily be established in multipolar prometaphases. Most of these cells would then bi-polarize before anaphase onset, and the residual merotelic attachments would produce chromosome mis-segregation due to anaphase lagging chromosomes. We propose this spindle pole coalescence mechanism as a major contributor to chromosome instability in cancer cells.

Materials and Methods

Cell lines and culture conditions.

All cell lines were obtained from the American Type Culture Collection. HCT116 and HT-29 cells were maintained in McCoy's 5A medium (Gibco), whereas SW620 cells were maintained in L-15 Medium (Gibco). All the media were supplemented with 10% fetal bovine serum, penicillin, streptomycin, and amphotericin B (antimycotic). All cell lines were grown in a 37^{o}C, 5% CO_2, humidified incubator. For experiments, cells were grown on sterile coverslips inside 35 mm Petri dishes.

Immunostaining.

Cells were rapidly rinsed in PBS, pre-fixed for 10 sec in 4% formaldehyde, permeabilized for 5 min in PHEM buffer containing 0.5% Triton X-100, and then fixed for 20 min in 4% formaldehyde. Subsequently, cells were washed in PBS, and then blocked in 10% boiled goat serum for 1 h at room temperature. The coverslips were then incubated overnight at 4°C in primary antibodies diluted in 5% boiled goat serum. Cells were finally washed in PBST (PBS with 0.05% Tween 20), incubated in secondary antibodies diluted in 5% boiled goat serum for 1 hour at room temperature, washed again, stained with DAPI, and mounted in an antifade solution containing 90% glycerol and 0.5% *N*-propyl gallate. For analysis of merotelic attachments in bipolar vs. multipolar cells, coverslips were first incubated in ice-cold medium (to disassemble non-kinetochore microtubules and preserve cold-stable kinetochore-microtubules) and kept at 4°C for 10 min; then they were processed as described above. Primary antibodies were diluted as follows: CREST (human anti-centromere protein, Antibodies Inc.), diluted 1:100; mouse

anti–α-tubulin (DM1A, Sigma-Aldrich), diluted 1:500; rabbit-anti-γ-tubulin (Abcam), diluted 1:100. Secondary antibodies were diluted as follows: X-Rhodamine goat-anti–human (Jackson ImmunoResearch Laboratories, Inc.), diluted 1:100; Alexa 488 goat-anti–mouse (Molecular Probes), diluted 1:400; Cy5-goat-anti-rabbit (Zymed Laboratories), diluted 1:100.

Confocal microscopy and image analysis.

Immunofluorescently stained cells were imaged with a Swept Field Confocal system (Prairie Technologies) on a Nikon Eclipse TE2000-U inverted microscope. The microscope was equipped with a 100X 1.4 NA Plan-Apochromatic phase–contrast objective lens, phase–contrast transillumination, transmitted light shutter, and automated ProScan stage (Prior Scientific). The confocal head was equipped with filters for illumination at 488, 568, and 647 nm from a 400 mW argon laser and a 150 mW krypton laser. Digital images were acquired with an HQ2 CCD camera (Photometrics). Image acquisition, shutter, Z-axis position, laser lines, and confocal system were all controlled by NIS Elements AR software (Nikon) on a PC computer. Z-series optical sections through each cell analyzed were obtained at 0.6 μm steps. Frequencies of multipolar prometaphases and anaphases, and anaphase lagging chromosomes were determined in 4 independent experiments, by viewing the samples via appropriate filter sets (Chroma Technologies). For experiments in which γ-tubulin staining was performed, each cell of interest was imaged as described above. For determination of the number of merotelic attachments in prometaphase cells, the acquired images were analyzed in multiple ways. First, both the kinetochore and microtubule images were processed through the "special

filtering" function of the NIS Elements AR software to increase the contrast. These two processed images were then merged and smoothed (using the "smooth" function of the NIS Elements AR software). Merotelically attached kinetochores were then identified by scrolling through the Z-axis to visualize kinetochores bound to microtubule bundles oriented in opposite directions. When a merotelic kinetochore was identified, a "ratio view" was also created for that specific focal plane. This view allowed the identification of regions of juxtaposition between a kinetochore and its microtubule bundle(s). All the differently processed views of the image were simultaneously analyzed and optical sections above and below were carefully examined to exclude all the cases in which a microtubule bundle ran past a kinetochore rather than ending on it.

Phase contrast live-cell imaging.

Coverslips at ~70% confluency were mounted into a Rose chamber [196] without top coverslip. The chamber was filled with L-15 medium with 4.5 g/L glucose, and mineral oil was added on top to prevent evaporation. Experiments were performed on a Nikon Eclipse TE2000-U inverted microscope equipped with phase–contrast transillumination, transmitted light shutter, ProScan automated stage (Prior Scientific), and HQ2 CCD camera (Photometrics). Cells were maintained at ~36°C by means of an air stream stage incubator (Nevtek). Images were acquired and analyzed through the NIS Elements AR software. Images of ten different fields of view were acquired at 30 sec intervals over a three-hour period with an ADL 20X 0.4 NA Achromatic phase-contrast objective. The time-lapse movies were subsequently analyzed to indentify cells undergoing mitosis during the period of recording. For each mitotic cell, complete

progression through mitosis, chromosome segregation phenotype (bipolar or multipolar), and cytokinesis completion were determined by simply playing the time-lapse movie and observing the cell undergoing mitosis. In addition, mitotic timing was measured (like in [197]) as the time elapsed between onset of cell rounding and anaphase onset.

Results

CIN colorectal cancer cells possess multipolar spindles in prometaphase, but not in anaphase.

Colorectal cancer cells can be divided in two groups [180, 198], those that exhibit CIN, and those that do not, traditionally named MIN because of their typical *M*icrosatellite *In*stability. Due to this characteristic, colorectal cancer cells represent a particularly interesting model for studying chromosome mis-segregation in cancer cells, because MIN cells can be used as an experimental control for CIN cells. For this study, we selected two CIN colorectal cancer cell lines (HT-29 and SW620) and one MIN colorectal cell line (HCT116). To identify mitotic defects potentially responsible for chromosome mis-segregation in CIN cells, we performed immunostaining experiments to label kinetochores (using CREST antibodies) and mitotic spindles (using anti-γ-tubulin antibodies) in CIN and MIN cells. We then used high-resolution confocal microscopy to identify prometaphase defects in both CIN and MIN cells (Figure 2.1). We found that the most prominent prometaphase defect in CIN cells was spindle multipolarity and that CIN prometaphase cells exhibited multipolar spindles (Figure 2.1A) at frequencies that were significantly higher than those found in MIN cells (Figure 2.1B). Most of the multipolar spindles exhibited a tripolar or tetrapolar morphology, although multipolar cells with 5-8 spindle poles (5.4%, 19.5%, and 7.9% of all multipolar HCT116, HT-29, and SW620, respectively) were also observed. We then looked at multipolarity in anaphase cells, and found that the frequencies of multipolar spindles in anaphase CIN cells were much lower than those found in prometaphase (Figure 2.1B). In addition, there was no difference between MIN and CIN cells in the frequency of multipolar anaphases (Figure 2.1B).

Both CIN and MIN cells divide in a bipolar fashion, but mitosis lasts longer in CIN cells.

The low frequencies of multipolar spindles in anaphase CIN cells suggested that multipolar prometaphases might not complete a multipolar division, but might instead encounter different fates. Some possibilities include mitotic arrest, mitotic cell death, or mitotic slippage. To determine the possible fate(s) of mitotic CIN cancer cells, we performed time-lapse experiments. In each experiment, multiple fields of view were selected and imaged by phase-contrast microscopy with a 20X objective on an inverted microscope equipped with a fully automated stage. Images were acquired every 30 sec for three hours. The time-lapse movies were subsequently analyzed to determine duration of mitosis and fate of cells entering mitosis during the period of recording. As expected from our fixed-cell data (Fig. 2.1B), we rarely observed chromosome segregation to occur in a multipolar fashion (Figure 2.2A). In most cells, chromosomes segregated into two groups at opposite sides of the cell, and one single cytokinetic furrow formed between them (data not shown). The number of cells exhibiting multipolar chromosome segregation in our live-cell experiments (Figure 2.2A) was not significantly different (χ^2, $P>0.37$ for all three cell lines) from the number of multipolar anaphase cells we found in fixed cell experiments (Figure 2.1B). In addition, we found that 40-67% of the CIN cells exhibiting multipolar chromosome segregation failed to complete cytokinesis (Figure 2.2A), whereas there were no cases of cytokinesis failure in cells exhibiting bipolar chromosome segregation. Finally, we did not find any indication of persistent mitotic arrest, cell death during mitosis, or mitotic slippage. These data indicate that most of the chromosome instability in CIN cells must derive from chromosome segregation defects

in cells dividing in a bipolar fashion and completing cell division. Our live-cell experiments also revealed that the time spent in mitosis, measured as the time elapsed from onset of cell rounding to anaphase onset, was significantly longer in CIN cells compared to MIN cells (Table 2.1), similarly to what others have found in other cancer cell lines [199].

Bipolar anaphase CIN cells exhibit high frequencies of merotelically attached lagging chromosomes.

As described above, multipolarity was common in CIN prometaphase cells, but it was rarely observed in anaphase (Figure 2.1B), and most CIN cells segregated their chromosomes in a bipolar fashion (Figure 2.2A). This indicated that multipolar chromosome segregation is an unlikely cause of chromosome instability in CIN cells, and suggested that errors occurring during bipolar chromosome segregation were the most likely cause of CIN. To identify such potential defects, we used high-resolution confocal microscopy to analyze anaphase cells with immunostained kinetochores and microtubules (Figure 2.2C). We found that bipolar CIN anaphase cells possessed merotelically attached lagging chromosomes (i.e., chromosomes that lagged behind at the spindle equator instead of segregating to the spindle pole, and whose kinetochore was bound to microtubule bundles from both spindle poles rather than just one; Figure 2.2C, right column) at higher frequencies than MIN cells (Figure 2.2B). Interestingly, the frequencies of anaphase cells with lagging chromosomes were very similar to the frequencies of multipolar prometaphase cells (compare Figure 2.1B with Figure 2.2B).

Both multipolar and bipolar CIN cells possess multiple centrosomes.

The low frequencies of multipolar anaphases compared to those of multipolar prometaphases (Figure 2.1B) and the bipolar chromosome segregation observed in live cells (Figure 2.2A) suggested that most of the multipolar spindles might bipolarize before anaphase onset. To test this hypothesis, we performed γ-tubulin staining in combination with microtubule and kinetochore immunostaining on CIN cells at different stages of mitosis (Figure 2.3A-B). High-resolution confocal microscopy revealed that in prometaphase CIN cells, γ-tubulin staining was present at all spindle poles in over 95% of the cells (Figure 2.3A). Next, we looked at bipolar metaphase/early anaphase cells (Figure 2.3B) and found that a significant number of cells exhibited multiple γ-tubulin-positive dots at a single spindle pole (Figure 2.3B-C), suggesting that some of the spindle poles present in multipolar prometaphase cells might move close together at later mitotic stages to generate two focused spindle poles, and hence a bipolar spindle. It should be noted that the observed frequencies (6.8% and 10.5% for HT-29 and SW620, respectively) could underestimate the actual number of spindle poles undergoing this coalescence process, as some of them might move so close to each other to appear as one by γ-tubulin staining.

Higher frequencies of merotelic attachments in multipolar vs. bipolar prometaphase CIN cells.

The multiple γ-tubulin signals at spindle poles of bipolar metaphase CIN cells, together with the occurrence of lagging chromosomes in bipolar anaphases at frequencies that closely resemble the frequencies of multipolar prometaphases, suggested that

merotelic attachments might be preferentially formed in multipolar prometaphase cells that subsequently bi-polarize by spindle pole coalescence. To test this hypothesis, we used high-resolution confocal microscopy combined with 3-D visualization and image processing (see Materials and Methods for details) to identify merotelic kinetochores in cold-treated prometaphase CIN cells immunostained for kinetochores and microtubules (Figure 2.4A-D). Cold treatment induced non-kinetochore microtubule disassembly, but preserve kinetochore microtubules. We determined the number of merotelic kinetochores in bipolar vs. multipolar prometaphase CIN cells by identifying all the kinetochores bound to two microtubule bundles oriented in opposite directions, and found that multipolar prometaphase cells possessed significantly higher numbers of merotelic attachments than bipolar prometaphase cells (Figure 2.4E), suggesting merotelic attachments in such multipolar prometaphases as a major source of lagging chromosomes in bipolar anaphase cells.

Discussion

Cytokinesis failure does not contribute to CIN.

Cytokinesis failure has been suggested in the past as a mechanism responsible for aneuploidy in cancer cells [182, 183]. Indeed, a number of studies have shown that polyploidy induced by experimentally inhibiting cytokinesis, can lead to malignant transformation and tumorigenesis [172, 200]. However, as pointed out in the introduction, cytokinesis failure *per se* would not be sufficient to explain CIN, i.e. high chromosome mis-segregation rates. Nevertheless, cytokinesis failure might be a contributing factor for CIN, thus we determined the frequency of cytokinesis failure both in cells exhibiting bipolar chromosome segregation and in cells with tripolar chromosome segregation. We never observed cytokinesis failure in cells undergoing bipolar cell division, and this phenomenon only occurred in about half of the cells undergoing multipolar cell division (Figure 2.2A). Because very few cells exhibit multipolar chromosome segregation, the observed rates of cytokinesis failure represent a very rare event in the overall cell population. Thus, cytokinesis failure fails to explain both the high rates of chromosome mis-segregation observed in CIN cells [179, 180] and the high rates of lagging chromosomes found in cancer cells [147, 192-195] (Figure 2.2B). In conclusion, although cytokinesis failure could represent a rare, early event in tumor development [172, 200], it does not seem to contribute significantly to CIN in cancer cells at later stages of tumor progression.

Multipolarity and multipolar chromosome segregation in CIN cancer cells.

Many cancer cells have been previously shown to exhibit centrosome amplification [184, 187, 201, 202], and mitotic spindle multipolarity has been observed in cancer cells from various sites [13, 147, 184, 187, 192, 195, 201-206]. It has been suggested that multipolar chromosome segregation would produce largely aneuploid daughter cells, which would most likely not survive subsequent cell cycles [190, 191]. Indeed, our live-cell experiments showed that multipolar cell division is a rare event in CIN cells (Figure 2.2A). In addition, a recent study showed that multipolar cell division in CIN cells results in either cell death or cell cycle arrest [207]. It was previously suggested that multipolar cancer cells can undergo a bipolarization process, which would occur via centrosome clustering, and would lead to bipolar chromosome segregation [188-190]. Recent studies have shown that multiple players can be involved in promoting centrosome clustering (reviewed in [208]). These include actin-associated mechanisms [188], dynein [189], kinesin 14s (Ncd/HSET) [188, 209], and maybe other proteins/mechanisms [188, 208, 209]. Recent studies [188, 199, 209] have also suggested a possible role of the spindle assembly checkpoint in allowing time for spindle bipolarization in multipolar cells, as Mad2 inhibition prevented spindle bipolarization [188, 209] and accelerated mitotic exit in multipolar cells [199]. In agreement with these studies, we find that cells with higher frequencies of multipolar spindles spend, on average, longer times in mitosis (Table 2.1). However, Mad2 inhibition accelerates mitosis exit regardless of spindle pole number and kinetochore attachment [136, 210, 211], so its effect on multipolar spindle bi-polarization might simply be a secondary effect. We also found that multipolar cells possess higher numbers of merotelic

kinetochores, but because merotelic attachments are not detected by the spindle assembly checkpoint (reviewed in [13]), this seems unlikely to be the reason for the mitotic delay. On the other hand, CIN cancer cells have excessive chromosome numbers, so it is easy to imagine that achieving stable attachments for all chromosomes will take longer in such cells compared to bipolar diploid cells. Yang et al. [199] recently showed that experimentally generated multipolar diploid RPE1 cells take twice as long to enter anaphase compared to their bipolar counterparts, suggesting that the increase in centrosome number might be enough to delay anaphase onset. The authors suggested that the presence of multiple microtubule asters might perturb the stability of kinetochore attachments [199], thus leading to an increase in the time necessary to complete kinetochore attachment, and consequently lengthening mitosis. This is an intriguing possibility, which will need to be tested in future experiments.

In conclusion, how extra centrosomes delay anaphase onset is still unclear, but studies such as the one performed by Yang and colleagues [199] suggest that both the extra chromosomes and the extra centrosomes in CIN cancer cells might contribute to the increase in average time spent in mitosis, during which the multipolar cells bipolarize via spindle pole coalescence. The centrosome clustering associated with spindle bi-polarization was previously suggested to confer cancer cells with a selective advantage that would prevent massive chromosome mis-segregation and allow cancer cells to keep dividing even in the presence of extra centrosomes [190, 191]. Thus, previous studies proposed such spindle pole coalescence process as a mechanism to prevent erroneous chromosome segregation. Conversely, we propose here that multipolar spindle assembly followed by spindle pole coalescence represents a major mechanism of chromosome mis-

segregation in CIN cancer cells (see next section for a detailed description of our proposed model).

Cancer cell multipolarity and merotelic kinetochore attachment: two sides of the same coin.

The low number of multipolar anaphases compared to multipolar prometaphases (Figure 2.1B), the low number of multipolar cell divisions (Figure 2.2A), and the presence of multiple γ-tubulin-positive signals at single spindle poles in metaphase/early anaphase CIN cells (Figure 2.3B-C), suggest that most of the multipolar prometaphases undergo a process of spindle pole coalescence before anaphase onset, as previously suggested [188-191].

We propose that when CIN cancer cells initially assemble multipolar spindles, single kinetochores are more likely than they would be within a bipolar spindle to face (Figure 2.5A), and become attached to (Figure 2.5B), two spindle poles (merotelic attachment). Thus, multipolar prometaphase cells would be expected to possess more merotelic attachments compared to bipolar prometaphases. Indeed, we found multipolar prometaphase cells to possess more merotelic kinetochores compared to bipolar prometaphases (Figure 2.4). As described above, multipolar spindles likely bipolarize via a spindle pole coalescence process (Figure 2.5B-C) before anaphase onset. Although correction mechanisms for merotelic kinetochore attachment exist [136, 142, 212], this kinetochore mis-attachment is not detected by the mitotic checkpoint [137, 138], and cells can enter anaphase before achieving complete correction [136, 138]. Because cells that transiently assemble multipolar spindles would start off with more merotelic

attachments compared to bipolar cells (Figure 2.4 and 2.5B), more of such mis-attachments are expected to persist through anaphase and produce lagging chromosomes (i.e., chromosomes that lag behind at the spindle equator rather than segregating to the spindle pole; Figure 2.5D), and hence chromosome mis-segregation and aneuploidy. Remarkably, we also found that the frequencies of anaphase cells with merotelically oriented lagging chromosomes were very similar to the frequencies of multipolar prometaphase cells (compare Figure 2.1B and Figure 2.2B), suggesting the intriguing possibility that most lagging chromosomes are found in those cells that initially assemble multipolar spindles. In summary, whereas spindle multipolarity and anaphase lagging chromosomes had been previously suggested as unrelated causes of CIN, we show here for the first time that large numbers of merotelic kinetochores form in multipolar prometaphase cells, thus unveiling the close connection between multipolarity and anaphase lagging chromosomes.

We should note that, although at much lower frequencies than in CIN cells, we found both multipolar prometaphase spindles (Figure 2.1) and anaphase lagging chromosomes (Figure 2.2B-C) in HCT116 (MIN) cells. Nevertheless, these cells have been previously shown not to exhibit CIN [179, 193], and they were shown not to tolerate experimentally-induced chromosome mis-segregation [193], suggesting that CIN must result from a combination of high chromosome mis-segregation rates (not observed in HCT116 cells) and some other phenotypic feature that makes the cells tolerant for aneuploidy [193].

Future experiments should be aimed at testing our model and its prediction that inhibition of spindle pole coalescence should result in lower frequencies of lagging

chromosomes in bipolar anaphase cells. Time-lapse imaging of cells with labeled kinetochores and microtubules would confirm the sequence of events proposed here (Figure 2.5) if merotelically attached anaphase lagging chromosomes were observed more frequently in cells starting mitosis with multipolar spindles compared to cells starting out with bipolar spindles. Moreover, spindle pole clustering could be inhibited to uncouple spindle multipolarity from anaphase lagging chromosomes, and thus demonstrate the causal relationship between these two phenomena. For instance, by performing a genome-wide RNAi screen in Drosophila S2 cells, Kwon et al. [188] found many different genes implicated in a variety of cellular processes, including spindle pole organization, cell shape and polarity, and cell adhesion, to be involved in centrosome clustering. According to our model, silencing of these genes in CIN cells should result in reduced frequencies of lagging chromosomes in bipolar anaphases, and future experiments should be aimed at testing this hypothesis. Although the reverse experiment (i.e., reducing merotelic attachment in multipolar cells) would be much more challenging, some experiments could provide indirect evidence that reducing merotelic attachment would result in a reduction in anaphase lagging chromosomes in cells that transiently assemble a multipolar spindle. For example, anaphase onset could be delayed by treatment of multipolar cells with a proteasome inhibitor. During the time of proteasome inhibition, the multipolar spindles are expected to bi-polarize, and the merotelic attachments are expected to be corrected. Thus, upon washout of the inhibitor, the cells should enter anaphase and exhibit low frequencies of lagging chromosomes.

Does any other mechanism contribute to CIN?

We do not rule out that other mechanisms might contribute to chromosome instability in cancer cells. For instance, recent studies suggested that the mechanisms of merotelic kinetochore correction are not very efficient in CIN cancer cells [160, 213]. This means that CIN cells would exhibit slower kinetochore-microtubule turnover (required for correction of mis-attachments [142]) compared to MIN (or other chromosomally stable) cells. However, accurate comparison of microtubule dynamics in CIN vs. MIN (or other chromosomally stable) cells has not been performed. Even if such reduced correction efficiency were confirmed, however, it would simply add up to the increased number of kinetochore mis-attachments in cells that start mitosis with multipolar spindles (Figures 2.4 and 2.5). Moreover, there could be additional, as yet unidentified, mechanisms contributing to formation of large numbers of mis-attached kinetochores in CIN cancer cells. However, whether additional mechanisms exist or not, the mechanism described in this study could explain a large fraction of the chromosome mis-segregation occurring in CIN cancer cells.

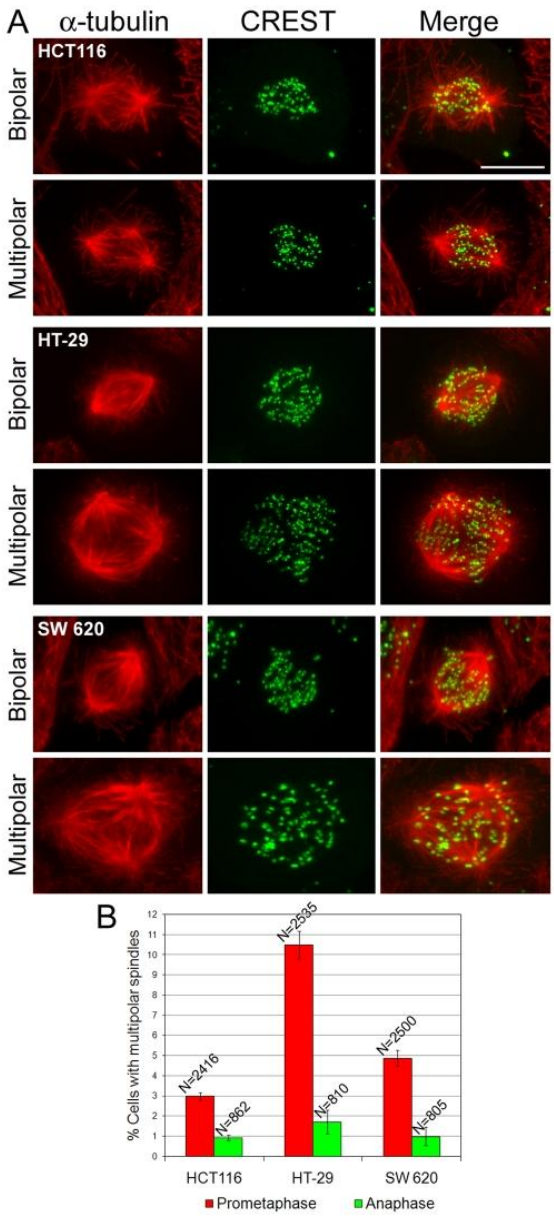

Figure 2.1. *CIN cells frequently assemble multipolar spindles in early mitosis*. A. Examples of MIN (HCT116) and CIN (HT-29, SW620) prometaphase cells immunostained for α-tubulin (red, left column) and kinetochores (green, middle column). All the images are maximum intensity projections of stacks of optical sections acquired at 0.6 μm intervals through the cell Z-axis. Merged images are shown in the right column. For each cell line, an example of bipolar prometaphase and one of multipolar prometaphase are shown. Scale bar, 5 μm. B. Frequencies of prometaphase and anaphase cells with multipolar spindles. The data shown here represent means and standard errors (bars) of four independent experiments. Multipolar CIN prometaphases were significantly more frequent than multipolar MIN prometaphases (χ^2 test, $P<0.001$ for both HT-29 and SW620 when compared to HCT116). However, multipolar CIN anaphases occurred at low frequencies that did not differ from those of multipolar MIN anaphases.

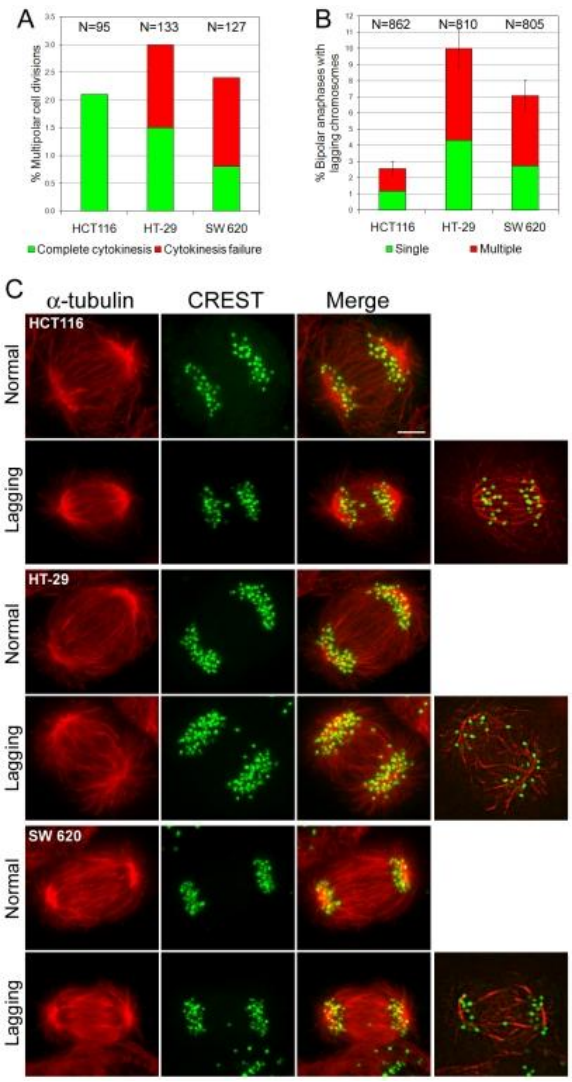

Figure 2.2. *Most CIN cells divide in a bipolar fashion, but exhibit lagging chromosomes in anaphase.* A. Frequencies of cells exhibiting multipolar chromosome segregation in phase-contrast time-lapse experiments. B. Frequencies of bipolar anaphase MIN (HCT116) and CIN (HT-29, SW620) cells with lagging chromosomes. The data shown here represent means and standard errors (bars) of four independent experiments. Frequencies of anaphase lagging chromosomes were significantly higher in CIN than MIN cells (χ^2 test, $P<0.001$ for both HT-29 and SW620 when compared to HCT116). C. Examples of MIN (HCT116) and CIN (HT-29, SW620) anaphase cells immunostained for α-tubulin (red, first column) and kinetochores (green, second column). The images are maximum intensity projections of stacks of optical sections acquired at 0.6 μm intervals through the cell Z-axis. Merged images are shown in the third column. For each cell line, an example of normal anaphase and an anaphase with a lagging chromosome are shown. The column at the far right shows the cells with lagging chromosomes at a single focal plane, in which the contrast has been enhanced to highlight the merotelic connections of the lagging chromosome kinetochore. Scale bar, 5 μm.

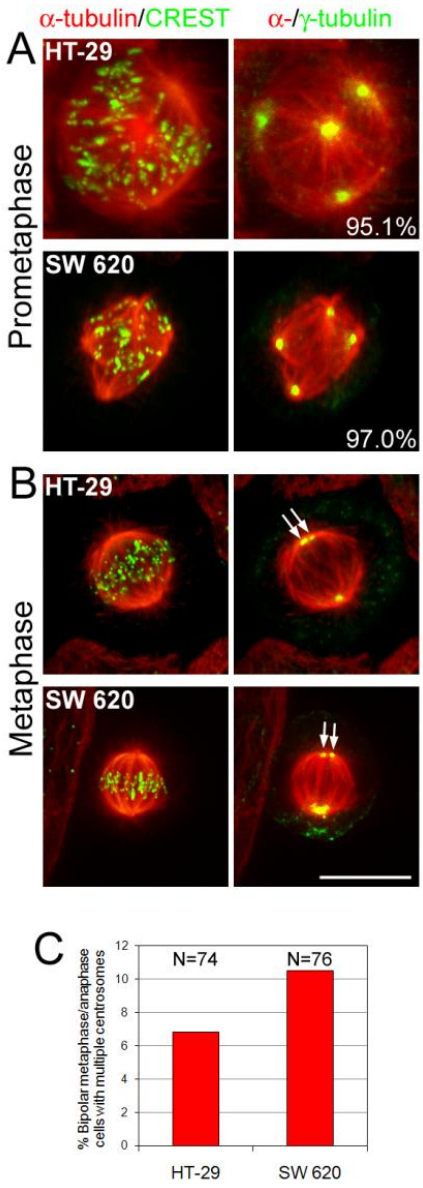

Figure 2.3. *Both multipolar prometaphase and bipolar metaphase CIN cells possess multiple centrosomes.* The figure shows examples of multipolar prometaphase (A) and bipolar metaphase (B) CIN cells immunostained for α-tubulin, kinetochores, and γ-tubulin. Images shown were obtained by merging maximum intensity projections of either α-tubulin and CREST (kinetochores) images (left column) or α-tubulin and γ-tubulin images (right column). A. Most multipolar prometaphase cells (exact percentages shown at the bottom right corner of the right panels) exhibited γ-tubulin staining at all spindle poles. B. Examples of bipolar metaphase CIN cells with multiple centrosomes at a single spindle pole (arrows point at γ-tubulin-stained dots). Scale bar, 5 μm. C. Frequencies of bipolar metaphase/early anaphase CIN cells possessing multiple centrosomes (as visualized by γ-tubulin staining) at a single spindle pole.

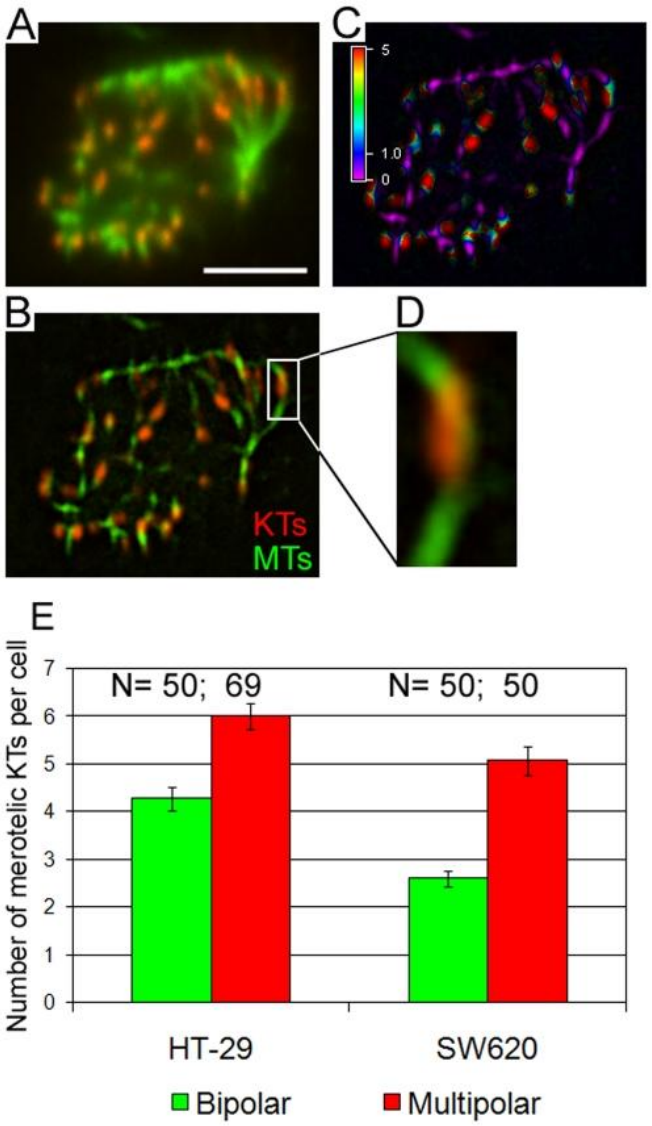

Figure 2.4. *Multipolar prometaphase CIN cells possess larger numbers of merotelic kinetochores than bipolar prometaphase CIN cells.* A. Single focal plane of an unprocessed HT-29 multipolar prometaphase. Scale bar, 2.5 μm. B. Same cell and same focal plane as in (A) obtained after processing of the images in the two channels by special filtering, merging, and smoothing (see Materials and Methods for details). A merotelic kinetochore is visible in the boxed area. KTs: kinetochores. MTs: microtubules. C. Ratio view of the focal plane shown in (A) and (B). Regions of juxtaposition between the kinetochore and its microtubule bundle(s) appear in green. D. Enlargement (400%) of the boxed area in (B). E. Average number of merotelic kinetochores in bipolar vs. multipolar prometaphase CIN cells. Multipolar prometaphases possess significantly more merotelic kinetochores than bipolar prometaphases (t-test, $P<0.001$ for both cell lines).

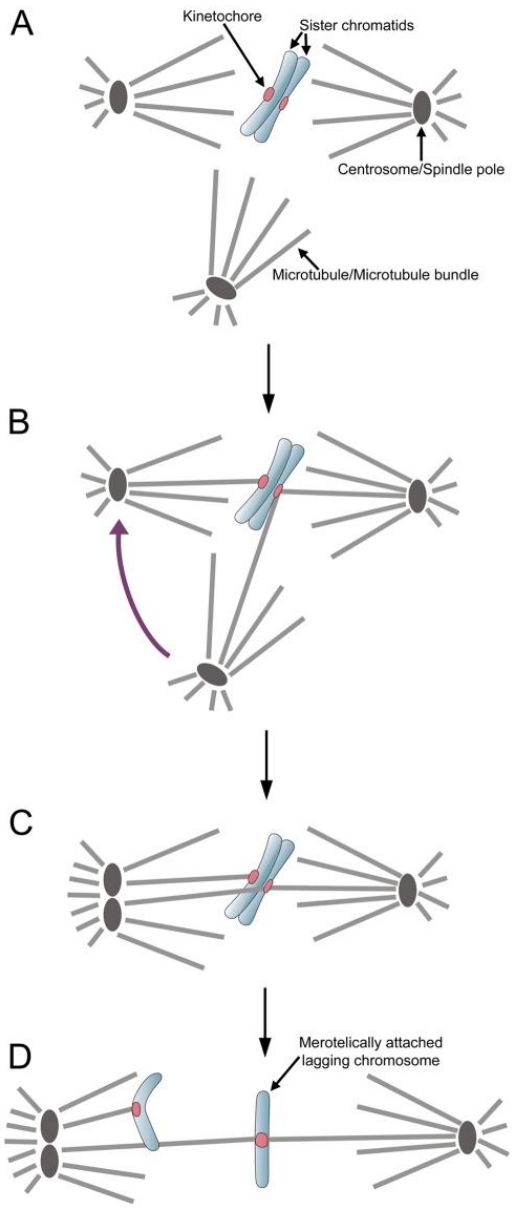

Figure 2.5. *Schematic representation of the mechanism by which multipolarity can lead to merotelic kinetochore attachment and mitotic chromosome mis-segregation.* A. Within a multipolar spindle, a single kinetochore is more likely to face two spindle poles than it would be in a bipolar spindle. B. Because of the multipolar spindle geometry, a single kinetochore can easily bind microtubules emanating from two spindle poles rather than from just one pole. After establishment of merotelic kinetochore attachment, the mitotic spindle bi-polarizes by a process of spindle pole coalescence (or centrosome clustering). C. Merotelic kinetochore attachment can persist through metaphase and into anaphase. D. During anaphase, the merotelic kinetochore attachment can give rise to a lagging chromosome.

Table 2.1. ***Duration of mitosis measured as time elapsed from onset of cell rounding to anaphase onset.***

Cell line	Cell rounding – anaphase onset (Mean±S.D.)	N
HCT 116	23.29±6.34 min	135
HT-29	30.74±8.90 min*	135
SW 620	64.24±29.8 min*	135

***t-test, P,0.001, when compared to HCT116**

Chapter 3

Timing of centrosome separation is important for accurate chromosome segregation.

Silkworth WT, Nardi IK, Paul R, Mogilner A, Cimini D.
Mol Biol Cell. 2012 Feb;23(3):401-11.

Author Contributions

Conceived and designed the experiments: WTS IKN DC. Performed the experiments: WTS IKN. Analyzed the data: WTS IKN DC. Contributed reagents/materials/analysis tools: AM DC. Development of the computational model: WTS RP AM DC. Performed computational simulations: RP AM. Wrote the paper: WTS AM DC

Abstract

Spindle assembly, establishment of kinetochore attachment, and sister chromatid separation must occur during mitosis in a highly coordinated fashion to ensure accurate chromosome segregation. In most vertebrate cells, the nuclear envelope must break down to allow interaction between microtubules of the mitotic spindle and the kinetochores. It has been previously shown that nuclear envelope breakdown (NEB) is not coordinated with centrosome separation, and that centrosome separation can be either complete at the time of NEB or can be completed after NEB. In this study, we investigated whether the timing of centrosome separation will affect subsequent mitotic events such as establishment of kinetochore attachment or chromosome segregation. We used a combination of experimental and computational approaches to investigate kinetochore attachment and chromosome segregation in cells with complete vs. incomplete spindle pole separation at NEB. We found that cells with incomplete spindle pole separation exhibit higher rates of kinetochore mis-attachments and chromosome mis-segregation compared to cells that complete centrosome separation before NEB. Moreover, our mathematical model showed that two spindle poles in close proximity do not "search" the entire cellular space, leading to formation of large numbers of syntelic attachments, which can be an intermediate stage in the formation of merotelic kinetochores.

Introduction

Accurate chromosome segregation during mitosis is critical to maintain genome stability and prevent aneuploidy. To this aim, assembly of the mitotic spindle must be coordinated with establishment of kinetochore (KT) attachment. The microtubules (MTs) of a bipolar mitotic spindle must interact with the chromosomes so that the two sister KTs on each chromosome interact with opposite spindle poles. This configuration will allow the two sister chromatids to be pulled to opposite ends of the cell upon sister chromatid separation, thus leading to the formation of two daughter cells with the correct chromosome number.

In most higher eukaryote cells interaction between spindle MTs and chromosomes is only possible after nuclear envelope breakdown (NEB). In fact, the nuclear envelope disassembles in early mitosis, and it is only after NEB that the MTs emanating from the centrosomes (spindle poles) can interact with the KTs. It has been known for many years that centrosome separation is not coordinated with NEB [214, 215]. Indeed, in several different cell types centrosome separation is completed before NEB in about 50% of mitotic cells within the same cell population, whereas in the other 50% centrosome separation is completed after NEB [215-220]. Several studies have shown that both the pre-NEB centrosome separation, referred to as the prophase pathway, and the post-NEB centrosome separation, referred to as the prometaphase pathway, rely on Eg5-dependent MT sliding [221-226]. However, other mechanisms are specific to each of the two pathways [reviewed in [221, 224]]. A major mechanism of prophase centrosome separation involves the interaction between astral MTs and the nuclear envelope, possibly

mediated by dynein [221, 224, 227, 228], whereas centrosome separation during prometaphase requires myosin activity at the cell cortex [217, 221, 224].

Whereas many studies have focused on identifying the molecules and mechanisms required for centrosome separation during these two mitotic stages, it is not known whether incomplete spindle pole separation at NEB will affect subsequent mitotic events such as establishment of KT attachment or chromosome segregation. When centrosomes achieve complete separation in prophase, at NEB the two spindle poles will be at opposite ends of the nuclear space and the MTs will grow from the centrosomes toward the chromosomes symmetrically. Conversely, when the centrosomes are not completely separated at NEB, the two spindle poles will be shifted to one side of the nuclear space and MT growth toward the chromosomes will be asymmetrical. Based on these differences, we speculated that incomplete spindle pole separation at NEB may lead to erroneous KT attachment, and possibly chromosome mis-segregation. To test this hypothesis, we used a combination of experimental and computational approaches and investigated KT attachment and chromosome segregation in PtK1 cells with complete vs. incomplete spindle pole separation at NEB. We found that cells with incomplete spindle pole separation at NEB exhibit KT mis-attachments and chromosome mis-segregation. In addition, our mathematical model showed that two spindle poles in close proximity do not “search” the entire cellular space, and this leads to formation of large numbers of syntelic attachments, which can be an intermediate stage in the formation of merotelic KTs.

Materials and Methods

Cell culture and drug treatments.

Both PtK1 cells (a generous gift from Ted Salmon, UNC, Chapel Hill, NC) and PtK-GFP-γ-tubulin (a generous gift from Alexey Khodjakov, Wadsworth Center, Albany, NY) were maintained in Ham's F-12 Medium (Gibco). The culture medium was supplemented with 10% fetal bovine serum, penicillin, streptomycin, and amphotericin B (antimycotic). Cells were grown in a 37°C, 5% CO_2, humidified incubator. For experiments, cells were grown on sterile coverslips inside 35 mm Petri dishes. Cells at ~80% confluency were incubated in media containing 20μM S-Trityl-L-Cystine (STLC) for 2 hours, and either fixed (0μm with pre-search) or washed out of the drug. STLC washout was performed by washing the cells in fresh media 4 times. After washout, cells were either immediately incubated in media containing 6μM Nocodazole (NOC) for 30 min (0μm without pre-search) or re-incubated in drug-free media for 15 min (2-3μm without pre-search) or 30 min (6-7μm without pre-search) before the NOC treatment. NOC was then washed out and cells were either fixed immediately (2.5 min), or re-incubated in drug-free media and fixed at regular time intervals.

Fixation and Immunostaining.

Cells were rapidly rinsed in 1x PHEM, and incubated in ice-cold 95% Methanol with 5mM EGTA for 5 min first and then again for 20 min at -20^{o}C. Subsequently, cells were washed in PBS, and then blocked in 10% boiled goat serum for 1 h at room temperature. The coverslips were then incubated overnight at 4°C in primary antibodies diluted in 5% boiled goat serum. Cells were finally washed in PBST (PBS with 0.05%

Tween 20), incubated in secondary antibodies diluted in 5% boiled goat serum for 1 hour at room temperature, washed again, stained with DAPI, and mounted in an antifade solution containing 90% glycerol and 0.5% *N*-propyl gallate. Primary antibodies were diluted as follows: ACA (human anti-centromere antigen, Antibodies Inc.), diluted 1:100; mouse anti–α-tubulin (DM1A, Sigma-Aldrich), diluted 1:500; rabbit-anti-γ-tubulin (Abcam), diluted 1:100. Secondary antibodies were diluted as follows: X-Rhodamine goat-anti–human (Jackson ImmunoResearch Laboratories, Inc.), diluted 1:100; Alexa 488 goat-anti–mouse (Molecular Probes), diluted 1:400.

Live-cell imaging.

Ptk1 cells expressing GFP-γ-tubulin were grown on coverslips to ~70% confluency and mounted into a Rose chamber [196] with a top coverslip. The chamber was injected with L-15 medium supplemented with 4.5 g/L glucose. Experiments were performed on a Nikon Eclipse Ti inverted microscope equipped with phase–contrast transillumination, transmitted light shutter, Lumen 200PRO fluorescence illumination system, ProScan automated stage (Prior Scientific), and HQ2 CCD camera (Photometrics). Cells were maintained at ~36°C by means of an air stream stage incubator (Nevtek). Image acquisition, shutters, Z-axis position, and Lumen 200PRO fluorescence illumination system were all controlled by NIS Elements AR software (Nikon) on a PC computer. To determine the time of NEB, the cells were monitored by phase contrast every 1-2 min, whereas simultaneous phase contrast and fluorescence images were acquired at a single focal plane every 3 min for a 1-2 hour period with a Plan-Apochromatic 60x 1.4 NA phase-contrast objective. Extra images were acquired

immediately following NEB, at which time the positions of the centrosomes were also recorded. To record the centrosome coordinates prior and upon NEB, the experiment was manually switched from time-lapse to live imaging, the centrosome positions were identified by focusing up and down along the Z-axis, and the coordinates were recorded. Time-lapse imaging was then resumed. To further confirm centrosome positioning and pole-to-pole distances, an additional set of cells with incomplete spindle pole separation was imaged by 4-D (3-D plus time) microscopy. For these cells, Z-series optical sections were obtained in seven 1.2 μm steps using a Plan-Apochromatic 60×1.4 NA phase-contrast objective. After completion of spindle pole separation, images were acquired at a single focal plane to follow the cells into anaphase. The collected images were subsequently analyzed to: (i) determine centrosome positions with respect to the nuclear space; (ii) measure pole-to-pole distances before and upon NEB; and (iii) determine the chromosome segregation phenotype. For re-localization experiments, cells were grown on coverslips photo-etched with an alpha-numeric grid pattern (Electron Microscopy Sciences) and imaged until mid-prometaphase (~10 minutes after NEB), at which time the specific alpha-numeric grid was recorded, and the cells were removed from the microscope and immediately fixed and immunostained as described above. After immunostaining, cells were re-localized (using previously recorded alpha-numeric grid), imaged, and analyzed as described below.

Confocal microscopy and image analysis.

Immunofluorescently stained cells were imaged with a Swept Field Confocal system (Prairie Technologies) on a Nikon Eclipse TE-2000U inverted microscope. The

microscope was equipped with a 100× 1.4 NA Plan-Apochromatic phase–contrast objective lens, phase–contrast transillumination, transmitted light shutter, and automated ProScan stage (Prior Scientific). The confocal head was equipped with filters for illumination at 488, 568, and 647 nm from a 400 mW argon laser and a 150 mW krypton laser. Digital images were acquired with an HQ2 CCD camera (Photometrics). Image acquisition, shutter, Z-axis position, laser lines, and confocal system were all controlled by NIS Elements AR software (Nikon) on a PC computer. Z-series optical sections through each cell analyzed were obtained at 0.6 μm steps. For determination of the numbers of merotelic KTs in re-localized cells and unattached, monotelic, amphitelic, syntelic and merotelic attachments in the fixed-cell time-course experiments, acquired images were analyzed as previously described [229].

Results

Incomplete spindle pole separation at NEB is associated with elevated frequencies of anaphase lagging chromosomes.

We first wanted to test the hypothesis that incomplete spindle pole separation at NEB causes KT mis-attachments and chromosome mis-segregation. Of all possible KT mis-attachments (monotelic, syntelic, and merotelic), merotelic attachments (a single KT bound to MTs from two spindle poles instead of just one) are not detected by the spindle assembly checkpoint [137-141] and can therefore persist through mitosis into anaphase, when they can induce anaphase lagging chromosomes [138, 145]. Thus, an easy way to test our hypothesis was to determine whether increased frequencies of anaphase lagging chromosomes are found in cells with incomplete vs. complete spindle pole separation at NEB. To this aim, we used PtK1 cells expressing GFP-γ-tubulin [a generous gift from Dr. Alexey Khodjakov, Wadsworth Center, Albany, NY [230]]. Although these cells had been previously shown [136] (Silkworth and Cimini, unpublished) to complete centrosome separation before NEB over 90% of the time, we fortuitously isolated a subclone of this cell line that exhibited incomplete spindle pole separation at NEB at higher rates, and used it for this study. We performed time-lapse experiments in which the cells from this clone were imaged from prophase through late anaphase. To discriminate between complete and incomplete spindle pole separation at NEB, we measured the pole-to-pole distance upon NEB (see Materials and Methods for details) and at the end of prometaphase. Moreover, we determined the positioning of the centrosomes with respect to the chromosomes prior to and upon NEB. We found that the configuration of centrosome positioning with respect to the chromosomes prior to NEB could fall into the

four different categories diagrammed in figure 3.1Ai-iv. In two of these categories (Figures 3.1Ai-ii), cells exhibited complete centrosome separation prior to NEB, but in one case the centrosomes were positioned along an axis parallel to the substrate (Figures 3.1Ai and 3.2A), whereas in the other the centrosomes were positioned along an axis perpendicular to the substrate (Figures 3.1Aii, 3S3.1A, and 3.2B). Notably, in this latter category the centrosomes repositioned to the central region of the nuclear space at the time of NEB (Figures 3.1Bii, 3S3.1A, and 3.2B), thus reverting the initial separation. In the other two groups the centrosomes were positioned either at the edge of the nuclear space (Figures 3.1A-Biii, 3S3.1B, and 3.2C) or one centrosome was positioned at the edge of the nuclear space and the other on the top surface of the nuclear space (Figures 3.1Aiv, 3S3.1C, and 3.3B). In this latter case, the centrosome on the top surface repositioned towards the center of the nuclear space upon NEB (Figures 3.1Biv and 3S3.1C). Because of the reduced pole-to-pole distance upon NEB (i.e., the time when kinetochore-microtubule interaction becomes possible), cells displaying centrosome configurations like those depicted in figure 3.1Bii-iv (and shown in figure 3S3.1) were classified as cells with incomplete centrosome separation. Cells with complete centrosome separation displayed centrosome positioning like that depicted in figure 3.1Bi (and shown in figures 3.2A and 3.3A). After an initial characterization of centrosome positioning in the overall population, an additional set of cells with incomplete centrosome separation was selectively imaged (see Materials and Methods for details) to confirm the results obtained in the initial screening. When all the data were taken together, we found that for cells with incomplete centrosome separation the mean interpolar distance upon NEB was 7.33±2.02 μm (mean±standard deviation; N=50),

which was less than 75% the distance measured at the end of prometaphase (13.63±1.98μm; Figure 3S3.2). In cells with complete centrosome separation the mean pole-to-pole distance was 15.81±4.99μm (N=31) upon NEB and 12.63±1.97μm at the end of prometaphase. Our measurements are consistent with previously reported pole-to-pole distances of 12-15μm in metaphase PtK1 cells [231, 232]. We also measured the distance across the long axis of the "nuclear space" (i.e., region occupied by the chromosomes) at NEB and found an average size of 16.27±3.39μm (N=67). This indicates that, whereas in cells with complete spindle pole separation the centrosomes were positioned at opposite ends of the nuclear space, in cells with incomplete spindle pole separation, the pole-to-pole distance at NEB was less than half that of the nuclear space. This suggests that the positioning of the centrosomes in such cells may cause a single KT to face both spindle poles and thus establish a merotelic attachment, which, if not corrected, will result in a lagging chromosome in anaphase. Indeed, cells with incomplete spindle pole separation upon NEB exhibited high frequencies of anaphase lagging chromosomes, which overall were ~3.5-fold the frequency of anaphase lagging chromosomes in cells with complete spindle pole separation (Figures 3.1D and 3.2D). In agreement with previous observations [218], there was no significant difference in the duration of mitosis for cells with complete vs. incomplete spindle pole separation (data not shown). Consistently, numerical simulations showed that at small initial distances between spindle poles, there are more persistent merotelic attachments, but those do not induce a mitotic delay [137]. Monotelic attachments, which can cause a mitotic delay, disappear in the simulations just 2-3 minutes more slowly in cells with incomplete spindle pole separation compared to cells with initial pole-to-pole distances of 12-15μm,

thus delaying mitosis insignificantly. Taken together, these data reveal that cells that start prometaphase with incompletely separated centrosomes/spindle poles are more likely than those with complete spindle pole separation to exhibit chromosome segregation defects in the form of anaphase lagging chromosomes (Figures 3.1D and 3.2).

Incomplete spindle pole separation at NEB promotes formation of merotelic kinetochore attachments.

Differences in frequencies of anaphase lagging chromosomes may be due to either differences in the rate of formation [136, 145, 229, 233-235], or differences in the rate of correction of merotelic KT attachments [76, 142, 236, 237]. To test whether formation of merotelic KTs was more frequent in cells with incomplete vs. complete spindle pole separation upon NEB, we performed a set of experiments in which GFP-γ-tubulin PtK1 cells were followed by time-lapse microscopy from (or before) NEB until mid-prometaphase, at which time the cells were fixed and immunostained for KTs and MTs (Figure 3.3A-B). The same cells were then re-localized, imaged by high-resolution confocal microscopy, and analyzed to determine the number of merotelic KTs. The mean pole-to-pole distance at NEB in cells with incomplete and complete spindle pole separation was found to be 7.09±2.79μm (N=19) and 15.83±3.86μm (N=36), respectively, values comparable to those found in the experiments described above. Cells with incomplete spindle pole separation at NEB were found to possess significantly (t-test, $p<0.01$) higher numbers of merotelic KTs in prometaphase compared to cells with complete spindle pole separation (Figure 3.3C). These results show that cells in which spindle pole separation is not complete upon NEB, and thus undergo spindle

bipolarization during prometaphase, are more likely to establish KT mis-attachments compared to cells in which spindle pole separation is complete at NEB. Our data also showed that overall the spindle poles were incompletely separated upon NEB in about 45% (N=122) of our PtK1 cell clone, similarly to what was previously found in HeLa, MCDKII, and PtK2 cells [215-218, 220, 226], making these cells a good model to study this phenomenon.

Merotelic kinetochore attachments can form through a syntelic intermediate.

We next wanted to understand how incomplete spindle pole separation influences the number and types of KT attachments formed and how merotelic attachments arise. To this aim, we experimentally inhibited spindle pole separation by inhibiting the kinesin Eg5 by a 2 hour S-Trityl-L-Cysteine (STLC) treatment [238]. We then washed out the STLC and added nocodazole (NOC) to completely disassemble the MTs. Next, we washed out the NOC and fixed the cells at regular time-intervals (Figure 3.4A). Pilot experiments were performed to identify the minimum dose of NOC and length of treatment that induced MT disassembly, but did not result in centrosome displacement or assembly of ectopic sites of MT nucleation after NOC washout. This experimental design allowed spindle pole separation to occur simultaneously with establishment of KT-MT interactions (i.e., search and capture occurs while the spindle poles are moving apart), as it would normally happen in untreated cells. Finally, we determined the number and types of KT attachments at different time points, until the end of prometaphase (Figure 3.4B-C). We found that at early time-points there were large numbers of unattached chromosomes, and that the attached chromosomes exhibited either syntelic or monotelic

attachments (Figure 3.4C). At later time-points, both merotelic and amphitelic attachments increased, while syntelic and monotelic decreased (Figure 3.4C), suggesting that some of the syntelic attachments were converted into merotelic ones. These results suggest that merotelic attachments can form through a syntelic intermediate, and that this mechanism may explain the higher frequency of merotelic attachments in cells with incomplete spindle pole separation compared to cells achieving complete centrosome separation before NEB. The types (monotelic and syntelic) of KT attachments (disregarding the unattached chromosomes) at the early time points of our experiment were very similar to those found in cells arrested with Eg5 inhibitors [17, 239]. Moreover, we performed an experiment in which cells were washed out of STLC after a 2-hour treatment, fixed at regular time intervals, and analyzed for numbers and types of KT attachments (initial pole-to-pole distance 0μm, with pre-search). We found that the changes in numbers and types of KT attachments over time (Figure 3S3.3A) were very similar to those observed in cells in which spindle pole separation and KT attachment occurred simultaneously (initial pole-to-pole distance 0μm, without pre-search). Although this experiment was not representative of the events occurring under physiological conditions, it provided useful information for the development of our mathematical model (see below and supplemental material).

Because the pole-to-pole distance upon NEB in untreated cells with incomplete spindle pole separation is never 0 μm, we further modified the experiment described above. We re-incubated the cells in drug-free media between the STLC wash-out and the NOC treatment to allow enough time for the spindle poles to move apart to a distance of 6-7 μm (Figure 3.4A), which represents the pole-to-pole distance in untreated cells with

incomplete spindle pole separation at NEB (Figure 3S3.1). We found that an initial pole-to-pole distance of 6-7 μm still resulted in a large number of syntelic chromosomes, but overall generated a more random distribution of different types of KT attachments at early time-points after NOC wash-out (see 2.5 and 5 min time-points in Figure 3.4D). It is also noteworthy that in this case, as opposed to when the search starts with spindle poles very close to each other (0 μm distance, Figure 3.4C), both amphitelic and merotelic attachments formed at early time points, suggesting that merotelic KT mis-attachments do not necessarily form through a syntelic intermediate. Finally, we also performed the experiment with an initial pole-to-pole distance of 2-3 μm and found that the numbers and types of KT attachments observed at early time-points (Figure 3S3.4) were intermediate between those observed with initial distances of 0 μm and 6-7 μm. In this case, both amphitelic and merotelic attachments appeared early, but at lower frequencies compared to when the initial distance was 6-7 μm. In all experiments, amphitelic attachments increased over time at the expense of syntelic and monotelic, as expected due to attachment of unattached KTs and correction of mis-attachments. An increase in merotelic attachments was also observed, which may be due to the conversion of syntelic attachments into merotelic ones due to partial correction of syntelic attachments. Finally, it is also worth noting that in all cases (but particularly in the 0 μm and 2-3 μm pole-to-pole distance) there was an initial increase in the number of syntelic attachments (see Figure 3.4C, 2.5 and 10 min; Figure 3.4D, 2.5 and 5 min; Figure 3S3.4, 2.5 and 5 min). This suggests not only that when the pole-to-pole distance is small chromosomes tend to establish syntelic attachments, but also that correction of syntelic attachments is not efficient when the spindle poles are not fully separated.

Computational modeling reveals that two spindle poles in close proximity do not search the entire cellular space.

To better understand how initial spindle pole distance affects establishment of KT-MT attachments, we took advantage of a computational model we recently developed to simulate spindle assembly in realistic geometry [240]. We adapted this previous model to our current experimental system (PtK1 cells) by taking into account a number of parameters, including size of the nuclear space (volume occupied by the chromosomes at NEB), chromosome number, and chromosome size (see Supplemental Material for information about parameters used in the simulations). We reverse-engineered the process of spindle assembly by using the quantitative experimental data described in the previous section and shown in Figures 3.4 C-D and 3S3.3A. Specifically, we simulated [using the same method as in [240]] the stochastic search for KTs by MTs growing from two poles (Figure 3.5A), the distance between which was changing as in the three experimental set-ups (Figures 3.4C-D and 3S3.3A). In the course of spindle assembly, the monotelically attached chromosomes rotated so that the uncaptured KT became shielded from the capturing pole [20, 241], thereby decreasing the probability of syntelic and merotelic attachments. Furthermore, the monotelically attached chromosomes moved away from the capturing pole, simulating CENP-E-dependent congression of monotelic chromosomes [85, 242], further decreasing the probability of syntelic and merotelic attachment and increasing the chance of amphitelic attachment by the opposing spindle pole. This bias of monotelic chromosomes to move away from the capturing pole increased with increasing pole-to-pole distances, reflecting the increase in number of k-

fibers along which the monotelic chromosomes can move (see Supplemental Material for details). Time-course simulations performed with such a computational model (details in Supplemental Material) closely reproduced the experimental results for all initial pole-to-pole distances (Figure 3.5B-C), and revealed that there are "blind spots" for each of the poles that are maximal when the poles are in close proximity, in which case each pole essentially searches in its own half-space (Figures 3.5A and 3.5D). Note that these blind spots are not an artificial assumption, but are simply the consequence of the steric hindrance that MTs of one centrosome present for MTs growing from the other centrosome when they are in close proximity. As the distance between the poles increases, each pole "sees" increasing fractions of chromosomes, until, when spindle pole separation is complete (~10 μm), almost all chromosomes are seen from both poles (Figure 3.5D). This "shielding" effect would explain our finding that there is a lag phase in the disappearance (correction) of syntelic attachments in cells with incomplete spindle pole separation (Figures 3.4C-D, 3S3.3A, and 3S3.4). Indeed, when the spindle poles are very close to each other a syntelic chromosome would likely only be seen by one pole, and therefore would keep forming syntelic attachments even if initially corrected. Finally, the mathematical model also explains why merotelic attachments (for which a single KT must be seen by both poles) do not form right away when the spindle poles are in close proximity (Figures 3.4C and 3S3.3A), but start forming at early time-points for increasing pole-to-pole distances (Figures 3S3.4 and 3.4D). The simulations also demonstrated that MTs attached to syntelic chromosomes have to be unstable, detaching after ~2 minutes, otherwise the number of erroneous attachments would be too great. Finally, the model indicates that chromosome rotations and movements toward the

spindle equator after the first capture are important for both rapid and accurate spindle assembly.

It is worth noting that the model invoking the shielding effect (Figure 3.5D) between the two spindle poles could reproduce the experimental results significantly better than alternative models, especially for very small initial pole-to-pole distances. Indeed, a model in which the two poles were allowed to search in the whole space (i.e., no shielding effect; Figure 3S3.5A-B), could not reproduce the experimental results in the case of an initial pole-to-pole distance of 0 μm (Figure 3S3.5A). Specifically, this model resulted in the formation of larger numbers of merotelic KTs at early time points and low numbers of amphitelic KTs at later time points (compare figure 3.4C and figure 3S3.5A). Results that better fit the experimental data were obtained when this latter model was modified by allowing merotelic and amphitelic KTs to frequently disassemble at small inter-polar distances and to become more stable with increasing pole-to-pole distances. Although this modification produced better results (Figure 3S3.5C-D), it could not reproduce the changes in frequency of monotelic and syntelic attachments over time for cells starting with an initial pole-to-pole distance of 0 μm (compare figure 3.4C and figure 3S3.5C).

Finally, we computationally tested additional conditions to account for observations reported in previous studies. Specifically, we varied the inter-KT angle to simulate spindle assembly in the presence of "plastic" KTs [243], we increased the KT target size to simulate the long k-fibers that form in cells arrested in mitosis by Eg5 inhibition [239], and we introduced small unevenness in chromosome distribution. None of these modifications led to better fits of the model results to the experimental data (see

supplemental material for details). This does not necessarily mean that the phenomena tested do not play any role in the spindle assembly process, but that they may be more subtle than the other mechanisms/processes considered in this study, and/or that the information about dynamic correlations between chromosome and centrosome positions and KT orientations in our hands is insufficient to detect an effect.

Discussion

Incomplete centrosome separation at NEB and kinetochore mis-attachment.

Our data reveal that the degree of centrosome separation upon NEB plays a critical role in determining the number and types of KT attachments that form in early prometaphase. Specifically, we showed that when the centrosomes are not located at opposite ends of the XY axis of the nuclear space at NEB there is an increase in formation of KT mis-attachments (Figures 3.3 and 3.4C-D), and consequently an increase in chromosome mis-segregation (Figures 3.1 and 3.2). Our data also indicate that incomplete spindle pole separation at NEB can lead to the formation of merotelic attachments through two different mechanisms (Figure 3.6): (i) when the spindle poles are very close to each other (<2-3μm), chromosomes tend to become syntelically attached (Figure 3.6A). Merotelic attachments will then be formed by partial correction of syntelic attachments during spindle bipolarization (Figure 3.6A, third and fourth panels). Indeed, our *in silico* data indicate that syntelic attachments are much more unstable than merotelic and amphitelic ones. This suggests that, *in vivo*, syntelic attachments may be corrected more efficiently than merotelic ones, as previously suggested by others [244-246]. Such an efficient correction may in turn explain why merotelic attachments are observed much more frequently than syntelic ones in tissue culture cells [13, 135]. Efficient correction of syntelic attachments may also be required for spindle bi-polarization. Indeed, if Aurora B kinase is inhibited in PtK1 cells recovering from an STLC arrest, both correction of syntelic attachments and bipolarization are inhibited/delayed in most cells (Silkworth, Nardi, and Cimini, unpublished). (ii) If the spindle poles are incompletely separated upon NEB, but far enough from each other (≥ 2-

3 μm), then merotelic attachments can also form through a second mechanism (Figure 3.6B), in which a single KT would be seen by and establish attachment with both spindle poles directly, without going through a syntelic intermediate. Interestingly, even though a certain degree of centrosome separation (6-7 μm) is always achieved before NEB, in many cells (~45%) this separation does not reach the maximum possible distance. Such partial spindle pole separation is enough to increase the rate of KT mis-attachment formation and chromosome mis-segregation compared to cells exhibiting complete spindle pole separation (>10 μm) at NEB (Figures 3.1 and 3.2).

Prophase vs. prometaphase centrosome separation.

As described here and in other studies [17, 215-218, 220, 247], spindle length and/or structure at the end of prometaphase are not affected by the position of the centrosomes at NEB because centrosome separation can be completed after NEB. It has been proposed that there is substantial redundancy during bipolar spindle assembly aimed at ensuring accurate chromosome segregation [221, 224], and the existence of mechanisms that allow completion of centrosome separation either in prophase or in prometaphase was believed to exemplify such redundancy [218, 220, 248]. However, we show here that, although cells in which centrosome separation is not completed before NEB do not exhibit permanent defects of spindle organization or structure, they do exhibit increased rates of chromosome mis-segregation compared to cells in which centrosome separation is completed before NEB. Thus, the mechanisms responsible for prometaphase centrosome separation may represent a back-up system that ensures progression of mitosis in spite of the potential risk. Interestingly, during the early stages

of embryonic development, the spindle poles are completely separated at NEB [221, 228], indicating that prophase centrosome separation is highly prevalent in this context. Likely, completion of centrosome separation before NEB at this stage of development ensures the accuracy of chromosome segregation required for development of a healthy adult organism. Similarly, RPE1 cells, known for maintaining a stable diploid chromosome number, were found to achieve complete centrosome separation prior to NEB 100% of the time [249].

Although traditionally the existence of two different pathways has been invoked to explain how centrosome separation can be completed either before or after NEB, our data on the pole-to-pole distance upon NEB (Figure 3S3.2) do not seem to support a two-pathway model. Indeed, if centrosome separation occurred through one of two alternative pathways, one would expect to find a bimodal distribution of pole-to-pole distances at NEB. Instead, we found a continuous distribution of distances upon NEB, suggesting that there are not two distinct pathways, but rather a number of mechanisms, some of which can be used in prophase (MT/nuclear envelope interaction), some in prometaphase (myosin activity at the cell cortex), and some in both (Eg5-dependent MT sliding). Nevertheless, it does appear that at least in some cell types centrosome separation and NEB are sufficiently uncoordinated that the number of cells in which centrosome separation is incomplete at NEB is relatively high [215-220]. At this time we only have limited information on how prevalent incomplete centrosome separation at NEB is in different cell types. However, we have preliminary data showing that in several different cancer cell lines a large proportion of cells exhibit incomplete centrosome separation in early mitosis (Silkworth, Nardi, and Cimini, unpublished). Thus, it is possible that under

normal conditions (e.g., early development and untransformed or primary cells) there would be a selective pressure against delayed centrosome separation due to its association with chromosome mis-segregation and aneuploidy, which may, in turn, reduce cell viability. However, situations in which there are high proliferation rates and mis-regulation of many physiological pathways, like in cancer cells, centrosomes may fail to achieve complete separation before NEB much more frequently. Interestingly, incomplete spindle pole separation in cancer cells may represent a mechanism associated with chromosomal instability, in addition to previously identified ones, such as transient spindle multipolarity [229, 233] and inefficient correction of KT mis-attachments [236].

Why does incomplete spindle pole separation at NEB induce kinetochore mis-attachments and chromosome mis-segregation?

The work presented here indicates that if the centrosomes are not in diametrically opposed positions along the XY axis of the nuclear space at the time of NEB, KTs are likely to establish erroneous attachments (Figures 3.3-3.5). A consequence of the high rates of mis-attachment formation is chromosome mis-segregation at later mitotic stages (Figures 3.1 and 3.2). Specifically, high rates of merotelic KT formation are expected to result in high rates of chromosome mis-segregation [136, 229, 233], because merotelic KT attachments are not detected by the spindle assembly checkpoint [137-141]. Over the years, several different factors have been shown to promote KT mis-attachments (in particular merotelic). These include altered centromere/chromosome architecture [250-254], and defects in mitotic spindle morphology/assembly [229, 233, 240, 255, 256]. In this study, we show that a delay in spindle bi-polarization also leads to increased rates of

merotelic KT formation (Figures 3.3-3.5). Specifically, both our experimental and computational data show that cells with incomplete spindle pole separation upon NEB establish a large number (20-60%) of syntelic attachments (Figures 3.3, 3.4, and 3S3.4). However, our data suggest that it is not the prometaphase bi-polarization *per se* that induces KT mis-attachment, rather the relative positions of the two centrosomes/spindle poles at the time of NEB with respect to the nuclear space. In fact, if the two spindle poles are not completely separated upon NEB, the early prometaphase spindle will be skewed and/or will have spindle poles positioned very close to each other. In two types of centrosome positioning configurations (Figures 3.1Biii-iv) we observed both a reduced pole-to-pole distance and a skewed placement of the centrosomes toward one half of the nuclear space. In a third type, initially separated centrosomes (Figure 3.1Aii) moved to the center of the nuclear space upon NEB (Figure 3.1Bii), which resulted in a symmetric configuration, but in very short pole-to-pole distance. This behavior was only observed in a small number of cells (<5% of the overall mitotic cell population), and it appears to exemplify a difference between PtK1 cells and several human cell types. Indeed, it has been previously shown that in human cells the centrosomes can reach diametrically opposing positions along the Z-axis before NEB. As opposed to what we observe in PtK1 cells, in human cells the centrosomes persist in those positions after NEB, and the spindle assembles perpendicularly to the substrate [249, 257-259]. This results in the chromosomes at the metaphase plate frequently appearing in what is known as a wheel-shaped rosette [259] or the toroidal configuration [249]. In our cells, when the centrosomes are positioned along the Z-axis prior to NEB, they move toward the center of the nuclear space upon NEB (Figures 3.1A-Bii and 3S3.1A), thus preventing spindle

assembly perpendicularly to the substrate. As a result, we never observed metaphase PtK1 cells with chromosomes in a rosette configuration. Thus, in human cells prophase centrosome separation along the Z axis is not expected to affect KT attachment or chromosome segregation [249]. Conversely, in PtK1 cells centrosome separation along the Z axis is not maintained upon NEB, and therefore it results in short pole-to-pole distances upon NEB, which are associated with KT mis-attachment and chromosome mis-segregation (this study). In summary, we find that incomplete centrosome separation upon NEB can result in asymmetric positioning of the spindle poles with respect to the nuclear space at the onset of prometaphase, and in all cases is characterized by a short pole-to-pole distance. As indicated by our mathematical model, the two spindle poles can only see a fraction of the chromosomes at short pole-to-pole distances (Figure 3.5D), and this gives rise to large numbers of KT mis-attachments.

Recent studies have shown that transient spindle multipolarity promotes formation of merotelic attachments in cancer cells [229, 233, 240]. Like transient multipolarity, incomplete spindle pole separation upon NEB leads to a temporary geometric defect of the mitotic spindle. However, although both situations will result in elevated rates of chromosome mis-segregation, they are mechanistically very different. In the case of a cell with two unseparated centrosomes, each chromosome can likely be seen by only one centrosome, and this results in high frequencies of syntelic attachments. Conversely, within a multipolar spindle each chromosome is likely seen by more than one centrosome, favoring merotelic attachment over syntelic.

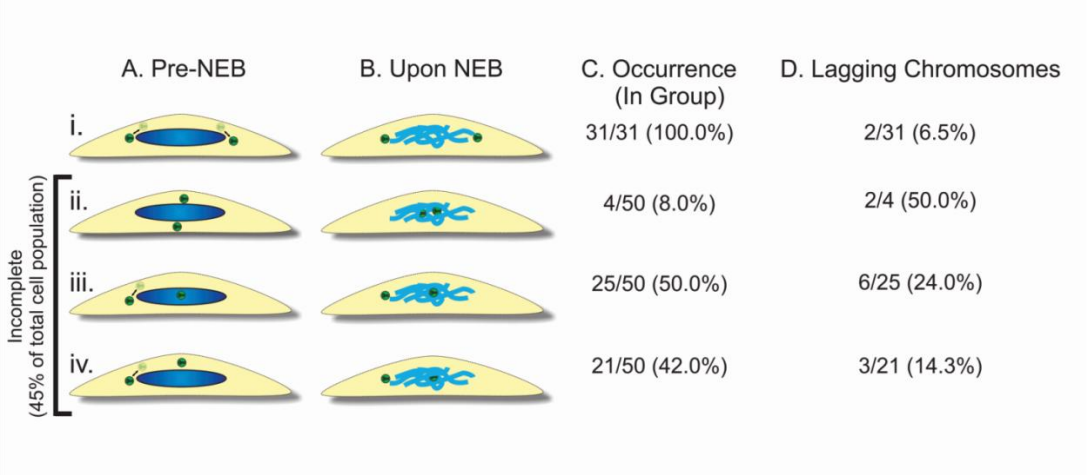

Figure 3.1 *Analysis of centrosome positioning before and immediately after NEB.* (A-B) Diagrams showing the different types of centrosome arrangements before (A) and upon NEB (B) in PtK1 cells with complete (i) or incomplete (ii-iv) centrosome separation. The arrow between a shadowed and a dark image of the centrosome in i, iii, and iv indicates that the centrosome could be positioned at any point between the two. Note that in those cases in which the centrosomes achieve positions at the top and bottom of the nucleus before NEB (Aii), they do not persist in such positions upon NEB, and instead they move toward the center of the nuclear space. See figure 3S3.1 for examples of cells with different centrosome configurations. (C) Rates of occurrence of the various configurations of centrosome positioning within the complete (i) and incomplete (ii-iv) spindle pole separation groups. (D) Rates of anaphase lagging chromosomes in cells from each subgroup.

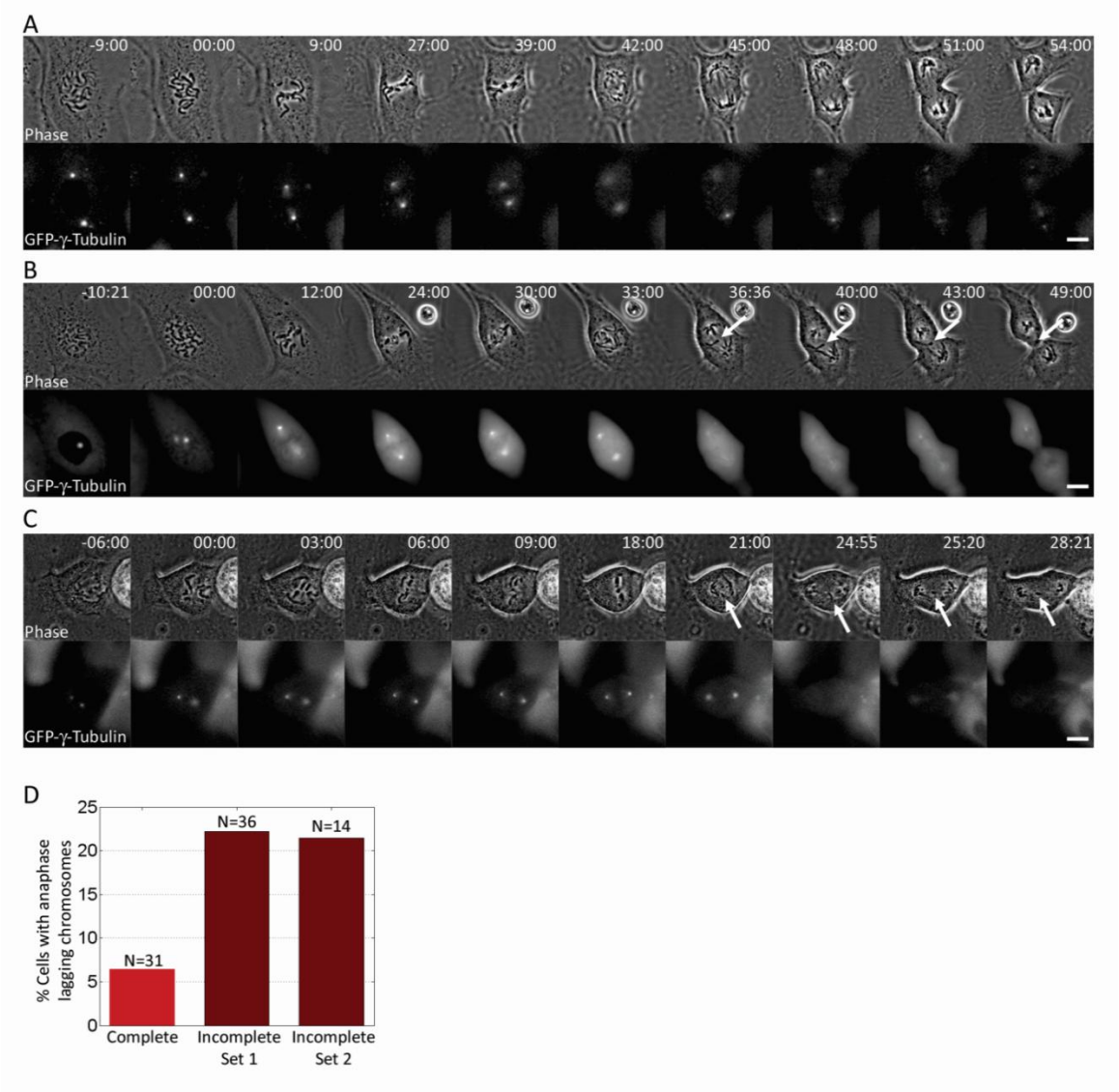

Figure 3.2. *Incomplete spindle pole separation at NEB is associated with elevated frequencies of anaphase lagging chromosomes.* (A-C) Still images from time-lapse movies of PtK1 cells expressing GFP-γ-tubulin. Phase contrast images are shown in the top row and single focal plane GFP images are shown in the bottom row of each panel. A cell in which the spindle poles were fully separated at NEB is shown in A. In the cell shown in B, the centrosomes were separated along the Z axis of the cell prior to NEB (-10:21 min time point; only one centrosome is in focus in the image), but moved toward the center of the nuclear space and in very close proximity upon NEB (00:00 min time point). The same cell exhibits an anaphase lagging chromosome (arrow). In the cell shown in C, the centrosomes were shifted to one side of the nuclear space prior to and upon NEB. (D) Frequencies of anaphase lagging chromosomes in cells with complete and incomplete spindle pole separation at NEB. The "Incomplete Set 2" data refer to an additional set of cells with incomplete centrosome separation imaged by 4-D (3-D plus time) time-lapse microscopy (See Materials and Methods for details). Scale bars, 10 μm.

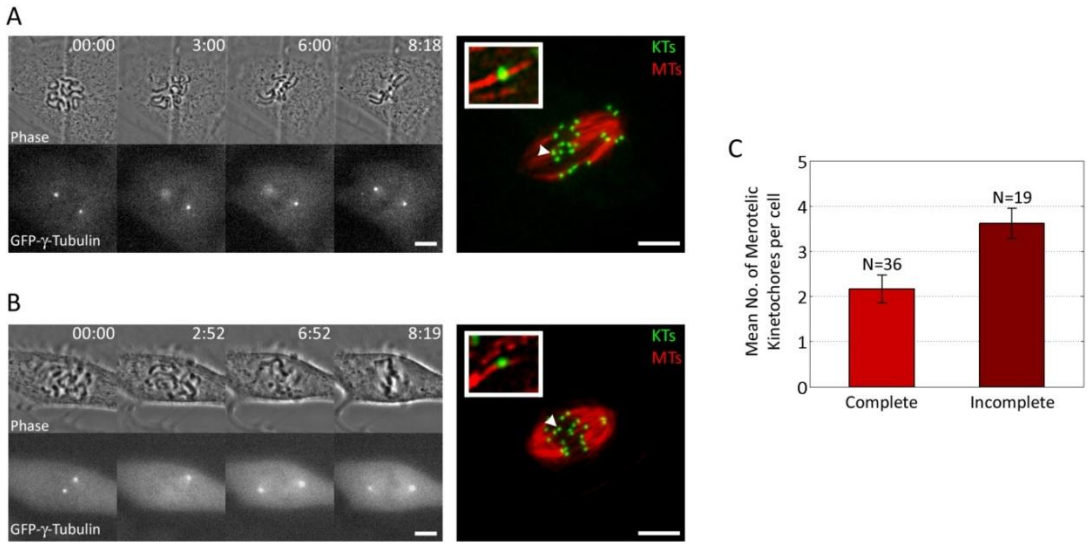

Figure 3.3. *Incomplete spindle pole separation at NEB promotes formation of merotelic kinetochore attachments.* (A-B) Examples of GFP-γ-tubulin PtK1 cells imaged by time-lapse microscopy from NEB to late prometaphase, then immunostained for KTs and MTs, relocalized, and imaged by confocal microscopy (far-right panels). A cell with complete spindle pole separation at NEB is shown in A, whereas a cell with incomplete spindle pole separation is shown in B. Insets represent 225% enlargements of the KTs indicated by the arrowheads. (C) The histogram shows that prometaphase cells with incomplete spindle pole separation at NEB exhibit higher (t-test, $p<0.01$) numbers of merotelic KTs compared to cells with complete spindle pole separation at NEB. Error bars represent standard errors of the mean. Scale bars in the time-lapse images represent 10 μm. Scale bars in the fixed cell images represent 5 μm.

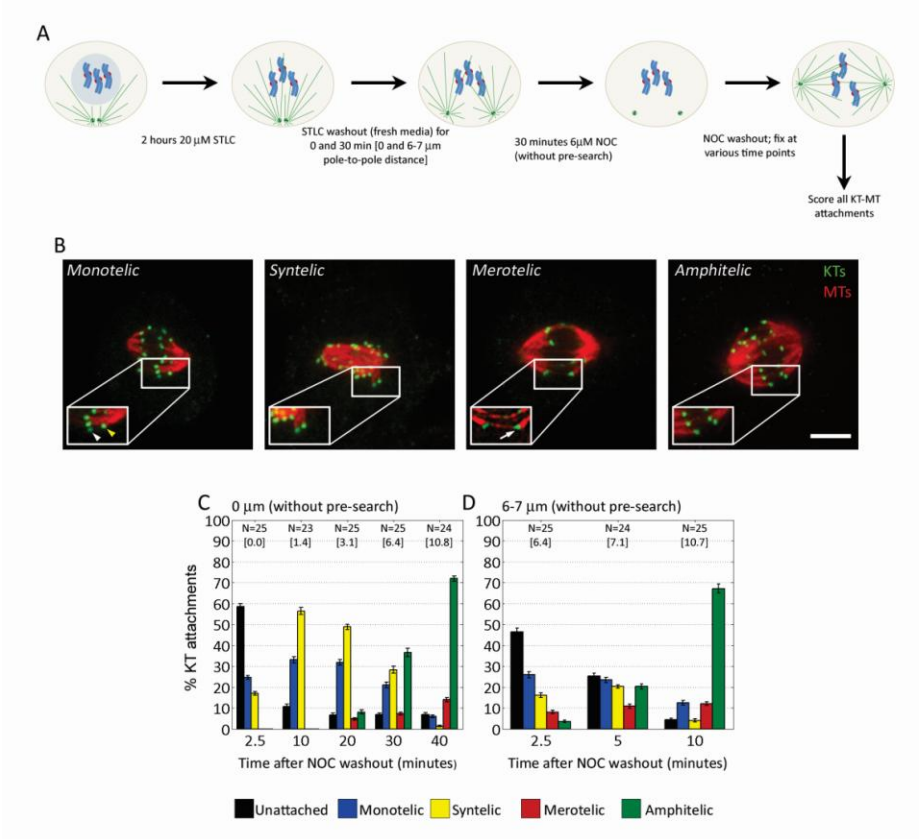

Figure 3.4. *Pole-to-pole distance at NEB determines the types and numbers of KT attachments that form in early prometaphase.* (A) Flow chart of experimental protocol used for the data summarized in C-D. (B) Examples of different types of KT attachment in PtK1 cells. The images are single focal planes or maximum intensity projections of 2-4 optical sections around the chromosome of interest. Insets are 150% enlarged views of the KT or KT pair in the boxed region. White and yellow arrowheads denote the unattached and attached sister KT, respectively. White arrow denotes merotelic KT. Scale bar, 5 μm. (C) Frequencies of different types of KT attachments in cells that were first treated with STLC for 2 hrs, then washed out and incubated in NOC for 30 min, and finally washed out of the NOC and fixed at subsequent time-points. In these cells, the spindle poles started at a distance of 0 μm, and gradually separated during MT assembly (spindle poles moving apart from 0 μm without pre-search). (D) Frequencies of different types of KT attachments in cells that were first treated with STLC for 2 hrs, washed out and re-incubated in STLC-free media for 30 min (to allow the spindle poles to move apart to a distance of 6-7 μm), then incubated in NOC for 30 min, and finally washed out of the NOC and fixed at subsequent time-points. In these cells, the spindle poles started at a distance of 6-7 μm, and gradually separated during MT assembly (to mimic incomplete spindle pole separation in untreated PtK1 cells). N represents the number of cells analyzed for each experimental point. For each cell, the type of KT attachment was determined for all the chromosomes (8.98±1.36, mean±standard deviation) that could be clearly visualized. The numbers in square brackets represent the average pole-to-pole distance (in μm) at each time-point.

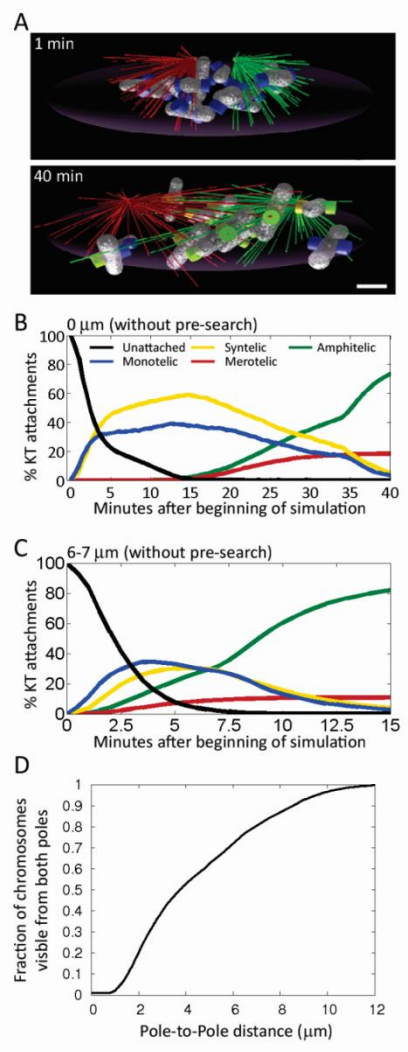

Figure 3.5. *Computer simulations of spindle assembly from different initial spindle pole distances can closely reproduce experimental results.* (A) Snap-shots of computer simulations of spindle assembly in a cell with incomplete spindle pole separation at NEB (top). MTs from different poles are shown in green and red to differentiate between their spindle pole of origin. Unattached KTs are blue, captured KTs are green. The complete separation of MTs coming from opposite poles in the top panel is an exemplification of the "shielding" effect occurring between the two poles when the pole-to-pole distance is very small (see text for details). (B-C) Time-course simulations of spindle assembly in the presence of a shielding effect between the two centrosomes. (B) Simulation starting with a spindle pole distance of 0 μm (as in figure 3.4C). (C) Simulation starting with a spindle pole distance of 6 μm (as in figure 3.4D). The simulation results closely reproduce the experimental results both at the initial pole-to-pole distance of 0 μm and at an initial distance of 6 μm. (D) The graph shows the correlation between pole-to-pole distance and the fraction of chromosomes seen from both poles.

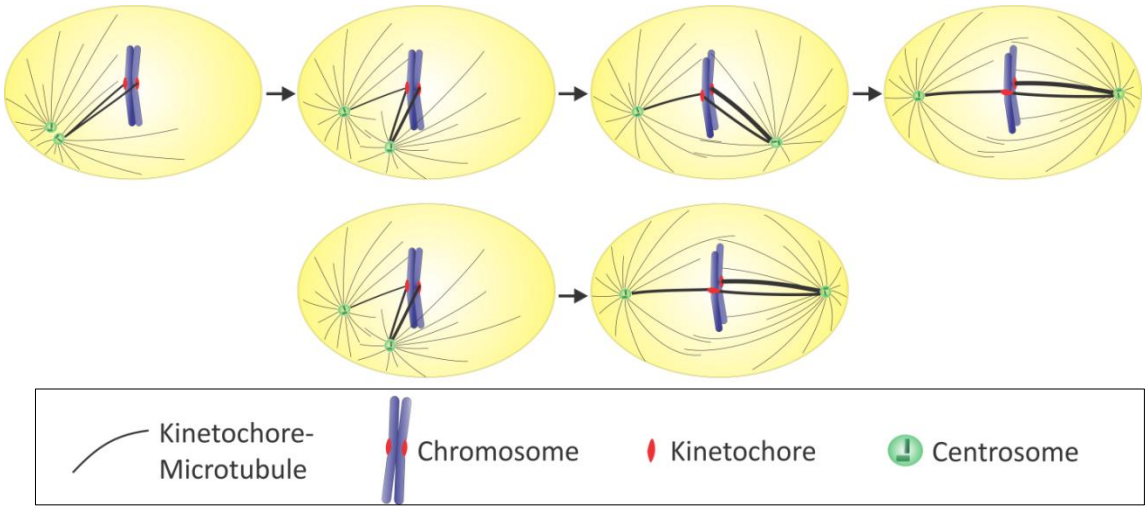

Figure 3.6. *Merotelic KT attachments can form through two different mechanisms in cells with incomplete spindle pole separation at NEB.* (A) When the spindle poles are very close to each other, chromosomes tend to become syntelically attached. Merotelic attachments will then be formed after partial correction of syntelic attachments during spindle bipolarization (third and fourth panels). (B) If the spindle poles are incompletely separated, but far enough from each other, a single KT can be seen by and establish attachment with both spindle poles right away, without going through a syntelic intermediate.

Supplemental Material

Development of a mathematical model for simulation of spindle assembly in PtK1 cells. Approximate kinetics of spindle assembly.

We recently considered an extremely simplified model [260] of microtubules (MTs) from two poles searching for a single chromosome equidistant from the poles. In the model, the MTs capture one of two kinetochores (KTs) with the rate k_{on} and the pole-KT connection is destabilized with the rate k_{off}. Thus, all pole-KT connections are transient, except for the amphitelic connection, which was assumed to be stable. We found, not surprisingly, that numbers of mono-, syn- and mero-telic attachments in this model increased at first, and then slowly decreased to zero, while the number of amphitelic connections increased monotonically to saturation.

Simulations of this model suggested starting with a numerical investigation of an approximate temporal dynamics of the spindle assembly to develop intuition without complications of the explicit spatial chromosome distribution. We will call the assembly of the spindle when the poles are initially very close to each other and the search takes place for 1-2 hours before pole separation **Experiment 1** (Figure 3S3A); the assembly when the poles are initially very close to each other and the search starts together with pole separation **Experiment 2** (Figure 3.4C); and finally the assembly when the poles start separating from the initial distance 6-7 μm together with the search **Experiment 3** (Figure 3.4D).

Experiment 1 informs that after 1-2 hours of search, most KTs are associated with MTs and that at pole separation onset there are almost no unattached, mero- and amphi-telic connections present. If MTs from each pole grow in all directions, then each

KT is 'seen' from almost the same angle from both poles because in this experiment the poles are so close together. In this scenario, there is an equal probability to capture any KT from either pole. Thus, in theory, if one KT is captured from one pole, there is an equal chance that the sister KT would be captured from the same as from the other pole. This argument suggests that at early time points following pole separation onset there would be a large number of merotelic and amphitelic attachments in addition to syntelic ones, which was not the case in the experimental results (Figure 3.4C). One of the most straightforward solutions for this conundrum is that when the centrosomes are very close together, then each searches in its own half-space (Figure 3.5A), so that each chromosome can only be captured from one of the poles. One possible explanation is that if the poles are close together, MTs from each pole can only cover a half-space because each pole 'shields' the other half-space from the other pole.

Furthermore, the data from Experiment 1 indicate clearly that MTs have to detach from the syntelically attached KTs. The respective MT detachment rate cannot be as fast as ~ 1/minute because in that case the attachment rate would have to be of the same order of magnitude, and the spindle would assemble within a couple of minutes, which does not happen. On the other hand, the detachment rate cannot be slower than ~ 1/30 min – in this case, the syntelic attachments would not have time to disassemble in all experiments. Thus, the detachment rate (conversion of syntelic to monotelic attachments) is of the order of one per 10-20 min. This means that during the initial 1-2 hrs, the numbers of syn- and mono-telic attachments equilibrate. Let N_1 and N_2 be the numbers of mono- and syntelic attachments, respectively, k_1 is the rate of monotelic attachment conversion into a syntelic one, and k_2 - the rate of syntelic attachment conversion into a

monotelic one (Figure 3S6). Then, $k_1 N_1 = k_2 N_2$. From the data at *t = 0* in Experiment 1, $2N_1 \approx N_2$, so $k_1 = 2k_2$: if $k_2 = 0.05/\min$, then $k_1 = 0.1/\min$. The complete spindle assembly time, about 15 min, scales as the logarithms of the KT number [260], so this time is of the order of $(1/k_0)\log 24 \sim 15$ min, where k_0 is the rate of the capture of one KT. Thus, we can estimate the rate of the capture of one KT as $k_0 = \log 24/15 = 0.2/\min$.

All three experiments (Figures 3S3A, 3.4C-D) show only increase of mero- and amphitelic connections over time. To account for this, we assumed that amphitelic and merotelic attachments do not disassemble. Although this is a simplification because correction of merotelic attachments is known to occur [212], mathematical models that predict the observed results but that also include disassembly of merotelic KT attachments are too complex, and were not considered.

Based on these arguments, we screened the parameters and found that if we assume that a monotelic attachment is established with the rate 0.3/min, syntelic one is established with the rate 0.6/min, destabilization rate of the syntelic attachment is 0.3/min, rate of merotelic attachment formation (from mono- or syntelic one) is 0.03/min, and finally if the rate of amphitelic attachment formation from the monotelic one is 0.15/min, we can semi-quantitatively explain the data of all three experiments. In addition to these rates, we also have to assume that the following fraction of chromosomes is *visible from both poles* as a function of the pole-to-pole distance: $f(r) = r^n/(r^n + s^n), n = 4, s = 5\,\mu$m. (Here *r* is the pole-to-pole distance in μm). Based on this function, each pole can access only half of the chromosomes for a pole-to-pole distance of up to 2 μm; between 2 and 8 μm pole-to-pole distance, the fraction of

chromosomes that both poles can reach linearly increases so that at 5 μm half of the chromosomes can be captured from both poles; and above 8 μm, almost all chromosomes are visible from both poles (Figure 3.5D).

Simulation of spindle assembly kinetics using the model described above explains the data of the beginning of experiment 1, and then it semi-quantitatively predicts that as the poles separate in this experiment and more chromosomes can be reached from both poles, the initially high monotelic and syntelic numbers decrease because stable amphitelic and merotelic attachments emerge. In experiments 2 and 3, this simple model predicts correctly that mono- and syntelic connection numbers increase in the first ~ 10 min, and then decrease. However, quantitative fits of the model predictions to the data are impossible for such a simple model. Specifically, very rapid increase of the amphitelic attachment number at the end of the search, as well as rapid increase of the merotelic attachment number at the beginning of the search are hard to capture numerically. In addition, the attachment rates that are constant in this model have to depend on actual location of the chromosomes in space. In order to reverse-engineer the data of the three experiments, we undertook the spatially explicit simulations described below.

Spatially explicit simulations.

We considered the nuclear space to be an oblate spheroid with dimensions 19 μm×19 μm × 5 μm (based on experimentally measured dimensions), with 12 chromosomes (24 kinetochores) inside and 2 centrosomes at the periphery. Chromosomes and KTs were cylindrical objects with dimensions given below. During the search, each

centrosome nucleated 100 MTs undergoing dynamic instability with the growth and shortening rates shown below. To account for the assumption that the poles search within a certain zone the width of which depends on the pole-to-pole distance, we introduced a spherical region with radius equal to 2 μm around each centrosome such that MTs from one pole invading this region around the other pole immediately catastrophe. This way, the poles search within certain cones in space such that MTs from opposite poles overlap little in space when the pole-to-pole distance is small, but mix more as the poles separate (Figure 3.5A). Starting with a given initial separation, the centrosomes in the simulations moved apart with a time-dependent velocity. From the data of Experiments 1-3 (Figures 3S3A, 3.4C-D), we extracted the pole-to-pole distances as functions of time and implemented these functions in the simulations. There are no spontaneous catastrophe and rescue events: recues prolong MT growth in 'wrong' directions, while frequent catastrophes make it hard to capture properly KTs that are too far from poles [261]. Instead, the MTs undergo catastrophe upon collisions with the nuclear space boundary. Unlike in [240], we did not make the MTs catastrophe upon a collision with the chromosome arm, because this effect is not very important in the geometry considered here. Instead, the assumption was that MTs 'slide off' the chromosome arms and continue to grow in a tangential direction.

In the simulations, syntelic MTs dissociate with the constant rate shown below, mero- and amphitelic connections are stable, and monotelic connections do not disassemble but can convert to syntelic or amphitelic ones. Importantly, we do not have fixed rates of making pole-KT connections. Instead, the connections are formed depending on the poles' and centrosomes' positions and MT numbers and growth/shortening rates. We

found that the following assumptions had to be made to achieve good fit to the data shown in Figures 3.4C-E:

- Each KT has 2 binding sites for MTs. The first MT interacting with a KT has a binding probability 1, whereas for the second MT the binding rate is reduced to 0.5 (to account for the significant probability of other MTs nucleated or transported on the first attached MT and saturating the second binding site). Having only two attachment sites is, of course, an over-simplification, because each KT binds 20-25 MTs [134], so we effectively think of MT bundles rather than individual MTs. Simulations with realistic numbers of the binding sites become too involved.
- Probability to establish the first, monotelic attachment increases linearly from zero to unity over a few minutes. This assumption can account for the gradual increase in the number of MTs involved in the search and increase in MT dynamicity for cells recovering from the drug treatments. Without this assumption, the fits are still good qualitatively, but quantitatively speaking, the assembly becomes too fast.
- We assume that monotelically attached chromosomes rotate, so that the non-captured KT faces away from the capturing pole [20, 241]. The rotation of monotelic chromosomes occurred within 10seconds during our simulations. Because the MTs do not penetrate chromosome arms, this effect makes syntelic attachments less frequent than monotelic ones. This also reduces the number of merotelic attachments as the distance between the poles increases, so that the pole

without a connection to the chromosome 'sees' the captured KT from such angle that the merotelic capture of this KT is less likely.

- Monotelically attached chromosomes move away from the poles to which they are connected, towards the spindle equator [85, 242]. This bias increases with growing pole-pole distance and effectively decreases the probability to establish a syntelic attachment but increases the probability to establish an amphitelic attachment with growing pole-to-pole distance.
- Effectively, the rotation and movement of the chromosomes create the following effects: 1) the probability to establish a syntelic attachment decreases with the pole-to-pole distance, r, as $p(r) = (1 - r/r_{max})$; 2) the probability to establish a merotelic attachment decreases with the pole-to-pole distance, as $p(r) = (1 - r/r_{max})^2$; 3) the probability to establish an amphitelic attachment increases with the pole-to-pole distance, r, as $p(r) = (r/r_{max})$. Here r_{max} is the model parameter, maximal pole-to-pole separation (12-15 μm in the simulations; results are not sensitive to the exact value).

Parameters used in the simulations.

Number of chromosomes = 12; Number of MTs from each pole = 100;

KT length = 0.5 μm; KT radius = 0.44 μm;

Chromosome radius = 0.5 μm; Chromosome length = 2 μm;

MT growth rate = 0.18 μm/s; MT shortening rate = 1 μm/s;

Rate of dissociation of a syntelic MT = 0.5/min.

Stochastic Monte Carlo simulations using the algorithm and parameters described here were performed as described in [240]. The results are reported in Figures 3.5B-C and Figure 3S3.3B.

We also tested a number of modifications of the model:

1) In order to test a possible effect of plastic KTs [243], we introduced varying random angles between the sister KTs and simulated spindle assembly with centrosomes starting at a distance of 0 μm. We found that the results did not fit the experimental data. Specifically, there was a dramatic decrease of amphitelic attachments from ~80% to less than 40% and a respective increase in the number of mis-attachments (syn-, mono- and merotelic attachments). The reasons for that were 'easy access' of MTs from both poles to unattached KTs, as well as more difficult access from the unconnected pole to the unattached KT of monotelic chromosomes. Note, that in our simulations, we tested various initial angles between sister KTs. During the course of running the simulations the initial angle remained static; it is entirely possible that a dynamic dependence of these angles on forces and/or attachments of MTs could remediate the errors of assembly. Moreover, in these simulations the angles between sister KTs were set at less than 180° before the establishment of any KT-MT interaction, but it is likely that this would not occur *in vivo* and that smaller angles would only be a consequence of prior establishment of syntelic attachment. However, our simulation results suggest that even in this case sister pairs that have previously established syntelic attachments would be unlikely to establish other types of attachments (mero- or apmhitelic).

2) To test possible effects of long K-fibers that could form during extensive pre-search [239], we repeated the simulations of Experiment 1 with an effective target size

(representing increased target length as a sum of KT and K-fiber lengths) equal to 2 μm. The results are shown in Figure 3S3.3C; comparison with Figure 3S3.3B illustrates that the increase in the effective target size has very little effect. This is in agreement with the results reported in [240] according to which the effective target size does not influence the accuracy of spindle assembly significantly. The K-fiber length is important for the speed of assembly on the scale of minutes, but on the scale of tens of minutes, characteristic for Experiment 1, this effect is not prominent.

3) In the simulations, the chromosome positions were not correlated with positions of the centrosomes, or with each other. We tried to introduce small unevenness in distributions of the chromosomes, and varied slightly restricted volumes within the oblate spheroid to which positions of the chromosomes were limited and found that these changes did not affect the predicted time series for the spindle assembly. Greater inhomogeneity and/or restriction of the chromosomes to more confined spaces did perturb the results significantly, but there are no clear indications from our experimental data that such effects take place.

4) We simulated the scenario in which the tendency for monotelic chromosomes to move away from the capturing pole was delayed by a few minutes. Within the delay period, a few amphitelic chromosomes appear, so the monotelic chromosomes can move along respective k-fibers. Such delay did not change the results significantly.

5) We allowed MTs to search the whole space. The results (Figure 3S3.5A-B) compare poorly to the experimental data. However, when we at the same time allowed amphitelic and merotelic attachments to disassemble as a function of pole-pole distance – faster at small distances and slower at greater distances, the model predicted time series

that better reproduce, despite residual discrepancies (see main text for details), the experimental data (Figure 3S3.5C-D). The rationale for such assumption is the possible effect of tension on the sister KTs exerted by attached MTs. Such tension depends on the angle between KTs connecting respective chromosomes to opposite poles, and therefore on the pole-pole distance. Specifically, we scaled the disassembly with probability of MT detachment equal to $P = 0.5 \times (1 - r/r_d)$ where r is the pole-pole distance, and r_d = 3.5μm is the maximal distance at which this effect takes place.

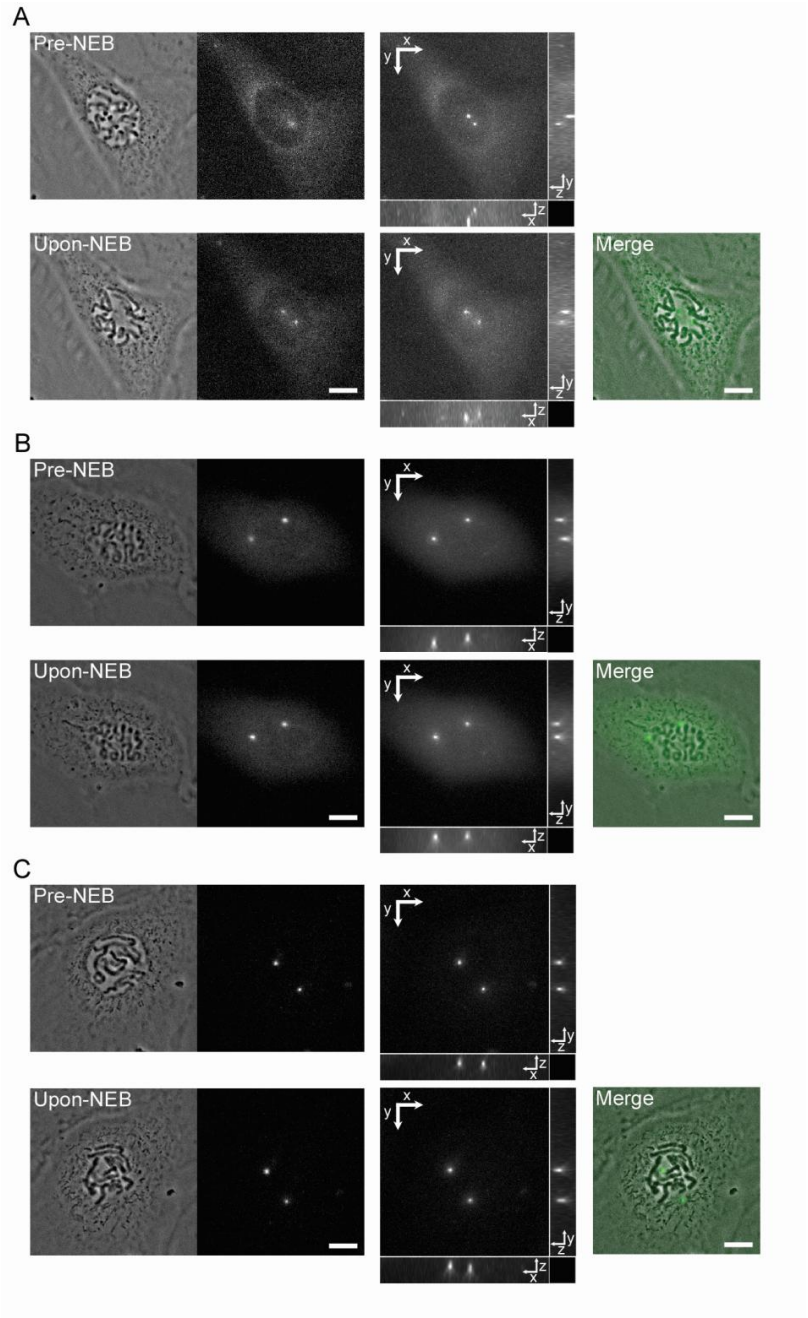

Figure 3S3.1. *Examples of cells with incomplete centrosome separation at NEB.* Examples of the three centrosome configurations [Top-bottom (A); side-side (B); top-side (C)] depicted in Figures 3.1A-Bii-iv in PtK1 cells expressing GFP-γ-tubulin. For each example, images of the cell prior to NEB (Pre-NEB) are shown in the top row and images of the cell upon NEB (Upon-NEB) are shown in the bottom row. Images of chromosomes and centrosomes at a single focal plane are shown in the first and second column, respectively. Maximum intensity projections in XY accompanied by YZ and XZ views are shown in the third column. The far-right column displays the overlay of phase contrast and fluorescence images at a single focal plane upon NEB. Scale bars, 5 μm.

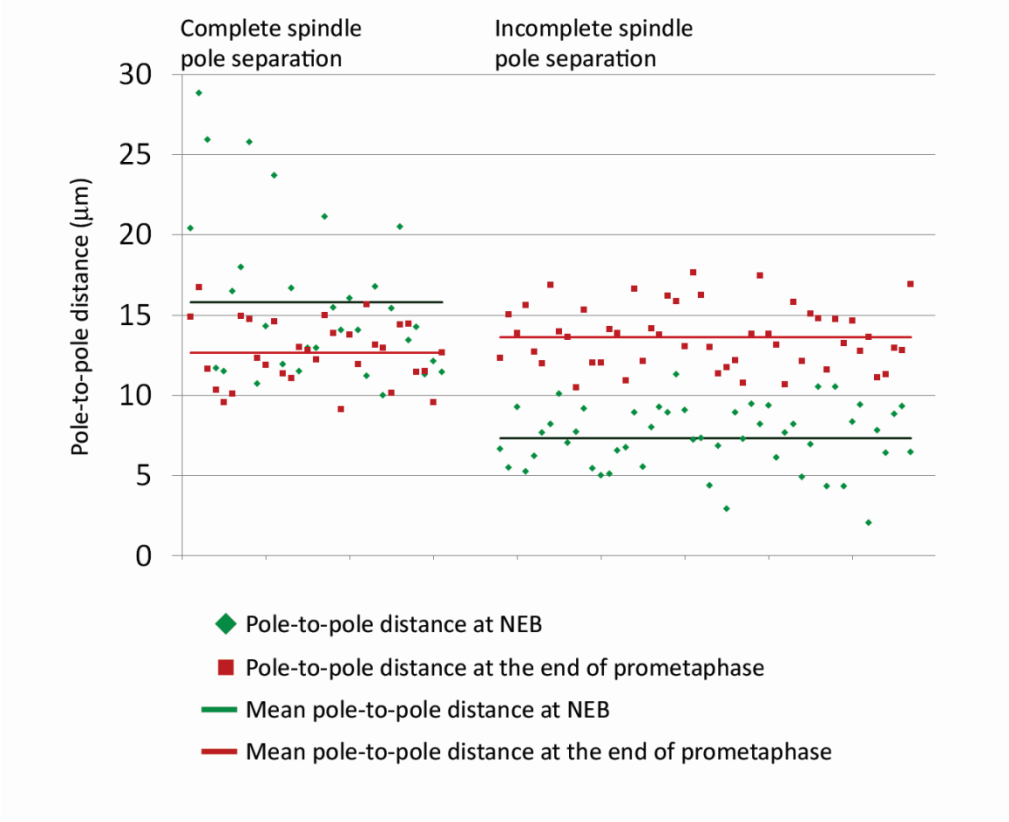

Figure 3S3.2. *Pole-to-pole distance in PtK1 cells with complete vs. incomplete centrosome separation at NEB.* Pole-to-pole measurements were obtained both upon NEB and at the end of prometaphase for all PtK1 cells imaged during the experiments summarized in figures 3.1 and 3.2.

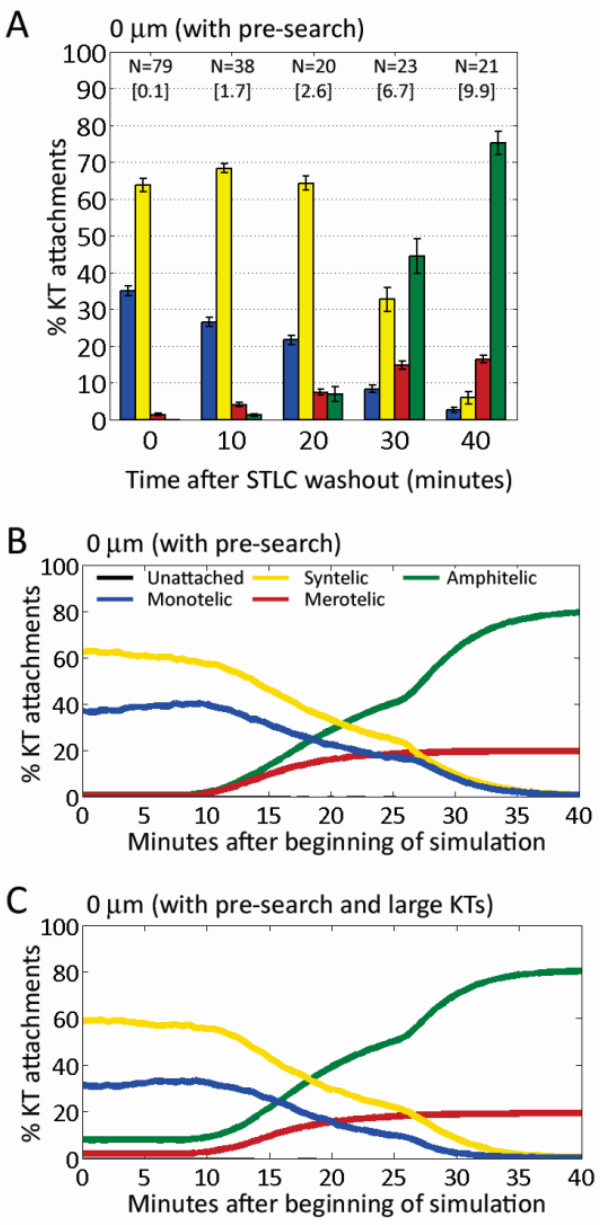

Figure 3S3.3. *The size of the KT target does not affect the numbers and types of KT attachments in cells recovering from a 2-hour STLC treatment.* (A) Frequencies of different types of KT attachments in cells washed-out of STLC after a 2-hr treatment. In these cells, the spindle poles gradually separated after persisting in very close proximity for 2 hrs and establishing KT attachment (spindle poles moving apart from 0 μm, with a 2-hr period of pre-search). N represents the number of cells analyzed. The numbers in square brackets represent the average pole-to-pole distance (in μm) at each time-point. (B) Computer simulation of spindle bipolarization with spindle poles starting at a distance of 0 μm after a 2-hr pre-search period (as in the experiment in A). (C) Computer simulation of spindle bipolarization under conditions identical to those used in B, except for the KT target size, which was set to 2 μm, as opposed to 0.5 μm in B.

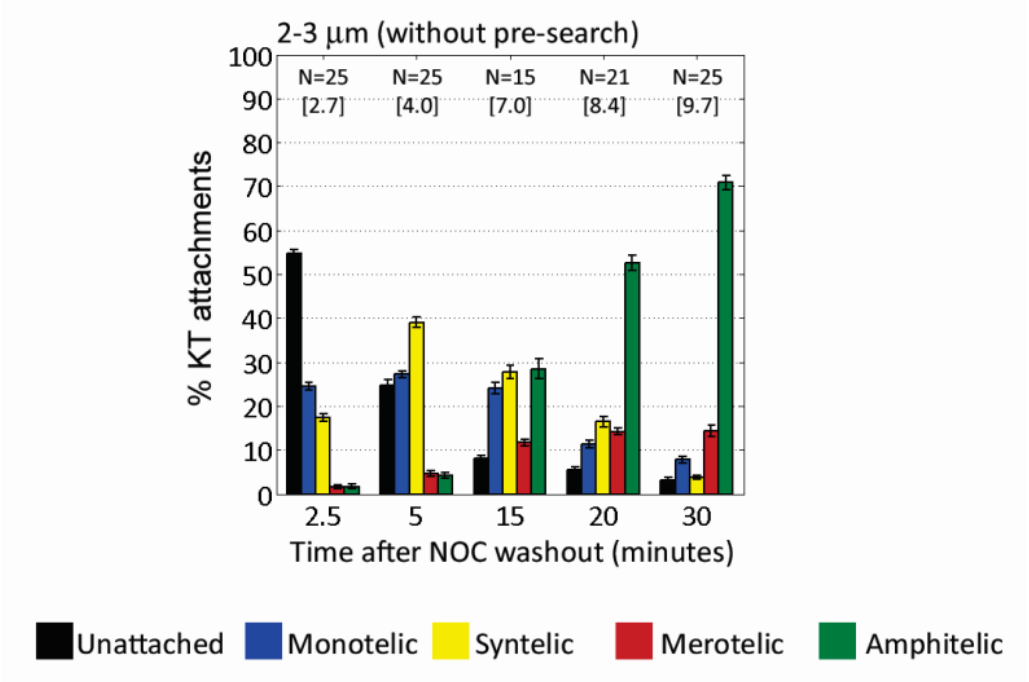

Figure 3S3.4. *Frequencies of different types of KT attachments in PtK1 cells with an initial pole-to-pole distance of 2-3 µm.* Cells were first treated with STLC for 2 hrs, then washed out and re-incubated in STLC-free media for 15 min (to allow spindle poles to move apart to an average distance of 2-3 µm), then incubated in NOC for 30 min, and finally washed out of the NOC and fixed at subsequent time-points. N represents the number of cells analyzed. The numbers in square brackets represent the average pole-to-pole distance (in µm) at each time-point.

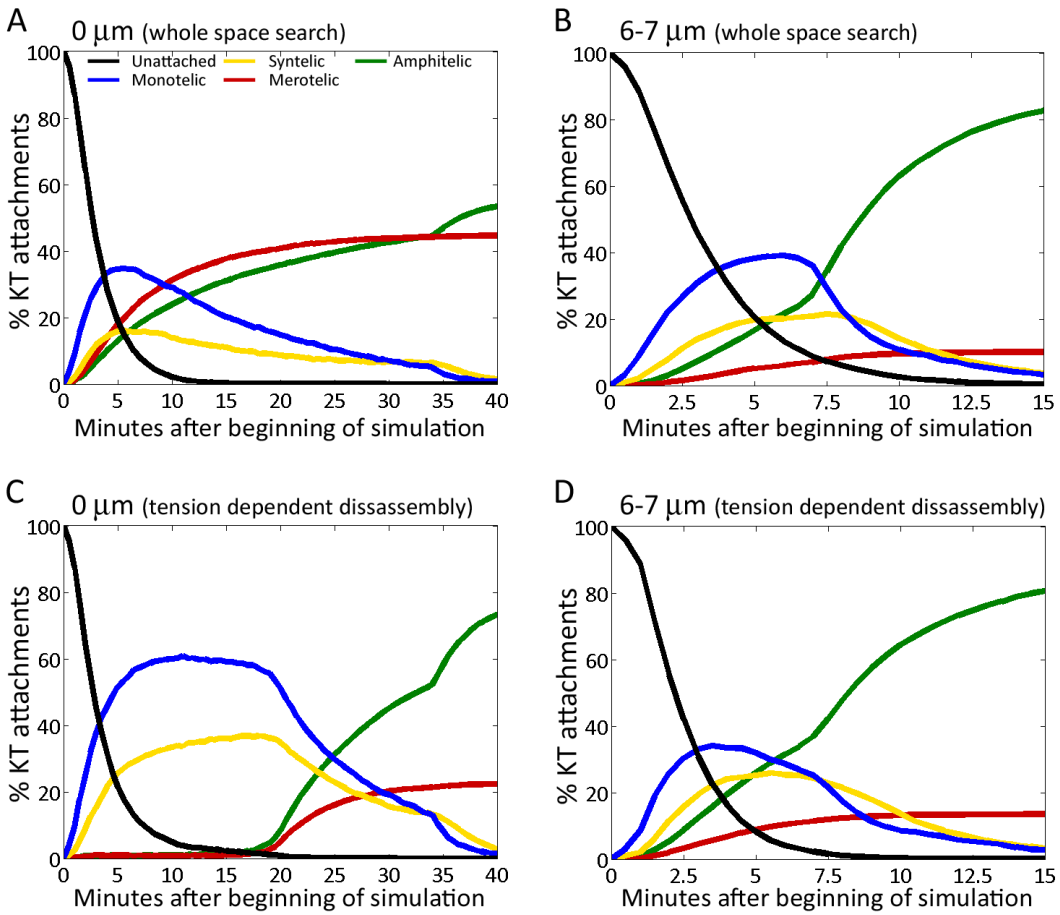

Figure 3S3.5. *Computer simulations of spindle assembly without shielding effect can reproduce experimental results only if merotelic and amphitelic KT attachments disassemble at very high rates at small pole-to-pole distances.* (A-B) Time-course simulations of spindle assembly in the absence of shielding effect between the two centrosomes (whole-space search). (A) Simulation starting with a spindle pole distance of 0 µm without pre-search (as in figure 3.4C). (B) Simulation starting with a spindle pole distance of 6 µm without pre-search (as in figure 3.4D). Whereas the simulation results at the initial distance of 6 µm fit the experimental results, the simulation results for an initial distance of 0 µm are very different from the experimental results. (C-D) Time-course simulations of spindle assembly with whole-space search and rapid disassembly of merotelic and amphitelic attachments at small pole-to-pole distances. (C) Simulation starting with a spindle pole distance of 0 µm without pre-search (as in figure 3.4C). (D) Simulation starting with a spindle pole distance of 6 µm without pre-search (as in figure 3.4D). At the initial pole-to-pole distance of 6 µm the simulation results fit well the experimental results, but that is not the case for an initial pole-to-pole distance of 0 µm.

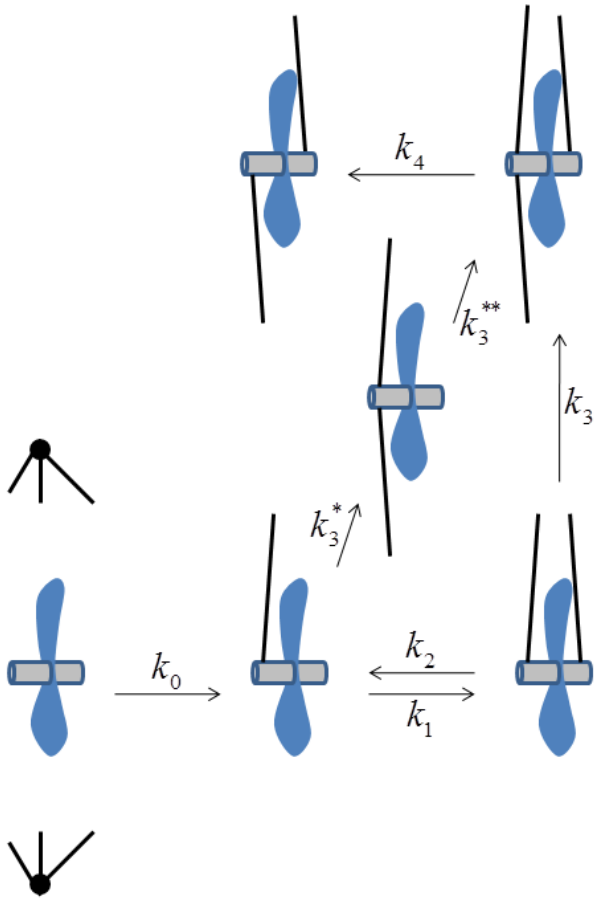

Figure 3S3.6. *Possible pathways of establishment of KT attachment during simulation of approximate kinetics of spindle assembly.* All the KTs are unattached (bottom left) at the beginning of the simulation. Merotelic and correct amphitelic attachments can be achieved through different pathways.

Chapter 4

Transient mitotic spindle defects as a cause of chromosomal instability in human cancer cells.

Silkworth WT, Nardi IK, and Cimini D.

Manuscript in preparation

Author Contributions

Conceived and designed the experiments: WTS IKN DC. Performed the experiments: WTS IKN. Analyzed the data: WTS DC. Contributed reagents/materials/analysis tools: DC. Wrote the paper: WTS DC

Abstract

Accurate chromosome segregation during mitosis is necessary for stability of the genome in developing organisms, and erroneous chromosome segregation is known to cause miscarriage, birth defects, and cancer in humans. Recent reports in both cancer and non-cancer cells have shown a link between transient abnormal mitotic spindle geometry and the establishment of kinetochore mis-attachments, which in turn cause chromosome mis-segregation in the form anaphase lagging chromosomes. In particular, two mechanisms have been described, one of which occurs in cells that assemble a multipolar spindle but bipolarize before anaphase onset (transient multipolarity mechanism, TM); and one that is characterized by a delay in centrosome separation (incomplete spindle pole separation mechanism, ISPS), by which the centrosomes are not completely separated at the time of nuclear envelope breakdown (NEB), and instead achieve complete separation after NEB. In this study, we investigated the role that these mechanisms play in cancer cell chromosomal instability (CIN). To this end, we screened a panel of cancer cells from various sites to determine the prevalence of mitotic spindle geometry defects in early mitosis and how such defects correlate to chromosome segregation defects. Our data show that human cancer cells from various sites exhibit one or both of the two transient mitotic spindle defects that can promote kinetochore mis-attachment and chromosome mis-segregation, thus indicating that transiently abnormal spindle geometry plays an important role in CIN.

Introduction

We have recently characterized two mechanisms [229, 262] that cause cells in early mitosis to establish many kinetochore mis-attachments (particularly merotelic, in which a single kinetochore is bound to microtubules from two spindle poles instead of just one). One of these mechanisms occurs in cells that assemble a multipolar spindle but bipolarize before anaphase onset (transient multipolarity mechanism, TM). During the multipolar stage, cells establish high rates of merotelic kinetochore attachments, which then cause chromosome mis-segregation and aneuploidy [229, 233]. The other mechanism we identified is characterized by a delay in centrosome separation (incomplete spindle pole separation mechanism, ISPS) [262]. Cells that display ISPS are cells in which the centrosomes are not completely separated at the time of nuclear envelope breakdown (NEB), and in which spindle pole separation is completed after NEB. These cells exhibit higher rates of merotelic kinetochore attachment and chromosome mis-segregation compared to cells that complete centrosome separation before NEB [262]. In the present study, we examined a selected panel of human cancer cell lines to infer whether and how much the above described mechanisms can explain chromosomal instability (CIN) in cancer cells (for a review on CIN see [263]. Although the TM mechanism was initially characterized in cancer cells [207, 229], and is already known to play a major role in CIN [229, 233], looking at both TM and ISPS in the same set of cells lines, allowed us to draw general conclusions. Thus, for this study we used the following CIN cancer cells lines: HT-29 (colorectal adenocarcinoma); H460 (lung carcinoma); HeLa (cervical adenocarcinoma); DU 145 (prostate carcinoma); MCF7 (breast adenocarcinoma); MDA-MB-231 (breast adenocarcinoma). These cells were

selected due to the fact that breast, prostate, lung, and colorectal cancers comprise the top 3 sites of cancer in both women and men in the US [264]. As controls, we used the MIN (microsatellite instability) colorectal cancer cell line HCT-116 and the immortalized, non-transformed retina pigmented epithelial cell line hTERT-RPE-1.

Materials and Methods:

Cell culture

HCT 116 (ATCC, Manassas, VA) cells were cultured in McCoy's 5a Medium (Invitrogen); HT-29 (ATCC, Manassas, VA) cells were cultured in McCoy's 5a Medium (Invitrogen); MCF-7 cells (a generous gift from Iuliana Lazar, Virginia Tech, Blacksburg, VA) were cultured in Eagle's Minimum Essential Medium (Invitrogen) supplemented with non-essential amino acids (Invitrogen) and 0.01mg/ml bovine insulin; DU-145 cells (ATCC, Manassas, VA) were cultured in Eagle's Minimum Essential Medium (ATCC, Manassas, VA); NCI-H460 (ATCC, Manassas, VA) cells were cultured in RPMI-1640 (Invitrogen); HeLa (ATCC, Manassas, VA) cells were cultured in Dulbecco's Modified Eagle's Medium (DMEM; Invitrogen); MDA-MB-231 cells (a generous gift from Young Ju, Virginia Tech, VA) were cultured in DMEM; hTERT RPE-1 (ATCC, Manassas, VA) cells were cultured with DMEM:Ham's F-12 (ATCC, Manassas, VA). All the culture media were supplemented with 10% fetal bovine serum (FBS), 100 units/mL penicillin, 100 μg/mL streptomycin, and 0.25 μg/mL amphotericin B (antimycotic). All cell lines were grown at 37°C in a 5% CO_2 humidified incubator.

Fixation and Immunofluorescence

Cells were grown on acid-washed coverslips in 30mm petri dishes to ~70% confluence. Prior to immunostaining, cells were rapidly rinsed in 1x phosphate-buffered saline (PBS), fixed for 10 seconds in 4% paraformaldehyde diluted in 1x PHEM pH 7.0 (60 mM PIPES, 25 mM Hepes, 10 mM EGTA, 2 mM $MgCl_2$), permeablized in 0.5%

Triton-X-100 in 1x PHEM, and then fixed for 20 minutes in 4% paraformaldehyde in 1x PHEM. Cells were then rinsed 3 times in PBS and incubated in 10% boiled goat serum (BGS) at room temperature for 1 hour and then incubated in primary antibodies diluted in 5% BGS at 4°C overnight. Cells were then rinsed 3 times for 5 minutes in 1xPBS-T (Phosphate Buffered Saline with 0.05% Tween-20 added) and incubated in secondary antibodies for 45-60 minutes at room temperature. Following the incubation in secondary antibodies cells were washed in PBS-T, stained with DAPI, washed again and then mounted in 90% glycerol and 0.5% N-propyl gallate (anti-fade). Primary antibodies were diluted as follows: mouse anti α-tubulin (DM1A, Sigma-Aldrich) was diluted 1:500, ACA (human anti centromere antigen, Antibodies, Inc.) was diluted 1:100, and rabbit anti γ-tubulin (Abcam) was diluted 1:100. Secondary antibodies were diluted as follows: Alexa488 goat anti-mouse (Molecular Probes) was diluted 1:400-1:500, goat anti rabbit X-Rhodamine (Jackson ImmunoResearch Laboratories, Inc.) was diluted 1:100, and goat anti human Cy5 (Zymed Laboratories) was diluted to 1:100.

Confocal microscopy

Immunostained cells were analyzed using a Nikon Eclipse TE2000-U inverted microscope equipped with a Swept Field Confocal system (Prairie Technologies) and 100X 1.4 NA Plan-Apochromatic phase–contrast objective, trans-illumination light source, diascopic shutter, and ProScan stage (Prior Scientific). The Swept Field Confocal system was outfitted with filters for illumination at 488 [Ar], 568 [Kr], and 647 [Kr] nm from a 150 mW krypton and 400 mW argon lasers. Digital images were captured using an HQ2 CCD camera (Photometrics). Laser lines, shutters, confocal system, and image

acquisition were controlled by a PC computer via the NIS Elements Software (Nikon). A 0.6μm step size was used to acquire z-series optical sections through imaged cells.

Results and Discussion

Cancer cells from different sites possess multipolar spindles in prometaphase, but not in anaphase

We first determined the frequencies of multipolar spindles in prometaphase and anaphase cells immunostained for microtubules and kinetochores. We found that all of the CIN cancer cells exhibited high frequencies of multipolar prometaphase cells (Figure 1A). As expected, the non-CIN HCT-116 cell line and the hTERT-RPE-1 cells displayed significantly lower frequencies of multipolar prometaphase spindles. In agreement with previous studies [207, 229], for most CIN cancer cells the frequencies of multipolarity in anaphase was significantly lower (<2.8%) (Figure 4.1A). This observation indicates that these cells can undergo the process of centrosome clustering/spindle pole coalescence previously described [188, 189]. These cells are also expected to form high numbers of merotelic kinetochore attachments during the transient multipolar stage and to exhibit high frequencies of anaphase lagging chromosomes as a consequence of the high rates of kinetochore mis-attachments. The exception to this trend was represented by the breast cancer cell lines MCF-7 and MDA-MB-231, in which the frequency of multipolar anaphases, although lower than in prometaphase, did not show the dramatic drop observed in the other CIN cell lines (Figure 4.1A). To better quantify the efficiency of multipolar spindle pole coalescence we calculated the multipolar prometaphase to anaphase ratio (Figure 4.1B). This ratio was 1.68 for hTERT-RPE-1 (Figure 4.1B), which suggested that most multipolar prometaphase cells underwent multipolar cell division. Non-CIN HCT 116 cells possessed a multipolar prometaphase/anaphase ratio of 3.23 indicating a moderate ability to cluster centrosomes. All the CIN cancer cell lines

displayed a ratio of 5.74 – 6.74, with the exception of the two breast cancer cell lines, with ratios of 1.74 (MCF-7) and 4.23 (MDA-MB-231) (Figure 4.1B). In summary, our data indicate that most CIN cancer cells can cluster the centrosomes of multipolar spindles and undergo bipolar mitosis, and that the TM mechanism can explain CIN in most cases. This was not the case for MCF-7 cells, which seem to behave more like non-transformed cells, and MDA-MB-231, which exhibited an intermediate behavior that was closer to that of non-CIN cancer cells than other CIN cell lines.

Incomplete spindle pole separation upon NEB is very common in breast cancer cells

Next, we determined the frequencies of ISPS in the same set of cell lines. To this end, we immunostained cells for microtubules, kinetochores, and γ-tubulin (a centrosome marker), and specifically analyzed prometaphase cells that had just undergone NEB. Identification of cells at this mitotic stage was determined by DAPI staining, because in cells that have just completed NEB, the chromosomes appeared arranged in a spherical configuration, but the outline of the periphery of the nuclear space was irregular in shape due to the chromosome arms becoming free of the nuclear envelope constraints, which suggested completion of NEB. Moreover, visualization of the kinetochores revealed that there is no metaphase plate and the kinetochores too are arranged in a spherical configuration, suggesting that they are not yet attached to microtubules. Because the ISPS was manifest with different degrees of centrosome separation (or lack thereof), cells that exhibited ISPS were categorized into 3 distinct categories based on centrosome arrangement: offset, close, and monopolar (see Figure 4.1C for examples of these phenotypes). Previous studies have found ISPS to occur approximately 45% of the time

in both non-transformed and transformed cell populations [215, 220, 262]. Here, we found that 30-68% of cancer cells exhibit ISPS (Figure 4.1D). Interestingly, MCF-7 and MDA-MB-231 cells exhibited the highest incidence of ISPS, with frequencies close to 70% in both cases (Figure 4.1D). These results suggest that ISPS may play an important role in promoting kinetochore mis-attachment and chromosome mis-segregation in breast cancer cells, and may explain the high frequencies of anaphase lagging chromosomes (Figure 4.1E), despite the reduced efficiency of the TM mechanism in these cells (Figures 4.1A-B).

Reduced frequencies of anaphase lagging chromosomes in some cancer cells prone to TM.

When analyzing anaphase lagging chromosomes, we found relatively low frequencies in H460 and DU 145 cells (Figure 4.1E), despite their apparent susceptibility to the TM mechanism (Figures 4.1A-B). It has been previously shown that microtubule dynamics, and hence correction of kinetochore mis-attachments, are impaired in certain cancer cells [213, 236]. It is possible that in H460 and DU 145 cells microtubule dynamics may instead be occurring at levels that lead to enhanced correction of mis-attachments.

Breast cancer cells at more advanced stage display more efficient centrosome clustering compared to breast cancer cells at earlier stage.

The multipolar prometaphase to anaphase ratio in MCF-7 cells was similar to that of RPE-1 cells, and lower than the ratio in HCT 116 cells (Figure 4.1B). Yet, the

frequency of anaphase lagging chromosomes in MCF-7 cells is significantly higher than that observed in either RPE-1 or HCT116 (Figure 4.1E). Being estrogen receptor-positive and progesterone-positive, MCF-7 cells are considered to be representative of early stage breast cancer, whereas MDA-MB-231 cells, being estrogen receptor-negative and progesterone-negative, are considered to be a more advanced breast cancer cell line. Interestingly, the multipolar prometaphase to anaphase ratio in MDA-MB-231 is higher than in MCF-7, indicating that these cells are more efficient at clustering the centrosomes of multipolar spindles. These data suggest that, at least in breast cancer, the CIN observed at early stages of cancer development may be largely linked to the increase in kinetochore mis-attachments caused by the ISPS mechanism. At later stages, cancer cells acquire the ability to cluster supernumerary centrosomes, and this may become the major source of kinetochore mis-attachment and CIN. However, the rate of chromosome mis-segregation ultimately depends both on the number of kinetochore mis-attachments formed in early mitosis and on the efficiency of the correction mechanisms (reviewed in [13, 265]). Thus, the lower rates of anaphase lagging chromosomes in MDA-MB-231 cells despite their high rates of both TM and ISPS, may depend on the ability to correct large numbers of kinetochore mis-attachments.

In conclusion, we have shown here that a number of different human cancer cell types display one or both of two transient mitotic spindle defects that have been previously shown to promote kinetochore mis-attachment and chromosome mis-segregation. While the specific mechanism by which the majority of cancer cells acquire supernumerary centrosomes remain unclear, once present, cells develop an ability to cluster extra centrosomes to avoid the deleterious effect of undergoing multipolar cell

division. Interestingly, cancer cells that cluster centrosomes less efficiently, such as MCF-7 cells, exhibit ISPS at very high frequencies. In MCF-7 cells it appears that the ISPS mechanism is the major mechanism by which merotelically attached anaphase lagging chromosomes are formed. Interestingly, both early and late stage breast cancer cells display similar rates of ISPS, suggesting that this mechanism may play an important role in breast cancer CIN. In addition, late stage breast cancer cells can also efficiently cluster supernumerary centrosomes, suggesting that ability to cluster centrosomes may be indicative of tumorigenic stage and potential. Finally, that ISPS has been observed at elevated frequencies in both early stage cancer (this study) and in non-transformed cells [214, 262] suggests that ISPS may contribute to early initiation events in cancer progression. Future studies should be aimed at the characterization of transient spindle defects in pre-malignant neoplasms. Studies such as these will allow for a systematic characterization of transient spindle defects throughout cancer development. Remarkably, both TM and ISPS appear to be common features of cancer cells from different sites, thus potentially representing general mechanisms of tumor progression.

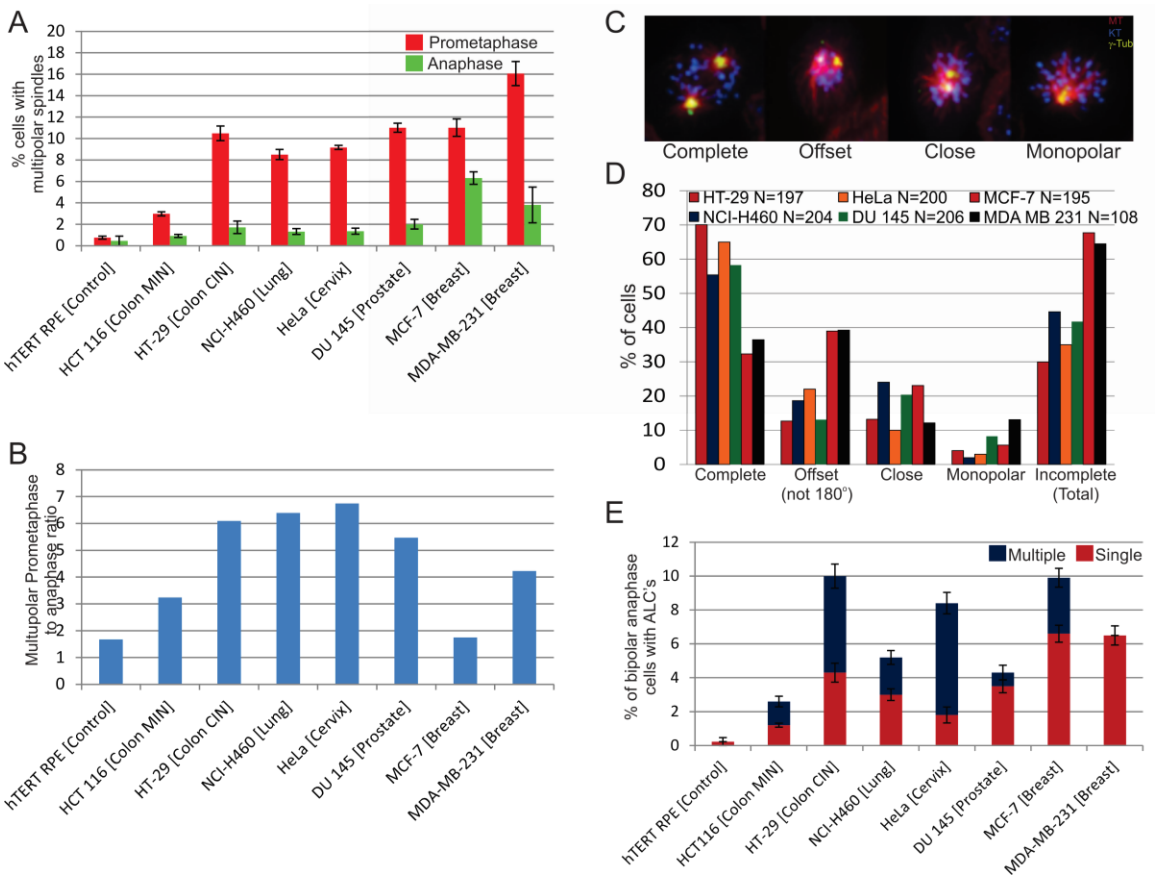

Figure 4.1 *Multiple cancer cells exhibit both transient multipolarity and incomplete spindle pole separation with high frequencies of lagging chromosomes.* (A) Histogram depicting the frequencies of both multipolar prometaphase (red) and anaphase (green) cells. Error bars denote SEM. (B) Multipolar prometaphase-to-multipolar anaphase ratio, R. R >1 indicate successful coalescence of supernumerary spindle poles before anaphase onset. Red upon NEB, R=1 multipolar spindles in prometaphase progress through anaphase as multipolar spindles. (C) Representative images of cancer cells with various types of incomplete spindle pole separation. (D) Quantification of incomplete spindle pole separation in a panel of cancer cells. (E) Rates of single (red) and multiple (blue) anaphase lagging chromosomes (ALC's) in cancer cells. Error bars denote SEM.

Table 4.1. ***Characteristics of a panel of cancer cells from different sites.***

Cell Line	Organ / Site	Disease	Cell Type	Modal Chromosome Number (range)	Gender (M/F) and Age
hTERT RPE-1	Retina	-	Epithelial	46 (No Data)	F (No Data)
HCT 116	Colon	colorectal carcinoma	Epithelial	45 (No Data)	M (Adult)
HT-29	Colon	colorectal Adeno-carcinoma	Epithelial	71 (68 – 72)	F (44)
NCI-H460	Lung/pleural effusion	carcinoma (large cell lung cancer)	Epithelial	57 (53 – 65)	M (No Data)
HeLa	Cervix	Adeno-carcinoma	Epithelial	82 (70 – 164)	F (31)
DU 145	Prostate/Brain metastasis	carcinoma	Epithelial	61; 62 (No Data)	M (69)
MCF-7	Mammary gland /pleural effusion	Adeno-carcinoma	Epithelial	82 (66 – 87)	F (69)
MDA-MB-231	Mammary gland / pleural effusion	Adeno-carcinoma	Epithelial	64 (52 – 68)	F (51)

Data compiled from the American Type Culture Collection, ATCC [266]

Chapter 5

Conclusions and future directions

Previous studies have shown that a number of different mechanisms can increase the rates of kinetochore mis-attachment formation (reviewed in [265]). The work presented here characterized two novel distinct mechanisms by which mammalian cells establish mis-attachments between microtubules and kinetochores. Both mechanisms are a result of transiently aberrant mitotic spindle geometry that is established during early mitosis. The mechanism described in chapter 2, multipolar spindle pole coalescence, has been shown to frequently occur in numerous cancer cell lines. Presence of supernumerary centrosomes, in cancer cells, leads to assembly of multipolar mitotic spindles during prometaphase. Because of the presence of multiple microtubule nucleation centers, microtubules emanating from different spindle poles frequently become attached to a single sister kinetochore (merotelic kinetochore attachment) [207, 229]. Interestingly, both computational and experimental approaches have shown that as the number of spindle poles increases so do the numbers of merotelic attachments [240]. As mitosis progresses from prometaphase to meta- and anaphase, the extra centrosomes cluster, which allows these cells to undergo bipolar cell division, thus avoiding the deleterious effect of multipolar cell division [207, 229]. However, the increase in merotelic attachments that are formed in early mitosis contributes to the increased rate of anaphase lagging chromosomes. The relationship between supernumerary spindle poles and mis-attachments reveals the significance of mitotic spindle geometry in the establishment of kinetochore-microtubule attachments, as it is not the extra spindle poles *per se* that cause mis-attachments but rather their position in relation to individual sister kinetochores.

The results from chapter 3 validated this idea. The work conducted confirmed previous observations that in ~45% of tissue culture cells isolated from both different

organisms and different sites/organs of the same organism (see previous chapter), the spindle poles failed to achieve diametrically opposed positions around the nucleus prior to NEB [214, 215, 218, 262]. Inability of the centrosomes to attain sufficient distance from one another results in a transient geometric defect of the mitotic spindle, in which a single sister kinetochore will likely face, and bind to microtubules from both spindle poles instead of just one. Indeed, results showed that as the proximity between spindle poles varies, so too did the number and types of kinetochore microtubule attachments. Overall, when the spindle poles begin mitotic spindle assembly at sufficiently close distances from one another, there is an increase in the number of kinetochore mis-attachments, (particularly merotelic), which will then promote elevated levels of chromosome mis-segregation in anaphase.

Finally, chapter 4 investigated how prevalent these two mechanisms were in a panel of human cancer cells from different sites. The data showed that both of these mechanisms occured frequently, albeit to varying degrees in cancer cells. Interestingly, both early and late stage breast cancer cells did not appear to efficiently cluster the centrosomes of multipolar spindles, but exhibited incomplete spindle pole separation at NEB at rates that are dramatically higher than those observed in other cancer cells. This suggests that the ISPS mechanism may largely explain the CIN observed in breast cancer cells. Furthermore, there are varying levels of chromosome mis-segregation in the panel of cancer cells analyzed, suggesting that other mechanisms may be at work that either suppress or facilitate chromosome mis-segregation events.

The specific mechanism for how cancer cells obtain supernumerary centrosomes is still a matter of some debate. Two promising ideas are that i) there are mutations in

genes that are required for centrosome duplication or ii) failure of cytokinesis during cell division results in polyploid cells with extra centrosomes (reviewed in [267]). Sequencing of genes responsible for centrosome duplication within specific cancer cell lines will elucidate if mutations are responsible for production of supernumerary centrosomes. In contrast, long term live cell imaging to assess the frequency of cytokinesis failure and overall survival of cells that fail abscission will allow to test if failure of cytokinesis is the mechanism by which cancer cells obtain supernumerary centrosomes. Moreover, biochemical studies of specific genes involved in focusing and separation of spindle poles both at the nucleotide and protein level will reveal the functionality and overall contribution of these genes in both formation of and coalescence of extra centrosomes. Additionally, the initial positioning of centrosomes upon NEB may also contribute to the efficiency of clustering. Experiments in which the position and movement of the multiple centrosomes is tracked over time to determine their ability to cluster, in combination with mathematical modeling, will prove useful in understanding the exact role of geometry in spindle organization.

Failure of centrosomes to occupy diametrical positions around the nucleus has been known since the mid-70s [214, 215]; however, the finding that this results in increased rates of chromosome mis-segregation is novel, and the work presented here (Chapter 3) formally demonstrated it for the first time. This phenomenon opens up an interesting avenue for study. It is well-known that in many tissues (e.g., epithelia) the cell division plane must be oriented in a specific direction in order to maintain tissue homeostasis. It is also widely acknowledged that the orientation of the mitotic spindle plays a key role in determining the position of the cleavage plane, and signals from the

cortex and/or the extracellular membrane are thought to determine spindle orientation [268]. It will be interesting to determine whether multipolar spindle pole coalescence and/or timely separation of the centrosomes also depends on signals from the plasma membrane, the extracellular matrix, or adjacent cells.

References

1. Nicklas, R.B., L.E. Krawitz, and S.C. Ward, *Odd chromosome movement and inaccurate chromosome distribution in mitosis and meiosis after treatment with protein kinase inhibitors.* J Cell Sci, 1993. **104 (Pt 4)**: p. 961-73.
2. Vandre, D.D. and V.L. Wills, *Inhibition of mitosis by okadaic acid: possible involvement of a protein phosphatase 2A in the transition from metaphase to anaphase.* J Cell Sci, 1992. **101 (Pt 1)**: p. 79-91.
3. Andreassen, P.R. and R.L. Margolis, *Induction of partial mitosis in BHK cells by 2-aminopurine.* J Cell Sci, 1991. **100 (Pt 2)**: p. 299-310.
4. Alberts, B., et al., *Molecular Biology of The Cell* fourth ed, ed. S. Gibbs2002, New York: Garland Science. 1463.
5. Hassold, T. and P. Hunt, *To err (meiotically) is human: the genesis of human aneuploidy.* Nat Rev Genet, 2001. **2**(4): p. 280-91.
6. Sanchez, J.M., et al., *Cytogenetic study of spontaneous abortions by transabdominal villus sampling and direct analysis of villi.* Prenat Diagn, 1999. **19**(7): p. 601-3.
7. Hassold, T., et al., *The relationship of maternal age and trisomy among trisomic spontaneous abortions.* Am J Hum Genet, 1984. **36**(6): p. 1349-56.
8. Sumner, A.T., *Chromosomes: Organization and Function*2003: Blackwell Science Ltd. 287.
9. Dunham, A., et al., *The DNA sequence and analysis of human chromosome 13.* Nature, 2004. **428**(6982): p. 522-8.
10. Hattori, M., et al., *The DNA sequence of human chromosome 21.* Nature, 2000. **405**(6784): p. 311-9.
11. Nusbaum, C., et al., *DNA sequence and analysis of human chromosome 18.* Nature, 2005. **437**(7058): p. 551-5.
12. Cimini, D. and F. Degrassi, *Aneuploidy: a matter of bad connections.* Trends Cell Biol, 2005. **15**(8): p. 442-51.
13. Cimini, D., *Merotelic kinetochore orientation, aneuploidy, and cancer.* Biochim Biophys Acta, 2008. **1786**(1): p. 32-40.
14. Weaver, B.A. and D.W. Cleveland, *Does aneuploidy cause cancer?* Curr Opin Cell Biol, 2006. **18**(6): p. 658-67.
15. Boveri, T., *Concerning the origin of malignant tumours by Theodor Boveri. Translated and annotated by Henry Harris.* J Cell Sci, 2008. **121, Supplement 1**: p. 1-84.
16. Rieder, C.L. and A. Khodjakov, *Mitosis through the microscope: advances in seeing inside live dividing cells.* Science, 2003. **300**(5616): p. 91-6.
17. Kapoor, T.M., et al., *Probing spindle assembly mechanisms with monastrol, a small molecule inhibitor of the mitotic kinesin, Eg5.* J Cell Biol, 2000. **150**(5): p. 975-88.
18. Kashina, A.S., et al., *A bipolar kinesin.* Nature, 1996. **379**(6562): p. 270-2.
19. Sharp, D.J., et al., *The bipolar kinesin, KLP61F, cross-links microtubules within interpolar microtubule bundles of Drosophila embryonic mitotic spindles.* J Cell Biol, 1999. **144**(1): p. 125-38.

20. Rieder, C.L. and S.P. Alexander, *Kinetochores are transported poleward along a single astral microtubule during chromosome attachment to the spindle in newt lung cells.* J Cell Biol, 1990. **110**(1): p. 81-95.
21. Skibbens, R.V., V.P. Skeen, and E.D. Salmon, *Directional instability of kinetochore motility during chromosome congression and segregation in mitotic newt lung cells: a push-pull mechanism.* J Cell Biol, 1993. **122**(4): p. 859-75.
22. Rieder, C.L. and E.D. Salmon, *Motile kinetochores and polar ejection forces dictate chromosome position on the vertebrate mitotic spindle.* J Cell Biol, 1994. **124**(3): p. 223-33.
23. Haering, C.H. and K. Nasmyth, *Building and breaking bridges between sister chromatids.* Bioessays, 2003. **25**(12): p. 1178-91.
24. Zhai, Y., et al., *Microtubule dynamics at the G2/M transition: abrupt breakdown of cytoplasmic microtubules at nuclear envelope breakdown and implications for spindle morphogenesis.* J Cell Biol, 1996. **135**(1): p. 201-14.
25. Azimzadeh, J. and M. Bornens, *Structure and duplication of the centrosome.* J Cell Sci, 2007. **120**(Pt 13): p. 2139-42.
26. Zimmerman, W., C.A. Sparks, and S.J. Doxsey, *Amorphous no longer: the centrosome comes into focus.* Curr Opin Cell Biol, 1999. **11**(1): p. 122-8.
27. Mitchison, T. and M. Kirschner, *Dynamic instability of microtubule growth.* Nature, 1984. **312**(5991): p. 237-42.
28. Compton, D.A., *Spindle assembly in animal cells.* Annu Rev Biochem, 2000. **69**: p. 95-114.
29. Hogan, C.J. and W.Z. Cande, *Antiparallel microtubule interactions: spindle formation and anaphase B.* Cell Motil Cytoskeleton, 1990. **16**(2): p. 99-103.
30. Hayden, J.H., S.S. Bowser, and C.L. Rieder, *Kinetochores capture astral microtubules during chromosome attachment to the mitotic spindle: direct visualization in live newt lung cells.* J Cell Biol, 1990. **111**(3): p. 1039-45.
31. Zimmerman, W. and S.J. Doxsey, *Construction of centrosomes and spindle poles by molecular motor-driven assembly of protein particles.* Traffic, 2000. **1**(12): p. 927-34.
32. Joshi, H.C., et al., *Gamma-tubulin is a centrosomal protein required for cell cycle-dependent microtubule nucleation.* Nature, 1992. **356**(6364): p. 80-3.
33. Fuller, S.D., et al., *The core of the mammalian centriole contains gamma-tubulin.* Curr Biol, 1995. **5**(12): p. 1384-93.
34. Wiese, C. and Y. Zheng, *Microtubule nucleation: gamma-tubulin and beyond.* J Cell Sci, 2006. **119**(Pt 20): p. 4143-53.
35. Manning, A.L. and D.A. Compton, *SnapShot: Nonmotor proteins in spindle assembly.* Cell, 2008. **134**(4): p. 694.
36. Loughlin, R., B. Riggs, and R. Heald, *SnapShot: motor proteins in spindle assembly.* Cell, 2008. **134**(3): p. 548-548 e1.
37. Khodjakov, A., et al., *Centrosome-independent mitotic spindle formation in vertebrates.* Curr Biol, 2000. **10**(2): p. 59-67.
38. Bonaccorsi, S., M.G. Giansanti, and M. Gatti, *Spindle assembly in Drosophila neuroblasts and ganglion mother cells.* Nat Cell Biol, 2000. **2**(1): p. 54-6.
39. Karsenti, E. and I. Vernos, *The mitotic spindle: a self-made machine.* Science, 2001. **294**(5542): p. 543-7.

40. Saredi, A., L. Howard, and D.A. Compton, *NuMA assembles into an extensive filamentous structure when expressed in the cell cytoplasm.* J Cell Sci, 1996. **109 (Pt 3)**: p. 619-30.
41. Merdes, A., et al., *A complex of NuMA and cytoplasmic dynein is essential for mitotic spindle assembly.* Cell, 1996. **87**(3): p. 447-58.
42. Compton, D.A., *Focusing on spindle poles.* J Cell Sci, 1998. **111 (Pt 11)**: p. 1477-81.
43. Maiato, H., et al., *The dynamic kinetochore-microtubule interface.* J Cell Sci, 2004. **117**(Pt 23): p. 5461-77.
44. Sharp, D.J., G.C. Rogers, and J.M. Scholey, *Microtubule motors in mitosis.* Nature, 2000. **407**(6800): p. 41-7.
45. Fleig, U., J.D. Beinhauer, and J.H. Hegemann, *Functional selection for the centromere DNA from yeast chromosome VIII.* Nucleic Acids Res, 1995. **23**(6): p. 922-4.
46. Schueler, M.G., et al., *Genomic and genetic definition of a functional human centromere.* Science, 2001. **294**(5540): p. 109-15.
47. Brenner, S., et al., *Kinetochore structure, duplication, and distribution in mammalian cells: analysis by human autoantibodies from scleroderma patients.* J Cell Biol, 1981. **91**(1): p. 95-102.
48. Musacchio, A. and E.D. Salmon, *The spindle-assembly checkpoint in space and time.* Nat Rev Mol Cell Biol, 2007. **8**(5): p. 379-93.
49. Chan, G.K., S.T. Liu, and T.J. Yen, *Kinetochore structure and function.* Trends Cell Biol, 2005. **15**(11): p. 589-98.
50. Kremer, L., et al., *Proteins responsible for anticentromere activity found in the sera of patients with CREST-associated Raynaud's phenomenon.* Clin Exp Immunol, 1988. **72**(3): p. 465-9.
51. Palmer, D.K., et al., *Purification of the centromere-specific protein CENP-A and demonstration that it is a distinctive histone.* Proc Natl Acad Sci U S A, 1991. **88**(9): p. 3734-8.
52. Yoda, K., et al., *Human centromere protein A (CENP-A) can replace histone H3 in nucleosome reconstitution in vitro.* Proc Natl Acad Sci U S A, 2000. **97**(13): p. 7266-71.
53. Stoler, S., et al., *A mutation in CSE4, an essential gene encoding a novel chromatin-associated protein in yeast, causes chromosome nondisjunction and cell cycle arrest at mitosis.* Genes Dev, 1995. **9**(5): p. 573-86.
54. Howman, E.V., et al., *Early disruption of centromeric chromatin organization in centromere protein A (Cenpa) null mice.* Proc Natl Acad Sci U S A, 2000. **97**(3): p. 1148-53.
55. Jansen, L.E., et al., *Propagation of centromeric chromatin requires exit from mitosis.* J Cell Biol, 2007. **176**(6): p. 795-805.
56. Keith, K.C. and M. Fitzgerald-Hayes, *CSE4 genetically interacts with the Saccharomyces cerevisiae centromere DNA elements CDE I and CDE II but not CDE III. Implications for the path of the centromere dna around a cse4p variant nucleosome.* Genetics, 2000. **156**(3): p. 973-81.
57. Okada, T., et al., *CENP-B controls centromere formation depending on the chromatin context.* Cell, 2007. **131**(7): p. 1287-300.

58. Perez-Castro, A.V., et al., *Centromeric protein B null mice are viable with no apparent abnormalities.* Dev Biol, 1998. **201**(2): p. 135-43.
59. Kapoor, M., et al., *The cenpB gene is not essential in mice.* Chromosoma, 1998. **107**(8): p. 570-6.
60. Amor, D.J. and K.H. Choo, *Neocentromeres: role in human disease, evolution, and centromere study.* Am J Hum Genet, 2002. **71**(4): p. 695-714.
61. Earnshaw, W.C., H. Ratrie, 3rd, and G. Stetten, *Visualization of centromere proteins CENP-B and CENP-C on a stable dicentric chromosome in cytological spreads.* Chromosoma, 1989. **98**(1): p. 1-12.
62. Cheeseman, I.M. and A. Desai, *Molecular architecture of the kinetochore-microtubule interface.* Nat Rev Mol Cell Biol, 2008. **9**(1): p. 33-46.
63. Cheeseman, I.M., et al., *KNL1 and the CENP-H/I/K complex coordinately direct kinetochore assembly in vertebrates.* Mol Biol Cell, 2008. **19**(2): p. 587-94.
64. Okada, M., et al., *The CENP-H-I complex is required for the efficient incorporation of newly synthesized CENP-A into centromeres.* Nat Cell Biol, 2006. **8**(5): p. 446-57.
65. Liu, S.T., et al., *Mapping the assembly pathways that specify formation of the trilaminar kinetochore plates in human cells.* J Cell Biol, 2006. **175**(1): p. 41-53.
66. Kwon, M.S., et al., *CENP-C is involved in chromosome segregation, mitotic checkpoint function, and kinetochore assembly.* Mol Biol Cell, 2007. **18**(6): p. 2155-68.
67. Desai, A., et al., *KNL-1 directs assembly of the microtubule-binding interface of the kinetochore in C. elegans.* Genes Dev, 2003. **17**(19): p. 2421-35.
68. Goshima, G., et al., *The role of Ppe1/PP6 phosphatase for equal chromosome segregation in fission yeast kinetochore.* EMBO J, 2003. **22**(11): p. 2752-63.
69. Kline, S.L., et al., *The human Mis12 complex is required for kinetochore assembly and proper chromosome segregation.* J Cell Biol, 2006. **173**(1): p. 9-17.
70. McAinsh, A.D., J.D. Tytell, and P.K. Sorger, *Structure, function, and regulation of budding yeast kinetochores.* Annu Rev Cell Dev Biol, 2003. **19**: p. 519-39.
71. Janke, C., et al., *The budding yeast proteins Spc24p and Spc25p interact with Ndc80p and Nuf2p at the kinetochore and are important for kinetochore clustering and checkpoint control.* EMBO J, 2001. **20**(4): p. 777-91.
72. Wigge, P.A. and J.V. Kilmartin, *The Ndc80p complex from Saccharomyces cerevisiae contains conserved centromere components and has a function in chromosome segregation.* J Cell Biol, 2001. **152**(2): p. 349-60.
73. DeLuca, J.G., et al., *Hec1 and nuf2 are core components of the kinetochore outer plate essential for organizing microtubule attachment sites.* Mol Biol Cell, 2005. **16**(2): p. 519-31.
74. Chen, Y., et al., *HEC, a novel nuclear protein rich in leucine heptad repeats specifically involved in mitosis.* Mol Cell Biol, 1997. **17**(10): p. 6049-56.
75. Hori, T., et al., *Dynamic behavior of Nuf2-Hec1 complex that localizes to the centrosome and centromere and is essential for mitotic progression in vertebrate cells.* J Cell Sci, 2003. **116**(Pt 16): p. 3347-62.
76. DeLuca, J.G., et al., *Kinetochore microtubule dynamics and attachment stability are regulated by Hec1.* Cell, 2006. **127**(5): p. 969-82.

77. Ciferri, C., A. Musacchio, and A. Petrovic, *The Ndc80 complex: hub of kinetochore activity.* FEBS Lett, 2007. **581**(15): p. 2862-9.
78. Cheeseman, I.M., et al., *The conserved KMN network constitutes the core microtubule-binding site of the kinetochore.* Cell, 2006. **127**(5): p. 983-97.
79. Emanuele, M.J., et al., *Measuring the stoichiometry and physical interactions between components elucidates the architecture of the vertebrate kinetochore.* Mol Biol Cell, 2005. **16**(10): p. 4882-92.
80. Cooke, C.A., et al., *Localization of CENP-E in the fibrous corona and outer plate of mammalian kinetochores from prometaphase through anaphase.* Chromosoma, 1997. **106**(7): p. 446-55.
81. Karess, R., *Rod-Zw10-Zwilch: a key player in the spindle checkpoint.* Trends Cell Biol, 2005. **15**(7): p. 386-92.
82. Weaver, B.A., et al., *Centromere-associated protein-E is essential for the mammalian mitotic checkpoint to prevent aneuploidy due to single chromosome loss.* J Cell Biol, 2003. **162**(4): p. 551-63.
83. Howell, B.J., et al., *Cytoplasmic dynein/dynactin drives kinetochore protein transport to the spindle poles and has a role in mitotic spindle checkpoint inactivation.* J Cell Biol, 2001. **155**(7): p. 1159-72.
84. Wood, K.W., et al., *CENP-E is a plus end-directed kinetochore motor required for metaphase chromosome alignment.* Cell, 1997. **91**(3): p. 357-66.
85. Kapoor, T.M., et al., *Chromosomes can congress to the metaphase plate before biorientation.* Science, 2006. **311**(5759): p. 388-91.
86. Yang, Z., et al., *Kinetochore dynein is required for chromosome motion and congression independent of the spindle checkpoint.* Curr Biol, 2007. **17**(11): p. 973-80.
87. Varma, D., et al., *Direct role of dynein motor in stable kinetochore-microtubule attachment, orientation, and alignment.* J Cell Biol, 2008. **182**(6): p. 1045-54.
88. Gassmann, R., et al., *A new mechanism controlling kinetochore-microtubule interactions revealed by comparison of two dynein-targeting components: SPDL-1 and the Rod/Zwilch/Zw10 complex.* Genes Dev, 2008. **22**(17): p. 2385-99.
89. Vergnolle, M.A. and S.S. Taylor, *Cenp-F links kinetochores to Ndel1/Nde1/Lis1/dynein microtubule motor complexes.* Curr Biol, 2007. **17**(13): p. 1173-9.
90. Bomont, P., et al., *Unstable microtubule capture at kinetochores depleted of the centromere-associated protein CENP-F.* EMBO J, 2005. **24**(22): p. 3927-39.
91. Sharp, D.J., G.C. Rogers, and J.M. Scholey, *Cytoplasmic dynein is required for poleward chromosome movement during mitosis in Drosophila embryos.* Nat Cell Biol, 2000. **2**(12): p. 922-30.
92. Li, Y., et al., *Kinetochore dynein generates a poleward pulling force to facilitate congression and full chromosome alignment.* Cell Res, 2007. **17**(8): p. 701-12.
93. Vorozhko, V.V., et al., *Multiple mechanisms of chromosome movement in vertebrate cells mediated through the Ndc80 complex and dynein/dynactin.* Chromosoma, 2008. **117**(2): p. 169-79.
94. Maiato, H., P. Sampaio, and C.E. Sunkel, *Microtubule-associated proteins and their essential roles during mitosis.* Int Rev Cytol, 2004. **241**: p. 53-153.

95. Nasmyth, K., *How might cohesin hold sister chromatids together?* Philos Trans R Soc Lond B Biol Sci, 2005. **360**(1455): p. 483-96.
96. Hauf, S., et al., *Dissociation of cohesin from chromosome arms and loss of arm cohesion during early mitosis depends on phosphorylation of SA2.* PLoS Biol, 2005. **3**(3): p. e69.
97. Rieder, C.L., et al., *The checkpoint delaying anaphase in response to chromosome monoorientation is mediated by an inhibitory signal produced by unattached kinetochores.* J Cell Biol, 1995. **130**(4): p. 941-8.
98. Rieder, C.L., et al., *Anaphase onset in vertebrate somatic cells is controlled by a checkpoint that monitors sister kinetochore attachment to the spindle.* J Cell Biol, 1994. **127**(5): p. 1301-10.
99. Rieder, C.L., et al., *Anaphase onset in vertebrate somatic cells is controlled by a checkpoint that monitors sister kinetochore attachment to the spindle.* J Cell Biol, 1994. **127**(5): p. 1301-10.
100. Waizenegger, I., et al., *Regulation of human separase by securin binding and autocleavage.* Curr Biol, 2002. **12**(16): p. 1368-78.
101. Gimenez-Abian, J.F., et al., *Proteasome activity is required for centromere separation independently of securin degradation in human cells.* Cell Cycle, 2005. **4**(11): p. 1558-60.
102. Hagting, A., et al., *Human securin proteolysis is controlled by the spindle checkpoint and reveals when the APC/C switches from activation by Cdc20 to Cdh1.* J Cell Biol, 2002. **157**(7): p. 1125-37.
103. King, R.W., et al., *A 20S complex containing CDC27 and CDC16 catalyzes the mitosis-specific conjugation of ubiquitin to cyclin B.* Cell, 1995. **81**(2): p. 279-88.
104. Visintin, R., S. Prinz, and A. Amon, *CDC20 and CDH1: a family of substrate-specific activators of APC-dependent proteolysis.* Science, 1997. **278**(5337): p. 460-3.
105. Fang, G., H. Yu, and M.W. Kirschner, *The checkpoint protein MAD2 and the mitotic regulator CDC20 form a ternary complex with the anaphase-promoting complex to control anaphase initiation.* Genes Dev, 1998. **12**(12): p. 1871-83.
106. Hoyt, M.A., L. Totis, and B.T. Roberts, *S. cerevisiae genes required for cell cycle arrest in response to loss of microtubule function.* Cell, 1991. **66**(3): p. 507-17.
107. Li, R. and A.W. Murray, *Feedback control of mitosis in budding yeast.* Cell, 1991. **66**(3): p. 519-31.
108. Hardwick, K.G., et al., *Activation of the budding yeast spindle assembly checkpoint without mitotic spindle disruption.* Science, 1996. **273**(5277): p. 953-6.
109. Kitagawa, K. and P. Hieter, *Evolutionary conservation between budding yeast and human kinetochores.* Nat Rev Mol Cell Biol, 2001. **2**(9): p. 678-87.
110. Taylor, S.S., M.I. Scott, and A.J. Holland, *The spindle checkpoint: a quality control mechanism which ensures accurate chromosome segregation.* Chromosome Res, 2004. **12**(6): p. 599-616.
111. Musacchio, A. and K.G. Hardwick, *The spindle checkpoint: structural insights into dynamic signalling.* Nat Rev Mol Cell Biol, 2002. **3**(10): p. 731-41.
112. Yen, T.J., et al., *CENP-E is a putative kinetochore motor that accumulates just before mitosis.* Nature, 1992. **359**(6395): p. 536-9.

113. Abrieu, A., et al., *CENP-E as an essential component of the mitotic checkpoint in vitro.* Cell, 2000. **102**(6): p. 817-26.
114. Skoufias, D.A., et al., *Mammalian mad2 and bub1/bubR1 recognize distinct spindle-attachment and kinetochore-tension checkpoints.* Proc Natl Acad Sci U S A, 2001. **98**(8): p. 4492-7.
115. DeLuca, J.G., et al., *Nuf2 and Hec1 are required for retention of the checkpoint proteins Mad1 and Mad2 to kinetochores.* Curr Biol, 2003. **13**(23): p. 2103-9.
116. Waters, J.C., et al., *Localization of Mad2 to kinetochores depends on microtubule attachment, not tension.* J Cell Biol, 1998. **141**(5): p. 1181-91.
117. Li, X. and R.B. Nicklas, *Mitotic forces control a cell-cycle checkpoint.* Nature, 1995. **373**(6515): p. 630-2.
118. Li, X. and R.B. Nicklas, *Tension-sensitive kinetochore phosphorylation and the chromosome distribution checkpoint in praying mantid spermatocytes.* J Cell Sci, 1997. **110 (Pt 5)**: p. 537-45.
119. Pinsky, B.A. and S. Biggins, *The spindle checkpoint: tension versus attachment.* Trends Cell Biol, 2005. **15**(9): p. 486-93.
120. Martin-Lluesma, S., V.M. Stucke, and E.A. Nigg, *Role of Hec1 in spindle checkpoint signaling and kinetochore recruitment of Mad1/Mad2.* Science, 2002. **297**(5590): p. 2267-70.
121. Tighe, A., O. Staples, and S. Taylor, *Mps1 kinase activity restrains anaphase during an unperturbed mitosis and targets Mad2 to kinetochores.* J Cell Biol, 2008. **181**(6): p. 893-901.
122. De Antoni, A., et al., *The Mad1/Mad2 complex as a template for Mad2 activation in the spindle assembly checkpoint.* Curr Biol, 2005. **15**(3): p. 214-25.
123. Howell, B.J., et al., *Spindle checkpoint protein dynamics at kinetochores in living cells.* Curr Biol, 2004. **14**(11): p. 953-64.
124. Sironi, L., et al., *Mad2 binding to Mad1 and Cdc20, rather than oligomerization, is required for the spindle checkpoint.* EMBO J, 2001. **20**(22): p. 6371-82.
125. Sudakin, V., G.K. Chan, and T.J. Yen, *Checkpoint inhibition of the APC/C in HeLa cells is mediated by a complex of BUBR1, BUB3, CDC20, and MAD2.* J Cell Biol, 2001. **154**(5): p. 925-36.
126. Yao, X., et al., *CENP-E forms a link between attachment of spindle microtubules to kinetochores and the mitotic checkpoint.* Nat Cell Biol, 2000. **2**(8): p. 484-91.
127. Mao, Y., A. Abrieu, and D.W. Cleveland, *Activating and silencing the mitotic checkpoint through CENP-E-dependent activation/inactivation of BubR1.* Cell, 2003. **114**(1): p. 87-98.
128. Nicklas, R.B., et al., *Checkpoint signals in grasshopper meiosis are sensitive to microtubule attachment, but tension is still essential.* J Cell Sci, 2001. **114**(Pt 23): p. 4173-83.
129. Reddy, S.K., et al., *Ubiquitination by the anaphase-promoting complex drives spindle checkpoint inactivation.* Nature, 2007. **446**(7138): p. 921-5.
130. Hoffman, D.B., et al., *Microtubule-dependent changes in assembly of microtubule motor proteins and mitotic spindle checkpoint proteins at ptk1 kinetochores.* Mol Biol Cell, 2001. **12**(7): p. 1995-2009.
131. Xia, G., et al., *Conformation-specific binding of p31(comet) antagonizes the function of Mad2 in the spindle checkpoint.* EMBO J, 2004. **23**(15): p. 3133-43.

132. Habu, T., et al., *Identification of a MAD2-binding protein, CMT2, and its role in mitosis.* EMBO J, 2002. **21**(23): p. 6419-28.
133. Yang, M., et al., *p31comet blocks Mad2 activation through structural mimicry.* Cell, 2007. **131**(4): p. 744-55.
134. McEwen, B.F., et al., *Kinetochore fiber maturation in PtK1 cells and its implications for the mechanisms of chromosome congression and anaphase onset.* J Cell Biol, 1997. **137**(7): p. 1567-80.
135. Hauf, S., et al., *The small molecule Hesperadin reveals a role for Aurora B in correcting kinetochore-microtubule attachment and in maintaining the spindle assembly checkpoint.* J Cell Biol, 2003. **161**(2): p. 281-94.
136. Cimini, D., et al., *Merotelic kinetochore orientation occurs frequently during early mitosis in mammalian tissue cells and error correction is achieved by two different mechanisms.* J Cell Sci, 2003. **116**(Pt 20): p. 4213-25.
137. Cimini, D., et al., *Merotelic kinetochore orientation versus chromosome mono-orientation in the origin of lagging chromosomes in human primary cells.* J Cell Sci, 2002. **115**(Pt 3): p. 507-15.
138. Cimini, D., L.A. Cameron, and E.D. Salmon, *Anaphase spindle mechanics prevent mis-segregation of merotelically oriented chromosomes.* Curr Biol, 2004. **14**(23): p. 2149-55.
139. Khodjakov, A., et al., *Chromosome fragments possessing only one kinetochore can congress to the spindle equator.* J Cell Biol, 1997. **136**(2): p. 229-40.
140. Wise, D.A. and B.R. Brinkley, *Mitosis in cells with unreplicated genomes (MUGs): spindle assembly and behavior of centromere fragments.* Cell Motil Cytoskeleton, 1997. **36**(3): p. 291-302.
141. Yu, H.G. and R.K. Dawe, *Functional redundancy in the maize meiotic kinetochore.* J Cell Biol, 2000. **151**(1): p. 131-42.
142. Cimini, D., et al., *Aurora kinase promotes turnover of kinetochore microtubules to reduce chromosome segregation errors.* Curr Biol, 2006. **16**(17): p. 1711-8.
143. Cimini, D., *Detection and correction of merotelic kinetochore orientation by Aurora B and its partners.* Cell Cycle, 2007. **6**(13): p. 1558-64.
144. Cimini, D., C. Tanzarella, and F. Degrassi, *Differences in malsegregation rates obtained by scoring ana-telophases or binucleate cells.* Mutagenesis, 1999. **14**(6): p. 563-8.
145. Cimini, D., et al., *Merotelic kinetochore orientation is a major mechanism of aneuploidy in mitotic mammalian tissue cells.* J Cell Biol, 2001. **153**(3): p. 517-27.
146. Fischer, W.H., et al., *Increased formation of micronuclei after hormonal stimulation of cell proliferation in human breast cancer cells.* Mutagenesis, 2001. **16**(3): p. 209-12.
147. Saunders, W.S., et al., *Chromosomal instability and cytoskeletal defects in oral cancer cells.* Proc Natl Acad Sci U S A, 2000. **97**(1): p. 303-8.
148. Bonassi, S., et al., *An increased micronucleus frequency in peripheral blood lymphocytes predicts the risk of cancer in humans.* Carcinogenesis, 2007. **28**(3): p. 625-31.
149. Weaver, B.A., A.D. Silk, and D.W. Cleveland, *Cell biology: nondisjunction, aneuploidy and tetraploidy.* Nature, 2006. **442**(7104): p. E9-10; discussion E10.

150. Mitelman, F., B. Johansson, and F. Mertens, *Mitelman Database of Chromosome Aberrations in Cancer.* http://cgap.nci.nih.gov/Chromosomes/Mitelman, 2007.
151. Borel, F., et al., *Multiple centrosomes arise from tetraploidy checkpoint failure and mitotic centrosome clusters in p53 and RB pocket protein-compromised cells.* Proc Natl Acad Sci U S A, 2002. **99**(15): p. 9819-24.
152. Cahill, D.P., et al., *Mutations of mitotic checkpoint genes in human cancers.* Nature, 1998. **392**(6673): p. 300-3.
153. Cahill, D.P., et al., *Characterization of MAD2B and other mitotic spindle checkpoint genes.* Genomics, 1999. **58**(2): p. 181-7.
154. Draviam, V.M., S. Xie, and P.K. Sorger, *Chromosome segregation and genomic stability.* Curr Opin Genet Dev, 2004. **14**(2): p. 120-5.
155. Myrie, K.A., et al., *Mutation and expression analysis of human BUB1 and BUB1B in aneuploid breast cancer cell lines.* Cancer Lett, 2000. **152**(2): p. 193-9.
156. Imai, Y., et al., *Mutational inactivation of mitotic checkpoint genes, hsMAD2 and hBUB1, is rare in sporadic digestive tract cancers.* Jpn J Cancer Res, 1999. **90**(8): p. 837-40.
157. Sato, M., et al., *Infrequent mutation of the hBUB1 and hBUBR1 genes in human lung cancer.* Jpn J Cancer Res, 2000. **91**(5): p. 504-9.
158. Yamaguchi, K., et al., *Mutation analysis of hBUB1 in aneuploid HNSCC and lung cancer cell lines.* Cancer Lett, 1999. **139**(2): p. 183-7.
159. Tighe, A., et al., *Aneuploid colon cancer cells have a robust spindle checkpoint.* EMBO Rep, 2001. **2**(7): p. 609-14.
160. Gascoigne, K.E. and S.S. Taylor, *Cancer cells display profound intra- and interline variation following prolonged exposure to antimitotic drugs.* Cancer Cell, 2008. **14**(2): p. 111-22.
161. Dai, W., et al., *Slippage of mitotic arrest and enhanced tumor development in mice with BubR1 haploinsufficiency.* Cancer Res, 2004. **64**(2): p. 440-5.
162. Michel, L.S., et al., *MAD2 haplo-insufficiency causes premature anaphase and chromosome instability in mammalian cells.* Nature, 2001. **409**(6818): p. 355-9.
163. Babu, J.R., et al., *Rae1 is an essential mitotic checkpoint regulator that cooperates with Bub3 to prevent chromosome missegregation.* J Cell Biol, 2003. **160**(3): p. 341-53.
164. Weaver, B.A., et al., *Aneuploidy acts both oncogenically and as a tumor suppressor.* Cancer Cell, 2007. **11**(1): p. 25-36.
165. Iwanaga, Y., et al., *Heterozygous deletion of mitotic arrest-deficient protein 1 (MAD1) increases the incidence of tumors in mice.* Cancer Res, 2007. **67**(1): p. 160-6.
166. Pihan, G.A. and S.J. Doxsey, *The mitotic machinery as a source of genetic instability in cancer.* Semin Cancer Biol, 1999. **9**(4): p. 289-302.
167. Duesberg, P. and R. Li, *Multistep carcinogenesis: a chain reaction of aneuploidizations.* Cell Cycle, 2003. **2**(3): p. 202-10.
168. Galipeau, P.C., et al., *17p (p53) allelic losses, 4N (G2/tetraploid) populations, and progression to aneuploidy in Barrett's esophagus.* Proc Natl Acad Sci U S A, 1996. **93**(14): p. 7081-4.
169. Rasnick, D. and P.H. Duesberg, *How aneuploidy affects metabolic control and causes cancer.* Biochem J, 1999. **340 (Pt 3)**: p. 621-30.

170. Shi, Q. and R.W. King, *Chromosome nondisjunction yields tetraploid rather than aneuploid cells in human cell lines.* Nature, 2005. **437**(7061): p. 1038-42.
171. Storchova, Z. and D. Pellman, *From polyploidy to aneuploidy, genome instability and cancer.* Nat Rev Mol Cell Biol, 2004. **5**(1): p. 45-54.
172. Fujiwara, T., et al., *Cytokinesis failure generating tetraploids promotes tumorigenesis in p53-null cells.* Nature, 2005. **437**(7061): p. 1043-7.
173. Wang, X., et al., *Overexpression of aurora kinase A in mouse mammary epithelium induces genetic instability preceding mammary tumor formation.* Oncogene, 2006. **25**(54): p. 7148-58.
174. Nguyen, H.G., et al., *Mechanism of Aurora-B degradation and its dependency on intact KEN and A-boxes: identification of an aneuploidy-promoting property.* Mol Cell Biol, 2005. **25**(12): p. 4977-92.
175. Duesberg, P., et al., *How aneuploidy may cause cancer and genetic instability.* Anticancer Res, 1999. **19**(6A): p. 4887-906.
176. Pogribny, I.P., I. Rusyn, and F.A. Beland, *Epigenetic aspects of genotoxic and non-genotoxic hepatocarcinogenesis: studies in rodents.* Environ Mol Mutagen, 2008. **49**(1): p. 9-15.
177. Foth, H., G.H. Degen, and H.M. Bolt, *New aspects in the classification of carcinogens.* Arh Hig Rada Toksikol, 2005. **56**(2): p. 167-75.
178. Lengauer, C., K.W. Kinzler, and B. Vogelstein, *Genetic instabilities in human cancers.* Nature, 1998. **396**(6712): p. 643-9.
179. Lengauer, C., K.W. Kinzler, and B. Vogelstein, *Genetic instability in colorectal cancers.* Nature, 1997. **386**(6625): p. 623-7.
180. Rajagopalan, H. and C. Lengauer, *CIN-ful cancers.* Cancer Chemother Pharmacol, 2004. **54 Suppl 1**: p. S65-8.
181. Yuen, K.W. and A. Desai, *The wages of CIN.* J Cell Biol, 2008. **180**(4): p. 661-3.
182. Gisselsson, D., *Mitotic instability in cancer: is there method in the madness?* Cell Cycle, 2005. **4**(8): p. 1007-10.
183. Masuda, A. and T. Takahashi, *Chromosome instability in human lung cancers: possible underlying mechanisms and potential consequences in the pathogenesis.* Oncogene, 2002. **21**(45): p. 6884-97.
184. Ghadimi, B.M., et al., *Centrosome amplification and instability occurs exclusively in aneuploid, but not in diploid colorectal cancer cell lines, and correlates with numerical chromosomal aberrations.* Genes Chromosomes Cancer, 2000. **27**(2): p. 183-90.
185. Fukasawa, K., *Centrosome amplification, chromosome instability and cancer development.* Cancer Lett, 2005. **230**(1): p. 6-19.
186. Lingle, W.L., K. Lukasiewicz, and J.L. Salisbury, *Deregulation of the centrosome cycle and the origin of chromosomal instability in cancer.* Adv Exp Med Biol, 2005. **570**: p. 393-421.
187. Lingle, W.L., et al., *Centrosome amplification drives chromosomal instability in breast tumor development.* Proc Natl Acad Sci U S A, 2002. **99**(4): p. 1978-83.
188. Kwon, M., et al., *Mechanisms to suppress multipolar divisions in cancer cells with extra centrosomes.* Genes Dev, 2008. **22**(16): p. 2189-203.
189. Quintyne, N.J., et al., *Spindle multipolarity is prevented by centrosomal clustering.* Science, 2005. **307**(5706): p. 127-9.

190. Brinkley, B.R., *Managing the centrosome numbers game: from chaos to stability in cancer cell division.* Trends Cell Biol, 2001. **11**(1): p. 18-21.
191. Godinho, S.A., M. Kwon, and D. Pellman, *Centrosomes and cancer: how cancer cells divide with too many centrosomes.* Cancer Metastasis Rev, 2009. **28**(1-2): p. 85-98.
192. Reing, J.E., S.M. Gollin, and W.S. Saunders, *The occurrence of chromosome segregational defects is an intrinsic and heritable property of oral squamous cell carcinoma cell lines.* Cancer Genet Cytogenet, 2004. **150**(1): p. 57-61.
193. Thompson, S.L. and D.A. Compton, *Examining the link between chromosomal instability and aneuploidy in human cells.* J Cell Biol, 2008. **180**(4): p. 665-72.
194. Wolf, K.W., M. Mentzel, and A.S. Mendoza, *DNA-containing cytoplasmic bridges in a human breast cancer cell line, MX-1: morphological markers of a highly mobile cell type?* J Submicrosc Cytol Pathol, 1996. **28**(3): p. 369-73.
195. Gisselsson, D., et al., *Telomere-mediated mitotic disturbances in immortalized ovarian epithelial cells reproduce chromosomal losses and breakpoints from ovarian carcinoma.* Genes Chromosomes Cancer, 2005. **42**(1): p. 22-33.
196. Rieder, C.L. and R. Hard, *Newt lung epithelial cells: cultivation, use, and advantages for biomedical research.* Int Rev Cytol, 1990. **122**: p. 153-220.
197. DeLuca, J.G., et al., *hNuf2 inhibition blocks stable kinetochore-microtubule attachment and induces mitotic cell death in HeLa cells.* J Cell Biol, 2002. **159**(4): p. 549-55.
198. Pellman, D., *Cancer. A CINtillating new job for the APC tumor suppressor.* Science, 2001. **291**(5513): p. 2555-6.
199. Yang, Z., et al., *Extra centrosomes and/or chromosomes prolong mitosis in human cells.* Nat Cell Biol, 2008. **10**(6): p. 748-51.
200. Nguyen, H.G., et al., *Deregulated Aurora-B induced tetraploidy promotes tumorigenesis.* Faseb J, 2009.
201. Pihan, G.A., et al., *Centrosome defects can account for cellular and genetic changes that characterize prostate cancer progression.* Cancer Res, 2001. **61**(5): p. 2212-9.
202. Sato, N., et al., *Correlation between centrosome abnormalities and chromosomal instability in human pancreatic cancer cells.* Cancer Genet Cytogenet, 2001. **126**(1): p. 13-9.
203. Jin, Y., et al., *Distinct mitotic segregation errors mediate chromosomal instability in aggressive urothelial cancers.* Clin Cancer Res, 2007. **13**(6): p. 1703-12.
204. Kaplan, K.B., et al., *A role for the Adenomatous Polyposis Coli protein in chromosome segregation.* Nat Cell Biol, 2001. **3**(4): p. 429-32.
205. Stewenius, Y., et al., *Structural and numerical chromosome changes in colon cancer develop through telomere-mediated anaphase bridges, not through mitotic multipolarity.* Proc Natl Acad Sci U S A, 2005. **102**(15): p. 5541-6.
206. Stewenius, Y., et al., *Defective chromosome segregation and telomere dysfunction in aggressive Wilms' tumors.* Clin Cancer Res, 2007. **13**(22 Pt 1): p. 6593-602.
207. Ganem, N.J., S.A. Godinho, and D. Pellman, *A mechanism linking extra centrosomes to chromosomal instability.* Nature, 2009.
208. Acilan, C. and W.S. Saunders, *A tale of too many centrosomes.* Cell, 2008. **134**(4): p. 572-5.

209. Basto, R., et al., *Centrosome amplification can initiate tumorigenesis in flies.* Cell, 2008. **133**(6): p. 1032-42.
210. Canman, J., E. Salmon, and G. Fang, *Inducing Precocious Anaphase in Cultured Mammalian Cells.* Cell Motil Cyto, 2002. **52**: p. 61-65.
211. Meraldi, P., V.M. Draviam, and P.K. Sorger, *Timing and checkpoints in the regulation of mitotic progression.* Dev Cell, 2004. **7**(1): p. 45-60.
212. Cimini, D., *Detection and correction of merotelic kinetochore orientationby Aurora B and its partners.* Cell Cycle, 2007. **6**(13): p. 1558-64.
213. Bakhoum, S.F., et al., *Genome stability is ensured by temporal control of kinetochore-microtubule dynamics.* Nat Cell Biol, 2009. **11**(1): p. 27-35.
214. Mole Bajer, J., *The role of centrioles in the development of the astral spindle (newt).* Cytobios, 1975. **13**: p. 117-140.
215. Rattner, J.B. and M.W. Berns, *Centriole behavior in early mitosis of rat kangaroo cells (PTK2).* Chromosoma, 1976. **54**(4): p. 387-95.
216. Aubin, J.E., M. Osborn, and K. Weber, *Variations in the distribution and migration of centriole duplexes in mitotic PtK2 cells studied by immunofluorescence microscopy.* J Cell Sci, 1980. **43**: p. 177-94.
217. Rosenblatt, J., et al., *Myosin II-dependent cortical movement is required for centrosome separation and positioning during mitotic spindle assembly.* Cell, 2004. **117**(3): p. 361-72.
218. Toso, A., et al., *Kinetochore-generated pushing forces separate centrosomes during bipolar spindle assembly.* J Cell Biol, 2009. **184**(3): p. 365-72.
219. Waters, J.C., R.W. Cole, and C.L. Rieder, *The force-producing mechanism for centrosome separation during spindle formation in vertebrates is intrinsic to each aster.* J Cell Biol, 1993. **122**(2): p. 361-72.
220. Whitehead, C.M., R.J. Winkfein, and J.B. Rattner, *The relationship of HsEg5 and the actin cytoskeleton to centrosome separation.* Cell Motil Cytoskeleton, 1996. **35**(4): p. 298-308.
221. Rosenblatt, J., *Spindle assembly: asters part their separate ways.* Nat Cell Biol, 2005. **7**(3): p. 219-22.
222. Sharp, D.J., et al., *Antagonistic microtubule-sliding motors position mitotic centrosomes in Drosophila early embryos.* Nat Cell Biol, 1999. **1**(1): p. 51-4.
223. Tanenbaum, M.E., et al., *Dynein, Lis1 and CLIP-170 counteract Eg5-dependent centrosome separation during bipolar spindle assembly.* EMBO J, 2008. **27**(24): p. 3235-45.
224. Tanenbaum, M.E. and R.H. Medema, *Mechanisms of centrosome separation and bipolar spindle assembly.* Dev Cell, 2010. **19**(6): p. 797-806.
225. Whitehead, C.M. and J.B. Rattner, *Expanding the role of HsEg5 within the mitotic and post-mitotic phases of the cell cycle.* J Cell Sci, 1998. **111 (Pt 17)**: p. 2551-61.
226. Woodcock, S.A., et al., *Tiam1-Rac signaling counteracts Eg5 during bipolar spindle assembly to facilitate chromosome congression.* Curr Biol, 2010. **20**(7): p. 669-75.
227. Gonczy, P., et al., *Cytoplasmic dynein is required for distinct aspects of MTOC positioning, including centrosome separation, in the one cell stage Caenorhabditis elegans embryo.* J Cell Biol, 1999. **147**(1): p. 135-50.

228. Robinson, J.T., et al., *Cytoplasmic dynein is required for the nuclear attachment and migration of centrosomes during mitosis in Drosophila.* J Cell Biol, 1999. **146**(3): p. 597-608.
229. Silkworth, W.T., et al., *Multipolar spindle pole coalescence is a major source of kinetochore mis-attachment and chromosome mis-segregation in cancer cells.* PLoS One, 2009. **4**(8): p. e6564.
230. Khodjakov, A., R.W. Cole, and C.L. Rieder, *A synergy of technologies: combining laser microsurgery with green fluorescent protein tagging.* Cell Motil Cytoskeleton, 1997. **38**(4): p. 311-7.
231. Brinkley, B.R. and J. Cartwright, Jr., *Ultrastructural analysis of mitotic spindle elongation in mammalian cells in vitro. Direct microtubule counts.* J Cell Biol, 1971. **50**(2): p. 416-31.
232. Cameron, L.A., et al., *Kinesin 5-independent poleward flux of kinetochore microtubules in PtK1 cells.* J Cell Biol, 2006. **173**(2): p. 173-9.
233. Ganem, N.J., S.A. Godinho, and D. Pellman, *A mechanism linking extra centrosomes to chromosomal instability.* Nature, 2009. **460**(7252): p. 278-82.
234. Salmon, E.D., et al., *Merotelic kinetochores in mammalian tissue cells.* Philos Trans R Soc Lond B Biol Sci, 2005. **360**(1455): p. 553-68.
235. Kline-Smith, S.L., et al., *Depletion of centromeric MCAK leads to chromosome congression and segregation defects due to improper kinetochore attachments.* Mol Biol Cell, 2004. **15**(3): p. 1146-59.
236. Bakhoum, S.F., G. Genovese, and D.A. Compton, *Deviant kinetochore microtubule dynamics underlie chromosomal instability.* Curr Biol, 2009. **19**(22): p. 1937-42.
237. Thompson, S.L., S.F. Bakhoum, and D.A. Compton, *Mechanisms of chromosomal instability.* Curr Biol, 2010. **20**(6): p. R285-95.
238. Piel, M., et al., *The respective contributions of the mother and daughter centrioles to centrosome activity and behavior in vertebrate cells.* J Cell Biol, 2000. **149**(2): p. 317-30.
239. Khodjakov, A., et al., *Minus-end capture of preformed kinetochore fibers contributes to spindle morphogenesis.* J Cell Biol, 2003. **160**(5): p. 671-83.
240. Paul, R., et al., *Computer simulations predict that chromosome movements and rotations accelerate mitotic spindle assembly without compromising accuracy.* Proc Natl Acad Sci U S A, 2009. **106**(37): p. 15708-13.
241. Nicklas, R.B., *How cells get the right chromosomes.* Science, 1997. **275**(5300): p. 632-7.
242. Cai, S., et al., *Chromosome congression in the absence of kinetochore fibres.* Nat Cell Biol, 2009. **11**(7): p. 832-8.
243. Loncarek, J., et al., *The centromere geometry essential for keeping mitosis error free is controlled by spindle forces.* Nature, 2007. **450**(7170): p. 745-9.
244. Yang, Z., et al., *Cells satisfy the mitotic checkpoint in Taxol, and do so faster in concentrations that stabilize syntelic attachments.* J Cell Biol, 2009. **186**(5): p. 675-84.
245. Khodjakov, A. and C.L. Rieder, *The nature of cell-cycle checkpoints: facts and fallacies.* J Biol, 2009. **8**(10): p. 88.

246. Nezi, L. and A. Musacchio, *Sister chromatid tension and the spindle assembly checkpoint.* Curr Opin Cell Biol, 2009. **21**(6): p. 785-95.
247. Kaseda, K., A.D. McAinsh, and R.A. Cross, *Walking, hopping, diffusing and braking modes of kinesin-5.* Biochem Soc Trans, 2009. **37**(Pt 5): p. 1045-9.
248. Kaseda, K., A. McAinsh, and R.A. Cross *A countdown clock in mitotic prophase*. 2009 ASCB Abstracts, 2009. **http://www.ascb.org/meetings/Abstract/2009_Regular_Abstracts.pdf**, 615/B562, p. 294.
249. Magidson, V., et al., *The spatial arrangement of chromosomes during prometaphase facilitates spindle assembly.* Cell, 2011. **146**(4): p. 555-67.
250. Cimini, D., et al., *Histone hyperacetylation in mitosis prevents sister chromatid separation and produces chromosome segregation defects.* Mol Biol Cell, 2003. **14**(9): p. 3821-33.
251. Gregan, J., et al., *The kinetochore proteins Pcs1 and Mde4 and heterochromatin are required to prevent merotelic orientation.* Curr Biol, 2007. **17**(14): p. 1190-200.
252. Manning, A.L., M.S. Longworth, and N.J. Dyson, *Loss of pRB causes centromere dysfunction and chromosomal instability.* Genes Dev, 2010. **24**(13): p. 1364-76.
253. Samoshkin, A., et al., *Human condensin function is essential for centromeric chromatin assembly and proper sister kinetochore orientation.* PLoS One, 2009. **4**(8): p. e6831.
254. Stear, J.H. and M.B. Roth, *Characterization of HCP-6, a C. elegans protein required to prevent chromosome twisting and merotelic attachment.* Genes Dev, 2002. **16**(12): p. 1498-508.
255. Heneen, W.K., *Kinetochores and microtubules in multipolar mitosis and chromosome orientation.* Exp Cell Res, 1975. **91**(1): p. 57-62.
256. Sluder, G., et al., *The checkpoint control for anaphase onset does not monitor excess numbers of spindle poles or bipolar spindle symmetry.* J Cell Sci, 1997. **110**(Pt 4): p. 421-9.
257. Chaly, N. and D.L. Brown, *The prometaphase configuration and chromosome order in early mitosis.* J Cell Sci, 1988. **91 (Pt 3)**: p. 325-35.
258. Mosgoller, W., et al., *Chromosome arrangements in human fibroblasts at mitosis.* Hum Genet, 1991. **88**(1): p. 27-33.
259. Nagele, R., et al., *Precise spatial positioning of chromosomes during prometaphase: evidence for chromosomal order.* Science, 1995. **270**(5243): p. 1831-5.
260. Mogilner, A. and E. Craig, *Towards a quantitative understanding of mitotic spindle assembly and mechanics.* J Cell Sci, 2010. **123**(Pt 20): p. 3435-45.
261. Wollman, R., et al., *Efficient chromosome capture requires a bias in the 'search-and-capture' process during mitotic-spindle assembly.* Curr Biol, 2005. **15**(9): p. 828-32.
262. Silkworth, W.T., et al., *Timing of centrosome separation is important for accurate chromosome segregation.* Mol Biol Cell, 2012. **23**(3): p. 401-11.
263. Nicholson, J.M. and D. Cimini, *How mitotic errors contribute to karyotypic diversity in cancer.* Adv Cancer Res, 2011. **112**: p. 43-75.

264. Group, U.S.C.S.W. *United States Cancer Statistics: 1999–2008 Incidence and Mortality Web-based Report.* 2012; Available from: Available at: www.cdc.gov/uscs.
265. Gregan, J., et al., *Merotelic kinetochore attachment: causes and effects.* Trends Cell Biol, 2011. **21**(6): p. 374-81.
266. Brattain, M.G., et al., *American Type Culture Collection (ATCC).* http://www.atcc.org, 2012.
267. Duensing, A. and S. Duensing, *Centrosomes, polyploidy and cancer.* Adv Exp Med Biol, 2010. **676**: p. 93-103.
268. Yamashita, Y.M., D.L. Jones, and M.T. Fuller, *Orientation of asymmetric stem cell division by the APC tumor suppressor and centrosome.* Science, 2003. **301**(5639): p. 1547-50.